FINAL TECHNICAL REPORT
AFOSR GRANT 85-0375

True Asymptotic Plasma - Sheath Matching with an
Asymptotically Correct Collisional Presheath

Principal Investigator: Geoffrey L. Main

School of Mechanical Engineering
Georgia Institute of Technology
Atlanta, Georgia 303032

Submitted to

Air Force Office of Scientific Research
Bolling Air Force Base
Washington, D.C., 20332-6448

AFOSR technical Officer:
Dr. Mitat Birkan

June, 1989

GEORGIA INSTITUTE OF TECHNOLOGY
A Unit of the University System of Georgia
Atlanta, Georgia 30332

GTRI
GEORGIA TECH RESEARCH INSTITUTE

Unclassified
SECURITY CLASSIFICATION OF THIS PAGE

REPORT DOCUMENTATION PAGE

Form Approved OMB No. 0704-01

1a REPORT SECURITY CLASSIFICATION: Unclassified	1b RESTRICTIVE MARKINGS:
2a SECURITY CLASSIFICATION AUTHORITY:	3 DISTRIBUTION/AVAILABILITY OF REPORT: Approved for public release; distribution is unlimited
2b DECLASSIFICATION/DOWNGRADING SCHEDULE:	
4 PERFORMING ORGANIZATION REPORT NUMBER(S): E25-664	5 MONITORING ORGANIZATION REPORT NUMBER(S):
6a NAME OF PERFORMING ORGANIZATION: Georgia Inst of Tech. / 6b OFFICE SYMBOL (If applicable):	7a NAME OF MONITORING ORGANIZATION: AFOSR/NA
6c ADDRESS (City, State, and ZIP Code): Mechanical Engineering Atlanta, GA 30332-0405	7b ADDRESS (City, State, and ZIP Code): Building 410, Bolling AFB DC 20332-6448
8a NAME OF FUNDING/SPONSORING ORGANIZATION: AFOSR/NA / 8b OFFICE SYMBOL (If applicable):	9 PROCUREMENT INSTRUMENT IDENTIFICATION NUMBER: AFOSR-85-0375
8c ADDRESS (City, State, and ZIP Code): Building 410, Bolling AFB DC 20332-6448	10 SOURCE OF FUNDING NUMBERS: PROGRAM ELEMENT NO. 61102F / PROJECT NO. 2308 / TASK NO A1 / WORK UNIT ACCESSION

11. TITLE (Include Security Classification)
(U) True Asymptotic Plasma-Sheath Matching with an Asymptotically Correct Collisional Presheath

12. PERSONAL AUTHOR(S)
Geoffrey L. Main

13a. TYPE OF REPORT	13b. TIME COVERED	14. DATE OF REPORT (Year, Month, Day)	15. PAGE COUNT
Annual Research Rpt	FROM 9/1/85 TO 10/31/88	30 June 89	134

16. SUPPLEMENTARY NOTATION

17. COSATI CODES			18. SUBJECT TERMS (Continue on reverse if necessary and identify by block number)
FIELD	GROUP	SUB-GROUP	Thermionic Energy Convertors, Plasmas, Sheath Presheaths

19. ABSTRACT (Continue on reverse if necessary and identify by block number)

This report covers work done on plasma sheaths and presheaths as applic Thermionic Energy Convertors (TECs) during the period 1 September 1985 31 October 1988 A code modelling the TEC has been completed with the and presheath work incorporated. Also additional work on presheaths v Fokker-Planck Collision terms has been done.

20. DISTRIBUTION/AVAILABILITY OF ABSTRACT	21. ABSTRACT SECURITY CLASSIFICATION	
☒ UNCLASSIFIED/UNLIMITED ☒ SAME AS RPT. ☐ DTIC USERS	Unclassified	
22a. NAME OF RESPONSIBLE INDIVIDUAL: Dr Mitat Birkan	22b. TELEPHONE (Include Area Code): (202) 767-4937	22c. OFFI AF

DD Form 1473, JUN 86 — Previous editions are obsolete. — SECURITY CLASSIFICA

Unclassifie

FINAL TECHNICAL REPORT
AFOSR GRANT 85-0375

True Asymptotic Plasma - Sheath Matching with an Asymptotically Correct Collisional Presheath

Principal Investigator: Geoffrey L. Main

School of Mechanical Engineering
Georgia Institute of Technology
Atlanta, Georgia 303032

Submitted to

Air Force Office of Scientific Research
Bolling Air Force Base
Washington, D.C., 20332-6448

AFOSR technical Officer:
Dr. Mitat Birkan

June, 1989

TABLE OF CONTENTS

INTRODUCTION

The work under this grant on plasma presheaths, which form a transition region between the collisionless electrode sheaths and the plasma, is directed toward the problems of the Thermionic Energy Convertor (TEC). Figure 1 shows a schematic of a TEC in a reactor core for space power applications and the basic physics. Cesium is put the gap between the emitter and collector for two purposes: first, to ionize and neutralize the space charge so that a useful electron current density can pass (10 - 100 amps/square cm), and second to reduce the electrode work functions by adsorption of cesium. Of the plasma physics of the the cesium filled gap of the TEC, the plasma-electrode interactions are the most significant part because these regions form boundary conditions which control the plasma density and temperatures of the entire gap. Thus the research under this grant has been directed toward the study of collisional presheaths which form the layer adjacent to an electrode on the order of one ion mean free path thick. However, the research pursued under this grant is not limited in applicabilty to TECs but is of interest to plasma-surface interactions in general. Other applications include electric propulsion where electrode erosion is a problem and not fully understood and more generally any plasma-surface interaction.

This report includes the asymptotic presheath theory developed, and is preceded by the basic theory of the Thermionic Energy Convertor (TEC) and is followed by the application of the theory to a time dependent model of the TEC in the program called TEC. As shown in the TEC results, the agreement with experiment is good except in the low current regime of the TEC where an unexplained disagreement remains. This is still a puzzle.

BASIC TEC THEORY

The basic theory of the TEC is set forth in the following paper published under this grant.

T-PS/15/3/13329

Effects of Emitter Sheath Ion Reflection and Trapped Ions on Thermionic Converter Performance Using an Isothermal Electron Model

G. L. Main
S. H. Lam

Reprinted from: IEEE TRANSACTIONS ON PLASMA SCIENCE, Vol. PS-15, No. 3, JUNE 1987.

Effects of Emitter Sheath Ion Reflection and Trapped Ions on Thermionic Converter Performance Using an Isothermal Electron Model

GEOFFREY L. MAIN AND S. H. LAM

Abstract—**This paper couples exact collisionless sheath calculations to an isothermal electron model of a thermionic converter. The emitter sheath structure takes into account reflected ions, trapped ions, and surface emission ions. It is shown that lessening the net loss of ions at the emitter in the ignited mode by these phenomena degrades performance. In addition, it is shown that when the emitter returns too many of the ions, the arc is extinguished because there is insufficient resistive heating to maintain the necessary plasma electron temperature for ionization. These results suggest that the ignited mode cannot be improved much. However, nonignited modes in which the electron temperature remains low, such as the pulsed mode, do not suffer from this adverse behavior.**

I. Introduction

EMITTER sheath phenomena are important in thermionic energy converters because the emitter sheath forms the emitter boundary condition for the plasma in the gap by controlling both the ion loss rate and the loss rate of hot (3000 K) plasma electrons to the emitter. This paper examines two expected emitter sheath phenomena and their effects on converter performance: reflection of ions coming from the plasma by a double emitter sheath, and ions trapped in the double emitter sheath. The authors have previously suggested that ion reflection might improve thermionic energy converter performance [1] and have subsequently shown that ion reflection at the emitter is likely to degrade the performance in the ignited mode and, in addition, that trapped ions in a double emitter sheath are also likely to degrade performance in the ignited mode [2]. Lundgren [3], [4] has also shown this with simplified ion and electron dynamics. In the present paper the effects of emitter ion reflection and ion trapping in the ignited mode are calculated using exact electron and ion dynamics in the collisionless (except for ion trapping) sheaths. The electrons entering the sheaths from the plasma are assumed to have a Maxwellian distribution, but no assumptions are made about the returning electrons, and the electron density in the sheath is calculated exactly. The ions entering the sheaths from the plasma are not assumed cold, but are given the correct ion temperature and shifted in velocity according to a generalization of the Bohm criterion [5], [6].

Both ion reflection and trapped ions in the emitter sheath reduce the normalized (by plasma density) net ion loss rate to the emitter. Also, both of these phenomena raise the normalized plasma density adjacent to the emitter. The higher plasma density at the emitter causes a greater increase in the loss of hot plasma electron energy to the emitter than the corresponding decrease in the loss of ionization energy (carried by the ions) to the emitter. Therefore, these emitter sheath phenomena increase arc-drop. Within the limitations of the present isothermal thermionic converter formulation, all three of these phenomena (which become significant at low currents) steepen the current-voltage characteristic. At low current densities, the present theory shows that the collector sheath height decreases, resulting in a larger electron diffusion velocity than can be justified for the continuum model used in the plasma region. The result of lower performance at lower current is in agreement with experimental studies. At some current density which depends strongly on the emitter sheath conditions, the ignited mode is no longer self-sustaining and the arc is extinguished.

Fig. 1 is a schematic diagram of the cesium diode converter. The emitter is heated externally to temperature T_E which is typically 1750 K or higher, and the collector is cooled to temperature T_C which is typically 900–1100 K. The gap space d, or converter length, which is typically 0.25 mm, separates the emitter from the collector. The cesium reservoir, which is sometimes imbedded in the collector, is kept at temperature T_R to maintain the desired cesium pressure (typically 1 to 2 torr) in the gap. The electrical load is connected across the emitter and collector to produce power.

II. The Isothermal Electron Formulation

In this section the isothermal thermionic converter formulation is developed. The formulation is similar to that of Lam [7] but is generalized to eliminate the assumption of high sheaths which has previously been used to simplify the electron dynamics. Since both low-emitter and low-collector sheath heights are encountered as a consequence of ion reflection and trapped ions, the assumption

Manuscript received October 8, 1986; revised December 11, 1986. This work was supported by the Air Force Office of Scientific Research.

G. L. Main is with the School of Mechanical Engineering, Georgia Institute of Technology, Atlanta, GA 30332.

S. H. Lam is with the Mechanical and Aerospace Engineering Department, Princeton University, Princeton, NJ 08544.

IEEE Log Number 8613329.

0093-3813/87/0600-0309$01.00 © 1987 IEEE

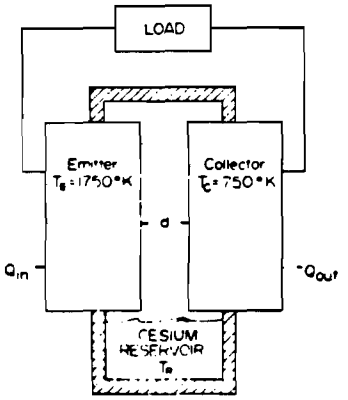

Fig. 1. The cesium diode converter.

of Boltzmann plasma electron distributions at the plasma-sheath interface must be abandoned. At both the emitter and collector, the low sheaths return few plasma electrons, leaving the distributions largely one sided. Furthermore, at the emitter sheath emitted electrons must be taken into account. Thus the ratio of electrons moving toward the sheath to the total density of electrons at the sheath edge is not 1/2, as in the Boltzmann assumption.

In Fig. 2 we define the potentials in the converter. All of the potentials are nondimensionalized by emitter temperature as follows:

$$\chi = \frac{q\phi}{kT_E} \tag{1}$$

where

- χ nondimensional potential,
- ϕ potential,
- q electron charge,
- k Boltzmann constant, and
- T_E emitter temperature.

We also use the following terminology for various potentials in the converter:

- Φ_E emitter work function,
- $\Delta\chi$ back sheath height,
- $\Delta\chi_s$ reflective potential,
- χ_E emitter sheath height,
- $\Delta\chi_p$ plasma potential drop,
- V_d arc-drop,
- χ_C collector sheath height,
- Φ_C collector work function, and
- V_{out} converter output voltage.

Inspection of Fig. 2 immediately yields the following relations:

$$V_d = V_{out} - (\Phi_E - \Phi_C) - \Delta\chi \tag{2}$$

$$V_d = (\chi_C - \chi_E) - \Delta\chi_p. \tag{3}$$

The Richardson current density of electrons from the emitter is

$$J_R\left(\frac{A}{cm^2}\right) = 120\, T_E^2(K^2) \exp(-\Phi_E). \tag{4}$$

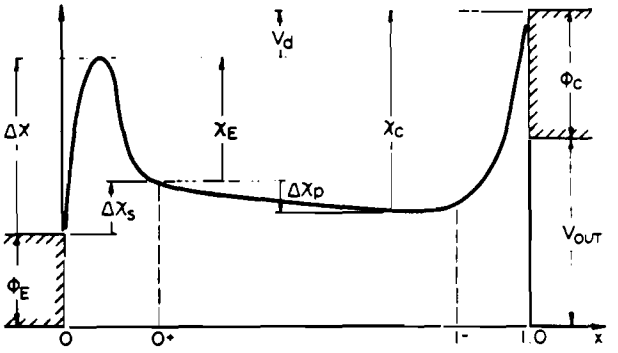

Fig. 2. The potential distribution in the converter.

The emitted current density which crosses the emitter sheath potential peak into the converter plasma region is

$$J_E = J_R \exp(-\Delta\chi), \qquad \Delta\chi > 0$$

$$J_E = J_R, \qquad \Delta\chi \le 0. \tag{5}$$

We also define the net current density through the converter J and the normalized current density

$$j = \frac{J}{J_E}. \tag{6}$$

We have assumed for convenience that the ion contribution to net current is negligible because the cesium-ion-to-electron-mass ratio is enormous. Ions will typically contribute no more than 1 percent of the net current. Electron temperature is nondimensionalized as

$$\tau = \frac{T_e}{T_E} \tag{7}$$

where T_e is the plasma electron temperature which, in this section, is constant by the isothermal assumption. Finally, we have the thermal speeds:

$$a_e = \sqrt{\frac{8kT_e}{\pi m}} \tag{8}$$

$$a_E = \sqrt{\frac{8kT_E}{\pi m}}. \tag{9}$$

The isothermal formulation is developed from here in the same way as the general formulation except that we take full advantage of the isothermal assumption by looking only at the global conservation equations instead of the local ones used in the general formulation. We then assume that the transport properties, collision frequencies, and the ionization source coefficient are constant across the converter because of the isothermal assumption. Also, we find only the steady-state solution. We carry out this development by deriving the global conservation equations for the isothermal case (current, momentum, and electron energy) and then reducing these to a set of three simultaneous equations in the variables τ, χ_E, and χ_C. In some cases the actual calculations are carried out

using different variables when χ_E or χ_C are small or zero. In the case, for instance, of a single ion-repelling emitter sheath we use j because χ_E is zero. These equations are nonlinear and solved numerically using a positive definite Newton's method.

First, we consider conservation of current. The collector is assumed to emit nothing; therefore, at the plasma–collector sheath interface we have

$$J = \frac{a_e \alpha_1 n(1)}{2} e^{-\chi_C/\tau} \tag{10}$$

where α_1 is the fraction of the total plasma density at the collector sheath which is moving toward the collector and $n(1)$ is the total plasma density at the plasma–collector sheath interface. Because we continue to assume that the part of the plasma electron distribution coming into the collector sheath is Maxwellian, we can write α_1 as

$$\alpha_1 = \frac{1}{1 + \frac{2}{\sqrt{\pi}} \int_0^{\chi_C/\tau} e^{-u^2}\, du} \tag{11}$$

which takes into account the plasma electrons reflected by the collector sheath. We still assume that the plasma electron distribution coming into the collector sheath is Maxwellian and that it does not have any velocity shift because the sheath is expected to be electron repelling. In the limit of a high collector sheath, $\alpha_1 = 1/2$ and we have a fully Boltzmann distribution of electrons at the collector sheath edge. The situation at the emitter is more complex because the emitted electrons must be taken into account. We have the backscattered current density J_{BS} which is the plasma electron current density moving into the emitter:

$$J_{BS} = \frac{n(0) a_e \alpha_0}{2} \exp\left(-\frac{\chi_E}{\tau}\right) \tag{12}$$

where $n(0)$ is the total plasma density at the emitter sheath–plasma interface and α_0 is the fraction of total plasma density at the interface moving toward the emitter.

Continuity of electron current demands

$$J_E = J_{BS} + J \tag{13}$$

which can be written as

$$J_E = J\left(1 + \frac{n(0)\alpha_0}{n(1)\alpha_1} \exp\left(\frac{\chi_C - \chi_E}{\tau}\right)\right). \tag{14}$$

This can be rewritten using (3) and (6) as

$$j = \frac{1}{1 + \frac{n(0)\alpha_0}{n(1)\alpha_1} \exp\left(\frac{V_d + \Delta\chi_p}{\tau}\right)}. \tag{15}$$

The quantity α_0 can be written as

$$\alpha_0 = \sqrt{\frac{\pi}{2}}\, Q\left(\frac{1}{j} - 1\right) \exp\left(\frac{\chi_E}{\tau}\right) \tag{16}$$

where

$$Q = \frac{(u_e)_0}{\sqrt{\frac{kT_e}{m}}}$$

is the electron Mach number at the emitter. This is just an application of (13).

Electron energy conservation is developed by considering energy exchange with the emitter and collector and energy lost to ionization. Power carried into the plasma by emitted electrons is

$$P_E = J_E(2 + \Phi_E + \Delta\chi)\frac{kT_E}{q}. \tag{17}$$

Power returned to the emitter is

$$P_{BS} = (J_E - J)(2\tau + \Phi_E + \Delta\chi)\frac{kT_E}{q}. \tag{18}$$

Power flowing into the collector is

$$P_C = J(2\tau + \Phi_E + V_d + \Delta\chi)\frac{kT_E}{q}. \tag{19}$$

Ionization power loss is

$$P_{ion} = J_{ion} V_{fi} \frac{kT_E}{q} \tag{20}$$

where J_{ion} is the total ion current into both the emitter and collector, and V_{fi} is the first ionization energy. Conservation of electron energy is

$$P_E = P_{BS} + P_C + P_{ion} \tag{21}$$

which can be reduced to

$$\tau = 1 - \tfrac{1}{2} j V_d - \tfrac{1}{2} j_i V_{fi} \tag{22}$$

where $j_i = J_{ion}/J_E$. In the ignited mode τ is generally about 2 (T_E = 1750 K and T_e = 3000 K), consequently the arc-drop V_d is negative. In other words, the high plasma electron temperature is generated by resistance heating.

Finally, we consider electron and ion momentum. From electron momentum conservation, we find the potential drop in the plasma region. By adding the electron and ion momentum equations as in the general case, we find our diffusion equation and boundary conditions to which the sheaths contribute flux terms. When we introduce the ionization source term into this, we have the complete formulation. Electron momentum conservation is

$$0 = -\frac{dp_e}{dx} - qn\frac{d\psi}{dx} - \frac{a_e m n u_e}{\lambda_e} \tag{23}$$

where λ_e is electron mean-free path. Using $p_e = nkT_e$ and $J = qnu_e$, we can rearrange (23) into

$$J = -\frac{q\lambda_e}{m a_e}\left(kT_e\frac{dn}{dx} + nq\frac{d\psi}{dx}\right). \tag{24}$$

This can be further reduced by dividing by J_E and using $\xi = x/d$ where d is the converter gap thickness:

$$j = -\frac{\pi}{4}\frac{\lambda_e}{d}\frac{1}{\sqrt{\tau}n_E}\left(\tau\frac{dn}{d\xi} + n\frac{d\chi}{d\xi}\right). \tag{25}$$

Integration of this equation from the emitter sheath interface to the collector sheath interface yields

$$\Delta\chi_p = \tau \ln\left(\frac{n(1)}{n(0)}\right) + jR \tag{26}$$

where

$$R = \frac{4}{\pi}\frac{d}{\lambda_e}\sqrt{\tau}\int_0^1 \frac{n_E}{n(\xi)}\,d\xi. \tag{27}$$

The quantity R is the normalized plasma resistance.

The ion and electron momentum equations can be written

$$kT_e\frac{dn}{dx} = -qn\frac{d\psi}{dx} - \frac{mnu_e a_e}{\lambda_e} \tag{28a}$$

$$kT_i\frac{dn}{dx} = qn\frac{d\psi}{dx} - \frac{Mnu_i a_i}{\lambda_i} \tag{28b}$$

where λ_i is ion mean-free path and a_i is ion thermal speed:

$$a_i = \sqrt{\frac{8kT_E}{\pi M}}.$$

Addition of (28a) and (28b) yields

$$(kT_e + kT_i)\frac{dn}{dx} = -\left(\frac{a_e m}{\lambda_e}u_e + \frac{a_i M}{\lambda_i}u_i\right)n \tag{29}$$

which is ambipolar diffusion. Equation (29) is differentiated to become

$$(kT_e + kT_i)\frac{d^2n}{dx^2} + \frac{a_e m}{\lambda_e}\frac{d}{dx}(nu_e) + \frac{a_i M}{\lambda_i}\frac{d}{dx}(nu_i) = 0. \tag{30}$$

We assume recombination is negligible and the ionization source term is

$$\frac{d}{dx}(u_e n) = \frac{d}{dx}(u_i n) = Sn. \tag{31}$$

Using (31) in (30) yields

$$\frac{d^2n}{d\xi^2} + \left|\left(\frac{a_e m}{\lambda_e} + \frac{a_i M}{\lambda_i}\right)Sd^2\right| n = 0. \tag{32}$$

Equation (29) taken at the boundaries of the plasma (at the emitter and collector sheath interfaces) forms the plasma boundary conditions

$$\left(\frac{dn}{d\xi}\right)_0 = \beta_0 n_0$$

$$\left(\frac{dn}{d\xi}\right)_1 = \beta_1 n_1 \tag{33}$$

where

$$\beta_0 = \frac{-d}{kT_e + kT_E}\left(\frac{a_e m}{\lambda_e}u_{e0} + \frac{a_i M}{\lambda_i}u_{i0}\right)$$

$$\beta_1 = \frac{d}{kT_e + kT_E}\left(\frac{a_e m}{\lambda_e}u_{e1} + \frac{a_i M}{\lambda_i}u_{i1}\right). \tag{34}$$

Equation (32) is written as

$$\frac{d^2n}{d\xi^2} + A^2(\tau)\,n = 0 \tag{35}$$

where

$$A^2(\tau) = d^2S\left(\frac{a_e m}{\lambda_e} + \frac{a_i M}{\lambda_i}\right) \tag{36}$$

where $A(\tau)$ is the ionization coefficient and is found from consideration of ionization kinetics of the cesium according to Lawless [8]. Its solution for n is

$$n(\xi) = B\sin(A\xi + C) \tag{37}$$

where B and C are constants of integration and $A = A(\tau)$. The quantities β_0 and β_1, which are the boundary conditions for (37), can be written as functions of τ, χ_E, χ_C, and $\Delta\chi_s$:

$$\beta_0 = \beta_0(\tau, \chi_E, \chi_C, \Delta\chi_s)$$

$$\beta_1 = \beta_1(\tau, \chi_E, \chi_C, \Delta\chi_s). \tag{38}$$

When there is no reflection, β_0 and β_1 are both large, i.e.:

$$\beta_0 = O\left(\frac{d}{\lambda_i}\right), \qquad \beta_1 = O\left(\frac{d}{\lambda_i}\right).$$

Significant reflection on the emitter side reduces β_0 and it may indeed attain negative values for sufficiently strong reflection.

The density equation (35) with the boundary conditions β_0 and β_1 is a linear eigenvalue problem; its solution yields A and C as functions of β_0 and β_1. The calculated results are shown in Fig. 3. Since $A(\tau)$ is a function of τ from the ionization kinetics, the value of τ is thus determined by a function of β_0 and β_1. The plasma resistance R also can be expressed in terms of functions of β_0 and β_1 through A and C using (27):

$$R = \frac{4}{\sqrt{2\pi}}\frac{d}{\lambda_e}\tau\frac{\sin C}{A}\ln\left(\frac{\tan\left(\frac{A+C}{2}\right)}{\tan\left(\frac{C}{2}\right)}\right). \tag{39}$$

The sheath results which provide j, Q, β_0, and β_1, complete the isothermal formulation. The sheath theory used is an exact solution to the Poisson equation and collisionless Boltzmann equation for warm plasma ion distribution with a 10 percent of Bohm speed cutoff velocity to approximate the effect of the collisional presheath [6]. The results are summarized below. The quantities β_0, β_1, Q,

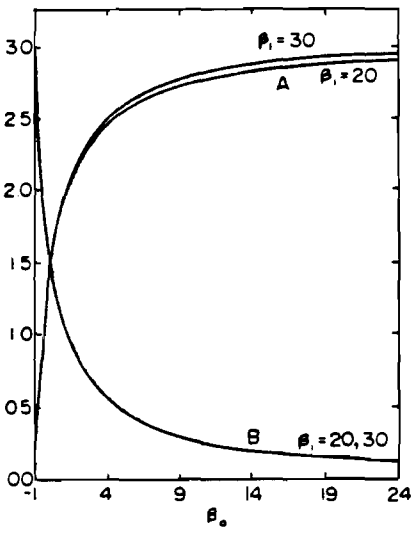

Fig. 3. The eigenvalue problem.

and j are found from the sheath calculations as functions of τ, χ_E, χ_C, and $\Delta\chi_s$, i.e.:

$$\beta_0 = \beta_0(\tau, \chi_E, \chi_C, \Delta\chi_s)$$

$$\beta_1 = \beta_1(\tau, \chi_E, \chi_C, \Delta\chi_s)$$

$$Q = Q(\tau, \chi_E, \chi_C, \Delta\chi_s)$$

$$j = j(\tau, \chi_E, \chi_C, \Delta\chi_s).$$

From the eigenvalue problem for the plasma density we then find

$$A(\tau) = A(\beta_0, \beta_1). \tag{40}$$

From the continuity equation for current we find

$$\chi_C - \chi_E = \tau \ln\left(\frac{\sin(A + C)}{\sin(C)}\right) + \tau \ln\frac{\alpha_1}{\alpha_0} + \tau \ln\left(\frac{1}{j} - 1\right) \tag{41}$$

and from the electron momentum equation we find

$$\chi_C - \chi_E = \tau \ln\left(\frac{\sin(A + C)}{\sin(C)}\right) + jR + \frac{2(\tau - 1)}{j} - \frac{j_i}{j} V_{fi}. \tag{42}$$

These three previous equations determine χ_E, χ_C, and τ when $\Delta\chi_s$ is given. This set of equations is valid for all $\Delta\chi_s$. Even in the case of $\Delta\chi_s \leq 0$ when there is no reflection, the calculations differ from previous isothermal calculations because the Boltzmann assumption on the electrons is not used as indicated by the presence of α_0 and α_1.

III. Calculated Results for Ion Reflection and Trapped Ions

In this section we develop isothermal solutions for the thermionic converter with the emitter sheath phenomena of ion reflection, trapped ions, and surface emission ions included. Emitter sheath effects on thermionic converter performance can be divided into two categories: 1) changes in net ion flux rate into the sheath which affect plasma density directly; and 2) changes in sheath potential distribution which affect the exchange of "hot" plasma electrons for "cold" emitter ions directly. A decreased influx of ions into the sheath, which occurs for all three emitter sheath phenomena, increases the plasma density at the neutral plasma emitter sheath interface. Theoretical intuition suggests that an increased plasma density at the emitter would benefit performance by reducing resistance through the plasma and therefore reducing arc-drop. However, this is not the case. While the plasma density at the emitter increases slightly, plasma density at the collector decreases. Consequently, total resistance increases.

TABLE I
Isothermal Solution Conditions

CASE 1	CASE 2
T_E = 1750 K	T_E = 1750 K
T_C = 750 K	T_C = 750 K
p_{cs} = 1 torr	p_{cs} = 1 torr
d = 10 mil	d = 10 mil
ϕ_E = 2.12 eV	ϕ_E = 2.67 eV
ϕ_C = 1.60 eV	ϕ_C = 1.60 eV
J_R = 20 amp/cm^2	J_R = 7.57amp/cm^2
J_{es+} = 1.80x10^{-5} amp/cm^2	J_{es+} = 2.10x10^{-3} amp/cm^2

All three of these phenomena increase in significance as net current density through the converter is reduced. Each of these reduces the net ion loss rate to the emitter and consequently increases arc-drop (therefore, degrading performance at low current densities). This increase in arc-drop is in agreement with the same tendency in the experimental results. However, the experimental results also show a plateau (of low arc-drop) at low current density. This plateau occurs at a current density corresponding to significant surface ion emission and is therefore thought to occur as surface emission replaces volume ionization as the dominant source of plasma ions. Unfortunately, the theoretical calculations cannot be carried into this region because the collisionless collector sheath matching (to the neutral plasma) fails.

To provide a realistic framework for presenting the results, we consider the converter conditions shown as case 1 in Table I. Case 2 is shown because it has the largest surface emission of any typical thermionic converter operating condition (because the work function is high and the temperature is also high). Instead of presenting case 2 separately, we demonstrate the effects of surface emis-

sion in case 1 by increasing the surface emission by a factor of 100 thereby bringing it up to the level in case 2. The net current density at which surface emission becomes significant can be estimated by multiplying J_{es+} by the square root of the ion to electron mass ratio (approximately 500). In case 1, this means that surface emission becomes significant at $J = 0.01$ A/cm^2 while in case 2 significant surface emission begins at $J = 1.0$ A/cm^2.

IV. Effects of Ion Reflection

In this section we discuss the isothermal results for case 1 with ion reflection, but without trapped ions and with the small amount of surface emission ions of case 1. Fig. 4 is the *CV* diagram for this case.

The dotted line extending upward from point A is the single electron-repelling emitter sheath solution. However, we have not taken recombination or the Schottky effect into account in this isothermal formulation which are expected to become important at current densities near J_R. The interest of this paper begins at point *A*, where the single sheath doubles over. Between points *A* and *B*, where the back sheath height $\Delta\chi$ is less than the sheath height χ_E, the emitter sheath is nonreflecting. In this region the sheath heights χ_E and χ_C remain constant while the plasma density is proportional to net current J (the normalized plasma density nc/J is constant). Only the back sheath height $\Delta\chi$ changes and the *CV* curve in this region is Boltzmann (the arc-drop is constant). Beginning at point *B* and continuing to point *C*, the double emitter sheath reflects plasma ions because the back sheath is larger than the front sheath; in other words, the reflective potential $\Delta\chi_s = \Delta\chi - \chi_E$ is positive. The result is that net ion loss rate into the sheath $\bar{u}$ decreases and that arc-drop increases. The quantity $\bar{u}$ is defined as the mean ion velocity into the sheath normalized by the Bohm speed, $\sqrt{kT_e/M}$. The dotted curve *BD* is the same double sheath except that it assumes no ions are reflected; therefore, $\bar{u}$ is constant and arc-drop is constant. The two curves *BC* and *BD* are almost indistinguishable because the increase in arc-drop is small until the net current density is extremely small. The reason for this is that the shift speed is approximately $u_s = 2$, and, therefore, a large increase in reflective potential is required to change $\bar{u}$ significantly (the half-reflection point is $\Delta\chi_s = 4.0$ or approximately $J = J_R \exp(-4) = 0.4$ A/cm^2). The shift speed u_s is defined as the velocity at the peak of the incoming ion distribution again normalized by the Bohm speed.

The curve *EF* is the single electron-repelling emitter sheath case. It is the limiting case for large amounts of trapped ions in which the double sheath peak has been completely suppressed by the trapped ions. For this case, the emitter sheath solutions gives $u_s = 0^6$. This curve is not topologically connected to the curve *ABC*; it will be shown in Section V that trapped ions move *ABC* toward the single ion-repelling sheath case. The curve is much steeper (a faster increase in arc-drop) in this case because $u_s = 0$ (the half-point in ion reflection is approximately J = 8 A/cm^2). Curve *EG* is the single ion-repelling case assuming no reflection and is therefore a Boltzmann line with constant arc-drop.

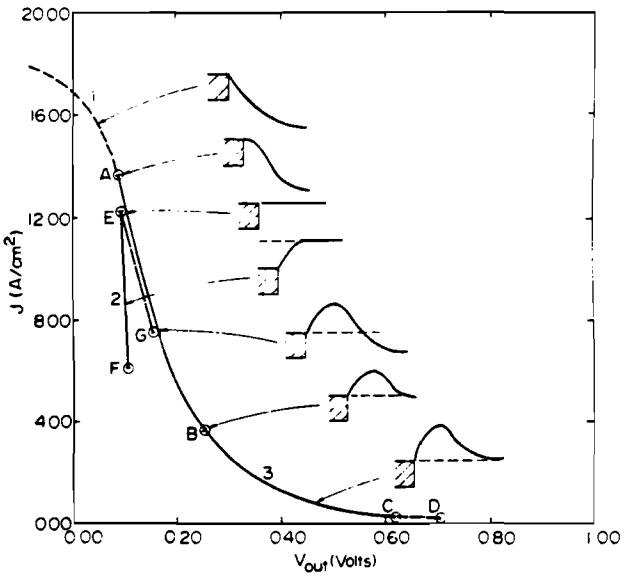

Fig. 4. *CV* diagram with ion reflection for case 1.

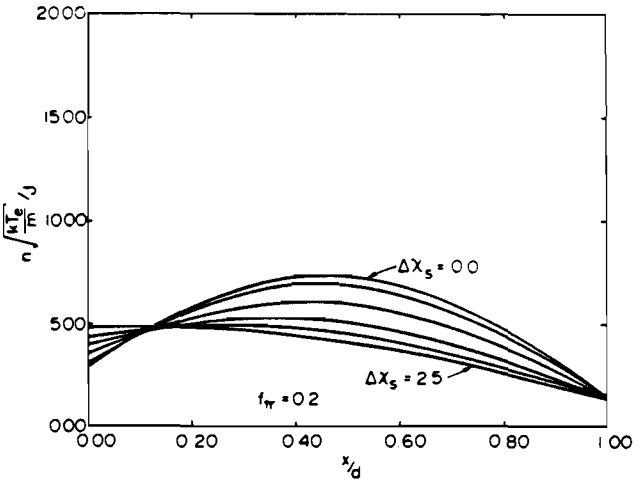

Fig. 5. Normalized plasma density with reflection.

At points *F* and *C* the solutions fail at the collector. The explanation for this failure is best given by examining Figs. 5–8.

Fig. 5 is the normalized plasma density through the converter gap. The highest curve with no reflection $\Delta\chi_s = 0$ has the largest plasma density at the collector but the lowest plasma density at the emitter. Ion reflection, which decreases the ion loss rate to the emitter, raises the plasma density at the emitter but lowers the plasma density at the collector. The lower plasma density at the collector forces a smaller collector sheath height to pass the net current density. This can be seen from (10). Fig. 6 is the potential through the converter under the same reflection conditions as in Fig. 5. In Fig. 6 the first two spaces on the left make up the double emitter sheath, and the last space on the

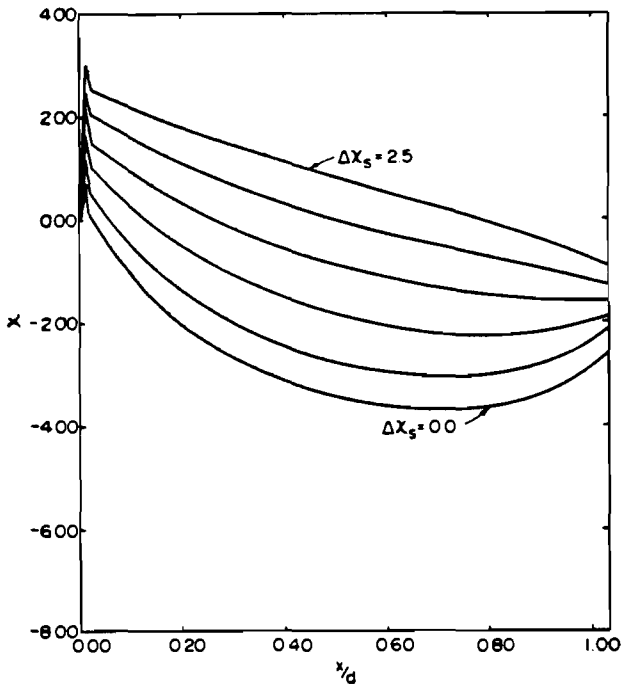

Fig. 6. Potential distribution in the converter.

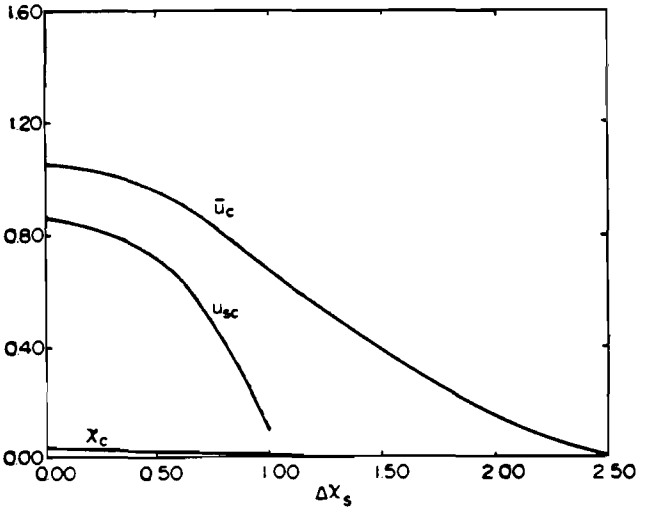

Fig. 7. Collector sheath failure.

right is the collector sheath. The region between the two sheaths is the neutral plasma region. In the no-reflection case, it can be seen that the potential has a pronounced well in the middle. This is the result of the large plasma density in the middle. As reflection increases, this well disappears on the collector side of the plasma because resistive drop there (due to low plasma density) increases to the degree that it is greater than the ambipolar rise (due to decreasing density toward the collector). Simultaneously with plasma potential gradient at the collector becoming negative, the collector sheath goes toward zero height. Fig. 7 shows the critical collector sheath quantities as the collector sheath failure occurs. Collector sheath height χ_C goes toward zero, the shift speed u_{sc} goes

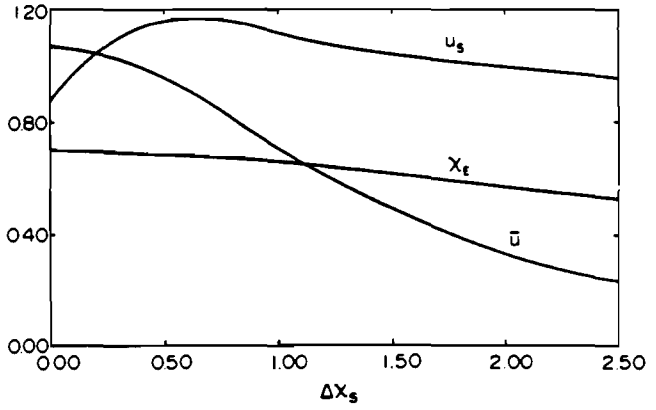

Fig. 8. Emitter sheath during reflection.

toward negative infinity, and the ion loss rate to the collector $\bar{u}_c$ is driven to zero. The two preceding quantities $\bar{u}_c$ and u_{sc} are defined at the collector sheath as $\bar{u}$ and u, were at the emitter sheath. Fig. 8 shows the changes in the emitter sheath height, ion shift speed and ion loss rate. When the collector sheath failure occurs, the ion loss rate to the collector is zero ($\bar{u}_c = 0$) and the corresponding plasma ion distribution at the collector is bunched at zero velocity ($u_{sc} = -\infty$). While the mathematics hold self-consistantly until $\bar{u}_c = 0$, the physics is clearly poor at this point because $\bar{u}_c = 0$ demands that the plasma ions at the collector have zero energy (zero temperature and zero mean velocity). An estimate of when the physics becomes poor is $u_{sc} = 0$. At this point the net ion loss rate is close to the thermal speed. A second physical difficulty that occurs with collector sheath failure is that the electron Mach number there Q_c (from (10)) becomes

$$Q_c = \sqrt{\frac{2}{\pi}}$$

because the collector sheath height approaches zero (actually about 0.001). In the present continuum formulation of the plasma region, it was assumed in (13) that Q_c is small so that the electron momentum term $u_e du_e/dx$ can be neglected.

One could take the solution below the collector sheath failure point if $\bar{u}_c$ could attain negative values or if Q_c could attain values larger than $\sqrt{2/\pi}$. There is no physical basis for assuming that $\bar{u}_c$ can become negative since the collector emits nothing. However, there is a physical basis for allowing Q_c to be larger than $\sqrt{2/\pi}$ (an electron distribution shift) as can be seen in Fig. 6: the potential drop nearing the collector becomes progressively more electron accelerating as the collector sheath fails, and, therefore, the electron distribution should be shifted as the ion distribution is in an electron-repelling sheath. However, this would clearly invalidate the assumption that the electron momentum term is negligible. Therefore, the momentum term must be added to explore further in this direction and this has not been done because of the resulting complexity in the equations.

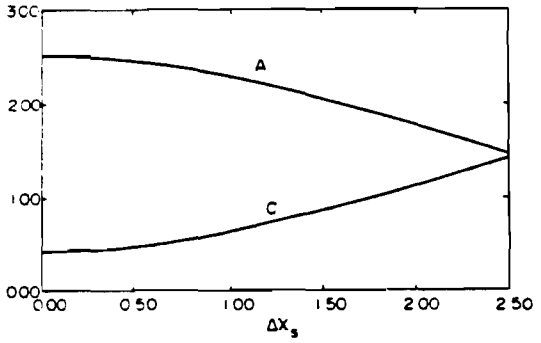

Fig. 9. Ionization coefficient A and C.

Comparison of Fig. 7 to Fig. 8 at the collector sheath failure point ($\Delta\chi_s = 2.5$, $u_c = 0$) shows that the ion loss rate to the emitter is positive. At this point the plasma is still ignited and generating ions as can be seen from Figs. 9 and 10. The ionization coefficient A has dropped by 50 percent, but the plasma electron temperature has dropped by only 5 percent. Finally, we note in Fig. 11 that the normalized plasma resistance R has risen by almost 100 percent. This is responsible for the increase in arc-drop and the decrease in performance. Plasma resistance increases in response to reflection because the loss of plasma electron energy to the emitter is more important than the loss of ionization energy to the emitter. Ion reflection at the emitter increases the normalized plasma density there, and consequently increases the normalized loss of plasma electron energy there. The basis of this can be seen from conservation of electron energy (22):

$$\tau = 1 - \tfrac{1}{2}jV_d - \tfrac{1}{2}j_iV_{fi}. \tag{43}$$

The ion energy loss term is generally small compared to the electron energy loss term:

$$\frac{\tfrac{1}{2}j_iV_{fi}}{\tfrac{1}{2}jV_d} = \frac{J_i}{J}\frac{V_{fi}}{V_d} \approx O(0.02). \tag{44}$$

Therefore, we take the electron energy equation as

$$\tau = 1 - \tfrac{1}{2}jV_d. \tag{45}$$

Since τ is nearly constant (because of the ionization kinetics), the product jV_d is nearly constant. Ion reflection decreases j (because the normalized plasma density increases) and therefore increases arc-drop V_d (makes V_d a more negative number).

If the equations are reformulated in such a way as to be valid past the collector sheath failure point, then we can eventually expect to see a decrease in arc-drop and a low-current plateau as the electron temperature approaches 1 (the ignited plasma is extinguished and the ionization source is surface emission). This can be seen from (43). However, as we see, the collector failure occurs before τ has dropped more than 5 percent. Consequently, we do not see any plateau or decrease in arc-drop as net current density is decreased in the present calculations.

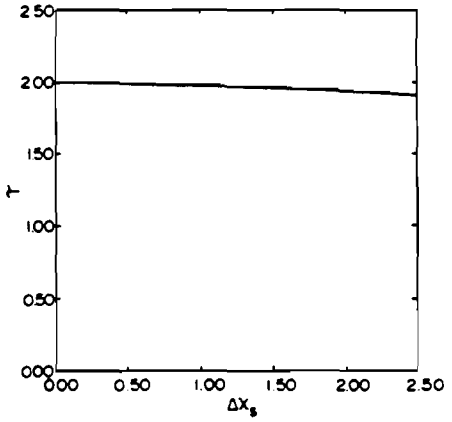

Fig. 10. Plasma electron temperature.

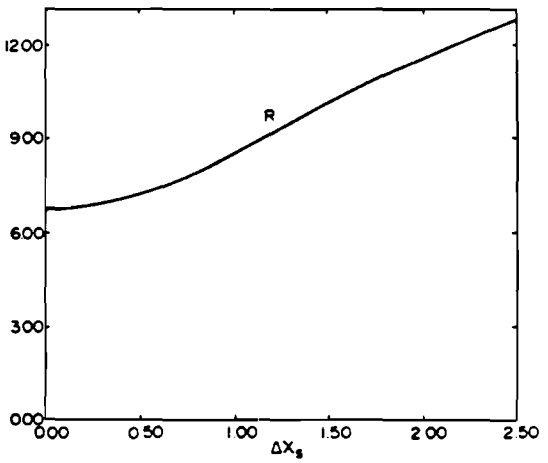

Fig. 11. Normalized plasma resistance.

V. Effects of Trapped Ions

Fig. 12 shows the effect of trapped ions on the CV characteristics. In this section the trapped ion distribution is assumed to have the temperature of plasma ion distribution, and 100-percent trapped ions ($f_{it} = 1.0$) is defined to complete the ion distribution at the double emitter sheath peak such that one has a Maxwellian distribution there. Based on physical reasoning about the trapping mechanism, one expects on the order of 10. Also, some trapping calculations have been done for approximate sheath formulations [9], [10] which support this.

Curve $AHIJ$ is the CV characteristic for $f_{it} = 0.10$. At point A there cannot be any trapped ions since the back sheath height $\Delta\chi$ is zero. Therefore, the trapped CV merges into the nontrapped curve there. The actual amount of trapped ions on the $f_{it} = 0.10$ curve increases from zero at point A to the full 10 percent of a thermal distribution at point H where the back sheath height $\Delta\chi$ is equal to the sheath height χ_E. The shift speed increases on AH from 1.95 to 3.00. This corresponds to what is seen in Fig. 12 where $\Delta\chi < \chi_E$.

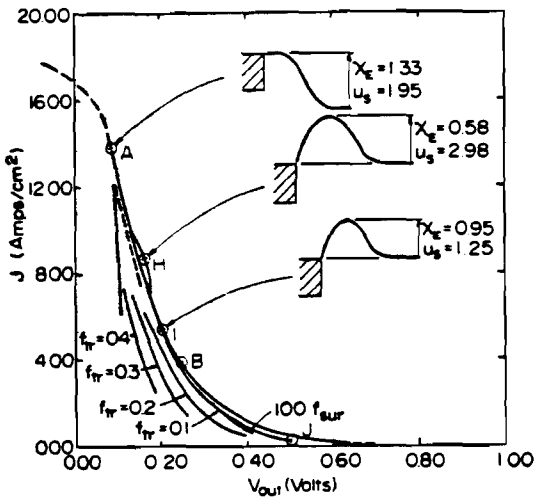

Fig. 12. *CV* diagram with trapped ions and surface emission.

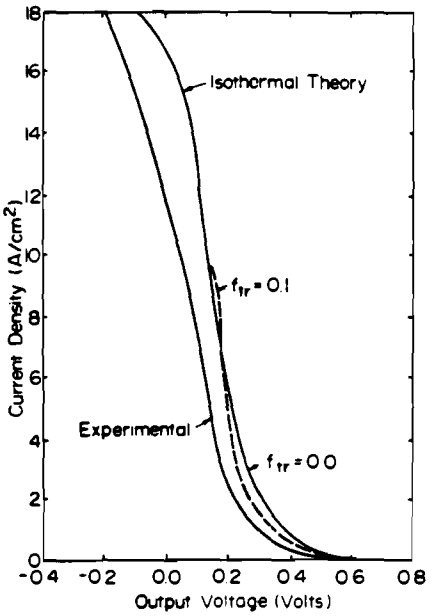

Fig. 13. Isothermal and experimental *CV* diagrams.

The rise in shift speed has been limited to 3.00. This limit is placed on the shift speed because a sheath with height of about 1.0 should not have a presheath region capable of shifting the entire distribution so far. In fact, limiting the shift speed is equivalent to increasing the cut-off speed for the ion distribution function.

The arc-drop decreases as a result of the increase in u_s and the consequent increase in the net ion loss rate to the emitter. A "hump" can be seen on *AH* where the shift speed hits 3.00. The arc-drop is lowest on this "hump" because the shift speed is at its maximum of 3.00. Between points *H* and *I* the back sheath height remains equal to the sheath height, $\Delta\chi - \chi_E = \chi_s = 0$. On this segment, u_s decreases to 1.25, therefore increasing arc-drop.

From point *I* to point *J*, the shift speed remains constant at 1.25 and the ion loss rate decreases because of reflection. The other trapped cases $f_{tr} = 0.2$, 0.3, and 0.4 have not been connected because they hit the 3.00 maximum shift speed much sooner than in the $f_{tr} = 0.1$ case.

Point *J* is the collector sheath failure point. Each of the $f_{tr} = 0.2$, 0.3, and 0.4 curves begins at $\Delta\chi_s = 0$ and ends at the collector sheath failure point. It should be noted that each of the trapped ion curves fails at a higher current than the last because the shift speed is lower.

VI. Effects of Emitter Surface Emission

Fig. 12 shows the effect of surface emission on the $f_{tr} = 0.10$ curve; surface emission is added by multiplying the actual small amount of surface emission in case 1 by a factor of 100. This brings the surface emission up to the level in case 2, making it significant at $J = 1.0$ A/cm^2. It can be seen that surface emission increases arc-drop; it does so in exactly the same way as reflection or trapped ions do—it decreases the net loss rate of ions to the emitter.

VII. Comparison with Experimental Results and Conclusions

Fig. 13 superimposes the isothermal results of Fig. 12 on the experimental results for a cesium reservoir temperature of 551 K which produces a 1-torr neutral cesium pressure. The experimental results are from [11]. The point of this comparison is that the steepness of the *CV* characteristic in the experimental converters can be explained by a decreasing ion loss rate to the emitter. We have shown that all three of the expected emitter sheath phenomena decrease the ion loss rate to the emitter. We cannot calculate the amount of trapped ions in a collisionless sheath without knowledge of the collisional processes. However, the experimental *CV* suggests that if the amount of trapped ions (f_{tr}) increases from 0 percent at $J = 14$ A/cm^2 (the double sheath formation point) to 10 percent at $J = 2$ A/cm^2, then the steepness could result from trapped ions reducing the ion loss rate to the emitter. Since these percentages are based on a thermal distribution of ions, they seem physically reasonable. Unfortunately, the collector sheath failure prevents us from going to the point in the calculations where τ drops enough to make surface emission the source of ions.

The experimental curve is nearly a constant 0.05 V below the isothermal result ($f_{tr} = 0.10$) except at high current densities and at the "hump." Comparison of the curves at high current density is not valid since neither the Schottky effect nor recombination has been included. The Schottky effect is important above 12 A/cm^2 in this case because the emitter sheath is single electron repelling (to the plasma) and therefore puts a strong electric field against the emitter with the appropriate sign. Recombination is also potentially important because the plasma density scales with current density, and at high current densities the plasma density in the middle of the converter approaches the Saha density. The 0.05-V difference may or may not be explained by a discrepency in the assumed collector work function. At 750 K the collector emits essentially nothing and therefore any change in the collector work function directly affects output voltage. If the collector work function were in fact 1.65 instead of 1.60 V, then the isothermal result would lie nearly on top of the

experimental result. We have not adjusted the assumed collector work function so as to illustrate the importance of it and therefore the importance of the surface physics of the adsorbed cesium layer. The "hump" should not be taken as an expected experimental result since it results from the interaction of the trapped ions with the plasma–emitter sheath interface. Instead it should be taken as a second reason (in addition to the cutoff of the ion distribution) for further study of the matching region between the collisionless sheath and the neutral plasma.

REFERENCES

[1] G. L. Main and S. H. Lam, in *Proc. 1982 Int. IEEE Conf. Plasma Sci.* (Ottawa, Canada), May 1982, p. 118.
[2] G. L. Main and S. H. Lam, in *Proc. Int. Energy Conversion Eng. Conf.* (Orlando, FL), Aug. 1983, p. 215.
[3] L. Lundgren, *J. Appl. Phys.*, vol. 58, p. 142, 1985.
[4] L. Lundgren, *J. Appl. Phys.*, vol. 58, p. 4032, 1985.
[5] E. R. Harrison and W. B. Thompson, *Proc. Phys. Soc. London*, vol. 74, p. 145, 1959.
[6] G. L. Main, Ph.D. dissertation, Princeton Univ., Princeton, NJ, 1984.
[7] S. H. Lam, "Preliminary report on plasma arc-drop in thermionic converters," Princeton Univ., Princeton, NJ, 1976.
[8] J. L. Lawless, Ph.D. dissertation, Princeton Univ., Princeton, NJ, 1980.
[9] C. Warner and L. K. Hansen, Tech. Summary Rep. AI-69-112 Contract NONR-3192(00), Dec. 1969.
[10] D. R. Wilkins and D. J. Rush, presented at Electrostatic Sheath Phenomena in Thermionic Converters, IEEE Thermionic Converter Specialist Conf., 1970.
[11] Thermo-Electron Corp., Waltham, MA, DOE Advanced Thermionic Tech. Program, Progress Rep. 48, Sept. 1981.

ASYMPTOTIC SHEATH THEORY

The Asymptotic Sheath Theory developed under this grant is set forth in the following paper.

Reprinted from

The Physics of Fluids

Volume 30 June 1987 Number 6

Asymptotically correct collisional presheaths

Geoffrey L. Main
School of Mechanical Engineering, Georgia Institute of Technology, Atlanta, Georgia 30332

pp. 1800-1809

a publication of the American Institute of Physics

Asymptotically correct collisional presheaths

Geoffrey L. Main
School of Mechanical Engineering, Georgia Institute of Technology, Atlanta, Georgia 30332

(Received 16 April 1986; accepted 19 February 1987)

Few exact solutions for collisional presheaths exist because of the difficulty of simultaneously satisfying both the collisional Boltzmann equation and the Poisson equation. The exact solutions that do exist are for very specialized collision terms such as constant cross-section charge exchange with cold neutrals. The present paper presents an asymptotic method which is applicable to a variety of collision terms and is applied in particular to constant collision frequency charge exchange with noncold neutrals. Constant collision frequency and constant cross-section collision with cold neutral results are also presented. The first-order terms for the presheath potential rise and ion distribution functions are calculated and it is shown that second- and higher-order terms can be calculated using a multiexponential expansion for presheath potential rise. The first-order cold neutral constant cross-section results correspond well to the exact solution. The calculated presheath potential rises are of the order expected from the Bohm criterion, and in some of the specialized cold neutral cases, exactly $kT_e/2$. The presheath potential rise is reduced by a neutral plasma potential gradient which accelerates ions toward the presheath. In all cases the collisional presheath is asymptotically matched to both the neutral plasma and the collisionless sheath.

I. INTRODUCTION

The majority of plasma–surface interaction work matches a neutral plasma to a collisionless sheath without detailed consideration of a collisional presheath. However, the collisional presheath structure is of great interest. Sheath theory, beginning with Bohm,[1] tends to assume that the plasma ion distribution is cold so that a minimum presheath potential rise may be calculated, which makes the collisionless sheath self-consistent. Harrison and Thompson[2] generalize the Bohm criterion to noncold ion distributions; however, the result is sensitive to the density of the low energy tail of the ion distribution, which in turn is strongly affected by the collisional presheath. And, a second difficulty in the absence of a collisional presheath is that the collisionless sheath and the surface beyond it may return no ions or a nonthermal distribution of ions which the collisional presheath must match to the neutral plasma region.

Some exact solutions exist for presheaths; notable is the work of Ecker and Kanne[3] and Riemann,[4] who derive exact solutions for collision terms based on charge exchange with cold neutrals and Emmert *et al.*,[5] who derive an exact collisionless solution in which there is an ionization source. In the present paper an asymptotically correct collisional presheath theory is developed which can be applied to a less restrictive range of collision terms. Potential in the presheath is expanded as a multiexponential series and the distribution functions are expanded in terms of presheath potential rise. First-order approximations are calculated for both constant collision frequency and constant cross-section charge exchange collisions.

II. FIRST-ORDER ASYMPTOTIC POTENTIAL FORMULATION

In this section it is assumed that the potential in the collisional presheath is of the form

$$U = U_0 + \Delta U = \alpha x + e^{\beta x}, \tag{1}$$

where $U_0 = \alpha x$ is the assumed linear potential in the neutral plasma and $\Delta U = e^{\beta x}$ is the additional potential rise in the collisional presheath, as shown in Fig. 1. In this paper the convention used is that $U = q\phi$, where q is the electron charge and ϕ is potential in electron volts so that U has units of energy. In addition, potential is defined in the reverse of the usual sign convention so that increasing potential repels electrons. With these conventions, the Boltzmann equation can be written as

$$\frac{dU}{dx}\left(v\frac{\partial f}{\partial U} \pm \frac{1}{m}\frac{\partial f}{\partial v}\right) = \left(\frac{\partial f}{\partial t}\right)_c. \tag{2}$$

In Eq. (2) and those following, the $\pm$ denotes the sign of the charged species in question; the upper sign refers to positively charged ions and the lower sign to electrons. The Boltzmann equation is expressed in terms of ΔU, which will be the expansion variable in the presheath:

$$v\beta\Delta U\frac{\partial f}{\partial \Delta U} \pm \frac{1}{m}(\beta\Delta U + \alpha)\frac{\partial f}{\partial v} = \left(\frac{\partial f}{\partial t}\right)_c. \tag{3}$$

The distribution function is then expanded as

$$f = f_0(v) + \Delta U f_1(v) + \Delta^2 f_2(v) + \cdots, \tag{4}$$

so that the derivatives are

$$\frac{\partial f}{\partial \Delta U} = f_1(v) + 2\Delta U f_2(v) + 3\Delta U^2 f_3(v) + \cdots \tag{5}$$

and

$$\frac{\partial f}{\partial v} = \frac{\partial f_0}{\partial v}(v) + \Delta U\frac{\partial f_1}{\partial v}(v) + \Delta U^2\frac{\partial f_2}{\partial v}(v) + \cdots. \tag{6}$$

Substitution of (5) and (6) into the Boltzmann equation (3) yields the terms

 0031-9171/87/061800-10$01.90

$$1: \quad \pm\frac{\alpha}{m}\frac{\partial f_0}{\partial v}(v) = \left[\left(\frac{\partial f}{\partial t}\right)_c\right]_1, \tag{7a}$$

$$\Delta U: \quad v\beta f_1(v) \pm \frac{\beta}{m}\frac{\partial f_0}{\partial v}(v) \pm \frac{\alpha}{m}\frac{\partial f_1}{\partial v}(v) = \left[\left(\frac{\partial f}{\partial t}\right)_c\right]_{\Delta U}, \tag{7b}$$

$$\Delta U^2: \quad 2v\beta f_2(v) \pm \frac{\beta}{m}\frac{\partial f_1}{\partial v}(v) \pm \frac{\alpha}{m}\frac{\partial f_2}{\partial v}(v) = \left[\left(\frac{\partial f}{\partial t}\right)_c\right]_{\Delta U^2}, \tag{7c}$$

$$\vdots$$

$$\Delta U^n: \quad nv\beta f_n(v) \pm \frac{\beta}{m}\frac{\partial f_{n-1}}{\partial v}(v) \pm \frac{\alpha}{m}\frac{\partial f_n}{\partial v}(v) = \left[\left(\frac{\partial f}{\partial t}\right)_c\right]_{\Delta U^n}. \tag{7d}$$

The quantity β, representing the presheath potential rise, is determined from the Poisson equation

$$\frac{d^2U}{dx^2} = 4\pi q^2\left(\int_{-\infty}^{\infty} f_i(v,\Delta U)dv - \int_{-\infty}^{\infty} f_e(v,\Delta U)dv\right), \tag{8}$$

where q is the electron charge. It is assumed that the ions are singly ionized for simplicity. The Poisson equation (8) is expanded as

$$\beta^2\Delta U = 4\pi q^2\left[\left(\int_{-\infty}^{\infty} f_{i1}(v)dv - \int_{-\infty}^{\infty} f_{e1}(v)dv\right)\Delta U + \left(\int_{-\infty}^{\infty} f_{i2}(v)dv - \int_{-\infty}^{\infty} f_{e2}(v)dv\right)\Delta U^2 + \cdots\right], \tag{9}$$

where charge neutrality at $\Delta U = 0$ has eliminated the terms containing f_{i0} and f_{e0}:

$$n_0 = \int_{-\infty}^{\infty} f_{i0}(v)dv = \int_{-\infty}^{\infty} f_{e0}(v)dv.$$

The quantity n_0 is the neutral plasma density of the asymptotic presheath, not of the neutral plasma.

III. FIRST-ORDER SOLUTION WITH A CONSTANT COLLISION FREQUENCY CHARGE EXCHANGE COLLISION TERM

The constant collision frequency charge exchange collision term is modeled as

$$\left(\frac{\partial f_i}{\partial t}\right)_c = \frac{1}{\tau n_n}\left(f_n(v)\int_{-\infty}^{\infty} f_i(u)du - f_i(v)\int_{-\infty}^{\infty} f_n(u)du\right), \tag{10}$$

where $f_n(v)$ is the neutral distribution and τ is the collision time. Previous work has assumed cold neutrals and results in an integral equation which is solvable only for constant collision cross section.[4]

A. Zero plasma potential gradient ($\alpha = 0$)

In this case Eqs. (7) become

$$\begin{aligned}
&1: \quad 0 = \frac{1}{\tau n_n}\left(f_n(v)\int_{-\infty}^{\infty} f_{i0}(u)du - f_{i0}(v)\int_{-\infty}^{\infty} f_n(u)du\right),\\
&\Delta U: \quad v\beta f_{i1}(v) + \frac{\beta}{m}\frac{\partial f_{i0}}{\partial v}(v) = \frac{1}{\tau n_n}\left(f_n(v)\int_{-\infty}^{\infty} f_{i1}(u)du - f_{i1}(v)\int_{-\infty}^{\infty} f_n(u)du\right),\\
&\quad\vdots\\
&\Delta U^n: \quad nv\beta f_{in}(v) + \frac{\beta}{m}\frac{\partial f_{i(n-1)}}{\partial v}(v) = \frac{1}{\tau n_n}\left(f_n(v)\int_{-\infty}^{\infty} f_{in}(u)du - f_{in}(v)\int_{-\infty}^{\infty} f_n(u)du\right).
\end{aligned} \tag{11}$$

Under the assumption that the neutral distribution is Maxwellian $f_n(v) = n_n\sqrt{m/2\pi kT}\ \exp(-mv^2/2kT)$, the solution to (11) is

$$\begin{aligned}
&f_{i0} = Cf_n(v),\\
&f_{i1}(v) = (1/kT)f_{i0}(v),\\
&\quad\vdots\\
&f_{in}(v) = (1/nkT)f_{i(n-1)}(v).
\end{aligned} \tag{12}$$

Thus

$$f_i(v,\Delta U) = Ce^{(\Delta U/kT)}f_n(v), \tag{13}$$

which is the expected result. In this case the mean ion velocity is zero throughout the collisional presheath since charge exchange collisions conserve ions and the mean ion velocity in the neutral plasma is zero. Thus, if $\alpha = 0$, constant collision frequency charge exchange collisions do not shift the ion distribution upward in velocity. This presheath can be matched to a collisionless sheath only if the collisionless sheath returns all the ions entering it from the collisional presheath.

With electron density assumed to follow

$$n_e(\Delta U) = n_0 e^{(-\Delta U/kT_e)},$$

the Poisson equation (9) yields, to first order,

$$\beta^2 = 4\pi q^2 n_0 (1/kT + 1/kT_e),$$

which is the length scale of the Debye length. Thus for $\alpha = 0$ the collisional presheath is not distinct from the collisionless sheath since there is no separate collisional presheath length scale.

B. Nonzero plasma potential gradient ($\alpha \neq 0$)

Under this condition there is a net flux of ions from the plasma into the sheath, which allows the construction of a collisional presheath that accelerates the ions and depopulates the ion distribution of returning ions. Thus the collisional presheath may be correctly matched to the collisionless sheath which returns no ions. In this case (7a) and (7b) can be written as

$$\frac{\alpha}{m}\frac{\partial f_0}{\partial v}(v) = \frac{1}{\tau n_n}[f_n(v)n_0 - n_n f_0(v)], \tag{14a}$$

$$v\beta f_1(v) + \frac{\beta}{m}\frac{\partial f_0}{\partial v} + \frac{\alpha}{m}\frac{\partial f_1}{\partial v}(v) = \frac{1}{\tau n_n}[f_n(v)n_1 - n_n f_1(v)]. \tag{14b}$$

The solution to Eqs. (14) are

$$f_0(v) = n_0 \exp\left(\frac{-mv}{\alpha\tau}\right)\frac{m}{\alpha\tau}\sqrt{\frac{m}{2\pi kT}}\int_{-\infty}^{v}\exp\left(-\frac{mu^2}{2kT}+\frac{mu}{\alpha\tau}\right)du \tag{15}$$

and

$$f_1(v) = \exp\left(-\frac{\beta m v^2}{2\alpha}-\frac{mv}{\alpha\tau}\right)\left[\int_0^v \exp\left(\frac{\beta m u^2}{2\alpha}+\frac{mu}{\alpha\tau}\right)\left[\frac{n_1 m}{\alpha\tau}\sqrt{\frac{m}{\alpha\pi kT}}\exp\left(\frac{mu^2}{2kT}\right)-\frac{\beta}{\alpha}\frac{\partial f_0}{\partial v}(u)\right]du + C\right], \tag{16}$$

where

$$n_0 = \int_{-\infty}^{\infty} f_0(v)dv \tag{17}$$

and

$$n_1 = \int_{-\infty}^{\infty} f_1(v)dv. \tag{18}$$

The constant of integration in (15) has been set so that f_0 goes to zero at $-\infty$; f_0 goes to zero at ∞ regardless of the constant of integration. Equation (17) is immediately satisfied by (15). The constant of integration C in (16) must be set so that (18), which represents self-consistency, is satisfied. It can be seen from (16) that f_1 goes to zero at $-\infty$ and ∞ regardless of the constant C. From (18), then

$$\begin{aligned} C = n_1\Bigg[1 - \int_{-\infty}^{\infty}\exp\left(-\frac{\beta m v^2}{2\alpha}-\frac{mv}{\alpha\tau}\right)\int_0^v \exp\left(\frac{\beta m u^2}{2\alpha}+\frac{mu}{\alpha\tau}\right)\frac{m}{\alpha\tau}\sqrt{\frac{m}{2\pi kT}}\exp\left(-\frac{mu^2}{2kT}\right)du\,dv\Bigg] \\ \times\left[\sqrt{\frac{2\pi\alpha}{m\beta}}\exp\left(\frac{m}{2\alpha\beta\tau^2}\right)\right]^{-1} + \left[\int_{-\infty}^{\infty}\exp\left(-\frac{\beta m v^2}{2\alpha}-\frac{mv}{\alpha\tau}\right)\int_0^v\frac{\beta}{\alpha}\exp\left(\frac{\beta m u^2}{2\alpha}+\frac{mu}{\alpha\tau}\right)\frac{\partial f_0}{\partial v}(u)du\,dv\right] \\ \times\left[\sqrt{\frac{2\pi\alpha}{m\beta}}\exp\left(\frac{m}{2\alpha\beta\tau^2}\right)\right]^{-1}. \end{aligned} \tag{19}$$

The exponential sheath rise β is determined from the Poisson equation under the simplifying assumption that

$$n_e = \int_{-\infty}^{\infty} f_e(v)dv = n_0\exp\left(-\frac{\Delta U}{kT_e}\right). \tag{20}$$

One might expect that the approximation should be $n_e = n_0\exp(-U/kT_e)$; however, this cannot be true in the asymptotic presheath because n_e must approach n_0 as U approaches negative infinity. With (20) the Poisson equation (9) to first order becomes

$$\beta^2 = 4\pi q^2(n_1 + n_0/kT_e). \tag{21}$$

Since the ion density is only calculated to first order, the same will be done for the electron density in (20).

To obtain a particular solution it is assumed here that the collisionless sheath to which the collisional presheath is joined at $\Delta U = \Delta U^*$ returns no ions. In particular,

$$\int_{-\infty}^{0} f(v,\Delta U^*)dv = 0, \tag{22}$$

or

$$\int_{-\infty}^{0} f_0(v)dv + \Delta U^* \int_{-\infty}^{0} f_1(v)dv = 0 \tag{23}$$

and

$$\int_{-\infty}^{0} vf(v,\Delta U^*)dv = 0, \tag{24}$$

or

$$\int_{-\infty}^{0} vf_0(v)dv + \Delta U^* \int_{-\infty}^{0} vf_1(v)dv = 0. \tag{25}$$

Because the approximation is only first order, it is not possible to impose the condition that $f(v)$ is uniformly zero for returning ions. Equations (23) and (25) represent zero returning ion density and zero returning ion flux. When higher-order terms are included, the conditions of zero returning ion momentum flux, zero returning ion energy flux, etc., can be applied in succession. Equations (21), (23), and (25) are solved for n_1, β, and ΔU^*, with all other quantities assumed constant. Equation (21) immediately satisfies the Bohm criterion at $\Delta U = \Delta U^*$ for the first-order approximation

$$n_1 + n_0/kT_e > 0. \tag{26}$$

The Poisson equation (21) can be written as

$$\beta^2 \lambda_D^2 = 1 + kT_e(n_1/n_0), \tag{27}$$

where

$$\lambda_D = \sqrt{kT_e/4\pi q^2 n_0} \tag{28}$$

is the Debye length. It is expected that the length scale of the presheath should be of the order $\beta = 1/\lambda_i$, where λ_i is the ion mean free path. In the circumstance that the Debye length is small compared to the ion mean free path, the product $\beta^2 \lambda_D^2$ is small and

$$n_1 = -n_0/kT_e. \tag{29}$$

The neutral plasma region is matched to the collisional presheath also at $\Delta U = \Delta U^*$, as shown in Fig. 1, to produce a three-scale uniform asymptotic solution. In particular, assuming constant collision frequencies, the momentum equations become

$$\left(kT_i - \frac{m_i \Gamma_i^2}{n^2}\right)\frac{dn}{dx} = n\frac{dU}{dx} - \frac{m_i \Gamma_i}{\tau} \tag{30}$$

and

$$\left(kT_e - \frac{m_e \Gamma_e^2}{n^2}\right)\frac{dn}{dx} = -n\frac{dU}{dx} - \frac{m_e \Gamma_e}{\tau_e}, \tag{31}$$

where

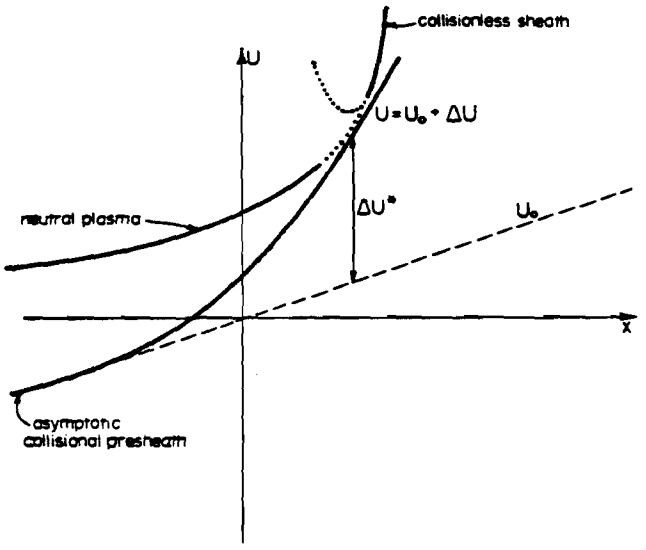

FIG. 1. Asymptotically correct potential in the collisional presheath.

$$n = n_0(1 - \Delta U^*/kT_e), \tag{32}$$

$$\frac{dn}{dx} = -n_0\beta\frac{\Delta U^*}{kT_e}, \tag{33}$$

and

$$\frac{dU}{dx} = \alpha + \beta\Delta U^*. \tag{34}$$

The quantity n is the plasma density at the matching point ΔU^* and Γ_i and Γ_e are, respectively, the ion and electron net fluxes.

Nondimensionalization results in

$$A = (\alpha\tau/m)\sqrt{m/2kT}, \tag{35}$$

$$B = \beta kT/\alpha, \tag{36}$$

$$R_e = T_e/T, \tag{37}$$

$$\omega = \sqrt{m/2kT}\, v, \tag{38}$$

where A and R_e are the parameters and B is a function of A and R_e. The quantity A represents the nondimensional asymptotic presheath potential gradient, B represents the nondimensional exponential presheath rise, R_e is the electron to neutral temperature ratio, and ω is the nondimensional velocity. The distribution functions can then be written as

$$F_0(\omega,A) = \frac{f_0(v)}{n_0\sqrt{m/2kT}} = \frac{\exp(-\omega/A)}{\sqrt{\pi}\,A}\int_{-\infty}^{\omega}\exp\left(-\xi^2 + \frac{\xi}{A}\right)d\xi \tag{39}$$

and

$$\begin{aligned} F_1(\omega,A,B) &= \frac{f_1(v)}{(n_0/kT_e)\sqrt{m/2kT}} \\ &= \frac{\exp(-B\omega^2 - \omega/A)}{\sqrt{\pi}}\left(\int_0^{\omega}\exp\left(B\xi^2 + \frac{\xi}{A}\right)\left\{-\frac{1}{A}\exp(-\xi^2)\right.\right. \\ &\quad \left.\left. - R_eB\left[\frac{1}{A}\exp(-\xi^2) - \frac{1}{A^2}\exp\left(-\frac{\xi}{A}\right)\int_{-\infty}^{\xi}\exp\left(-\eta^2 + \frac{\eta}{A}\right)d\eta\right]\right\}d\xi + C\right), \end{aligned} \tag{40}$$

where

$$\begin{aligned} C = &-\left[1 - \frac{1}{\sqrt{\pi}A}\int_{-\infty}^{\infty}\exp\left(-B\omega^2 - \frac{\omega}{A}\right)\int_0^{\omega}\exp\left(B\xi^2 + \frac{\xi}{A} - \xi^2\right)d\xi\,d\omega\right]\left[\sqrt{\frac{1}{B}}\exp\left(\frac{1}{4BA^2}\right)\right]^{-1} \\ &+ \frac{R_eB}{\sqrt{\pi}}\int_{-\infty}^{\infty}\exp\left(-B\omega^2 - \frac{\omega}{A}\right)\int_0^{\omega}\exp\left(B\xi^2 + \frac{\xi}{A}\right) \\ &\times\left[\frac{1}{A}\exp(-\xi^2) - \frac{1}{A^2}\exp\left(-\frac{\xi}{A}\right)\int_{-\infty}^{\xi}\exp\left(-\eta^2 + \frac{\eta}{A}\right)d\eta\right]d\xi\,d\omega\left[\sqrt{\frac{1}{B}}\exp\left(\frac{1}{4BA^2}\right)\right]^{-1}. \end{aligned} \tag{41}$$

Thus (23) and (25) become

$$\int_{-\infty}^{0}F_0(\omega,A)d\omega + \frac{\Delta U^*}{kT_e}\int_{-\infty}^{0}F_1(\omega,A,B)d\omega = 0 \tag{42}$$

and

$$\int_{-\infty}^{0}\omega F_0(\omega,A)d\omega + \frac{\Delta U^*}{kT_e}\int_{-\infty}^{0}\omega F_1(\omega,A,B)\,d\omega = 0. \tag{43}$$

Figure 2 presents the presheath potential rise $\Delta U^*/kT_e$ and the nondimensional exponential rise B as a function of the nondimensional asymptotic presheath potential gradient A for a range of electron to neutral temperature ratios R_e. As would be intuitively expected, the presheath potential rise decreases with increasing A. Figure 3 presents the ion distribution functions at the neutral plasma–collisional presheath interface $F_0(\omega)$, the first-order correction to the distribution function $F_1(\omega)$, and the resulting distribution function at the collisional presheath–collisionless sheath interface $F_0(\omega) + \Delta U^*F_1(\omega)$. Although the resulting distribution is not uniformly zero for $\omega < 0$, its net returning density and flux are zero by (42) and (43). It is expected that higher-order corrections to the distribution function and potential with the corresponding application of higher-order moment conditions of zero returning momentum, energy, etc., will converge the returning distribution function toward a uniform zero.

In the limit of cold neutrals, the constant collision frequency charge exchange solution is considerably simplified. Equations (14a) and (14b) become

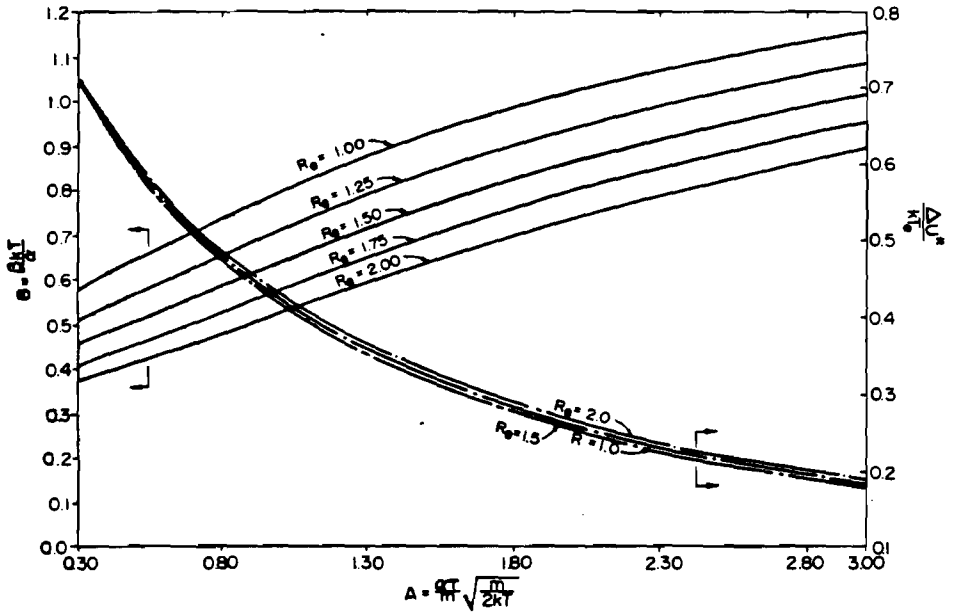

FIG. 2. Constant collision frequency presheath potential rise.

$$\frac{\alpha}{m}\frac{\partial f_0}{\partial v}(v) = \frac{1}{\tau n_n}[n_n \delta_n(v) n_0 - n_n f_0(v)] \tag{44}$$

and

$$v\beta f_1(v) + \frac{\beta}{m}\frac{\partial f_0}{\partial v} + \frac{\alpha}{m}\frac{\partial f_1}{\partial v}(v) = \frac{1}{\tau n_n}[n_n \delta_n(v) n_1 - n_n f_1(v)]. \tag{45}$$

The solutions to (44) and (45) are

$$f_0(v) = \begin{cases} n_0(m/\alpha\tau)\exp(-mv/\alpha\tau), & v>0, \\ 0, & v<0, \end{cases} \tag{46}$$

and

$$f_1(v) = \begin{cases} \exp\left(-\dfrac{\beta m v^2}{2\alpha} - \dfrac{mv}{\alpha\tau}\right)\left[C^+ + \dfrac{\beta}{\alpha} n_0 \left(\dfrac{m}{\alpha\tau}\right)^2 \displaystyle\int_0^v \exp\left(\frac{\beta m u^2}{2\alpha}\right) du\right], & v>0, \\ \exp\left(-\dfrac{\beta m v^2}{2\alpha} - \dfrac{mv}{\alpha\tau}\right)(C^-), & v<0, \end{cases} \tag{47}$$

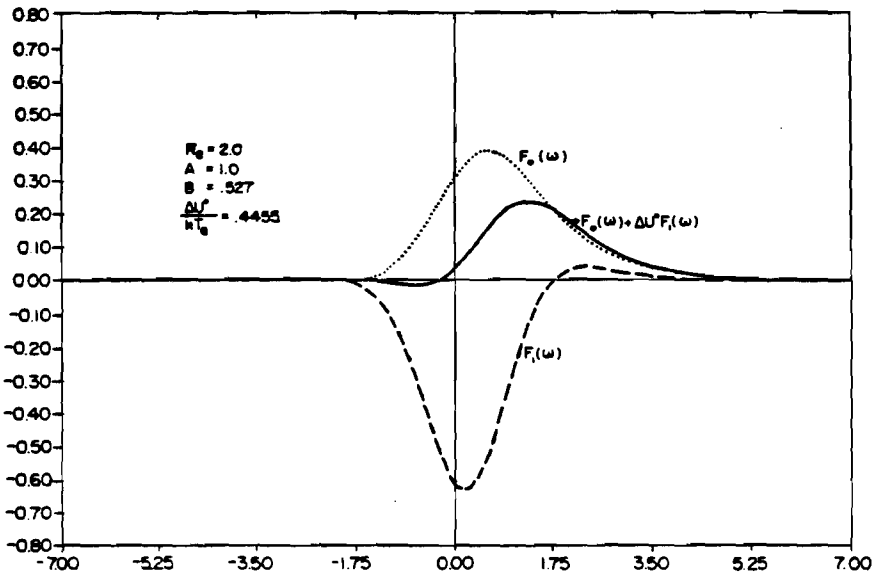

FIG. 3. Constant collision frequency ion distributions in the neutral plasma and at the presheath–sheath boundary.

such that

$$C^+ - C^- = (m/\alpha\tau)[n_1 - (\beta/\alpha)n_0]. \tag{48}$$

Equation (46) immediately satisfies $n_0 = \int_{-\infty}^{\infty} f_0(v)dv$. No returning ions implies that

$$C^- = 0 \tag{49}$$

and

$$C^+ = (m/\alpha\tau)[n_1 - (\beta/\alpha)n_0] \tag{50}$$

since f_0 on $v<0$ is already zero. The final condition is then that $n_1 = \int_0^{\infty} f_1(v)dv$, or

$$n_1 = \int_0^{\infty} \exp\left(-\frac{\beta m v^2}{2\alpha} - \frac{mv}{\alpha\tau}\right)\left[\frac{n_1 m}{\alpha\tau} - \frac{\beta n_0}{\alpha}\frac{m}{\alpha\tau} + \frac{\beta n_0}{\alpha}\left(\frac{m}{\alpha\tau}\right)^2 \int_0^{v} \exp\left(\frac{\beta m u^2}{2\alpha}\right)du\right]dv. \tag{51}$$

The application of $n_1 = -n_0/kT_e$ yields

$$\frac{\beta kT_e}{\alpha} = \left\{1 - \int_0^{\infty} \exp\left(-\frac{\beta\alpha\tau^2}{2m}\xi^2 - \xi\right)d\xi\right\}\left\{\int_0^{\infty} \exp\left(-\frac{\beta\alpha\tau^2}{2m}\xi^2 - \xi\right)\left[1 - \int_0^{\xi} \exp\left(\frac{\beta\alpha\tau^2}{2m}\eta^2\right)d\eta\right]d\xi\right\}^{-1}. \tag{52}$$

In this case, ΔU^* is defined by

$$f_0(0^+) + \Delta U^* f_1(0^+) = 0, \tag{53}$$

which yields

$$\Delta U^*/kT_e = 1/(\beta kT_e/\alpha + 1), \tag{54}$$

as expected. In the limit of $\beta\alpha\tau^2/2m \to 0$ we have

$$\beta kT_e/\alpha = 1 \tag{55}$$

and

$$\Delta U^* = kT_e/2, \tag{56}$$

which corresponds to the Bohm criterion. Figure 4 presents the variation of $B = \beta kT_e/\alpha$, with $\beta\alpha\tau^2/2m$ for the cold neutral case. A particular β for the parameters can be conveniently found by drawing a line from the origin, with slope $2mkT_e/\tau^2\alpha^2$, so that the intersection is the solution. Figure 5 presents an example cold neutral ion distribution. Examination of the ion distribution function at $v = 0$ shows that the slope is discontinuous. This is because the neutral source is a delta function at $v = 0$. It appears that the Bohm criterion cannot be satisfied at ΔU^* because the integral $\int_0^{\infty}[f(v)/v^2]dv$ is singular; however, the use of this integral in the Bohm criterion assumes that the ions accelerated are not replaced. In this case the ions accelerated from $v = 0$ are replaced by ions from the cold neutral distribution which, of course, is a delta function at $v = 0$.

IV. FIRST-ORDER SOLUTION WITH A QUASICONSTANT CROSS-SECTION COLLISION TERM

First-order asymptotic solutions can also be developed for a quasiconstant cross-section collision term

$$\left(\frac{\partial f}{\partial t}\right)_c = \sigma\left(\int_{-\infty}^{\infty} f_n(v)f(u)|v-u|du - \int_{-\infty}^{\infty} f(v)f_n(u)|v-u|du\right). \tag{57}$$

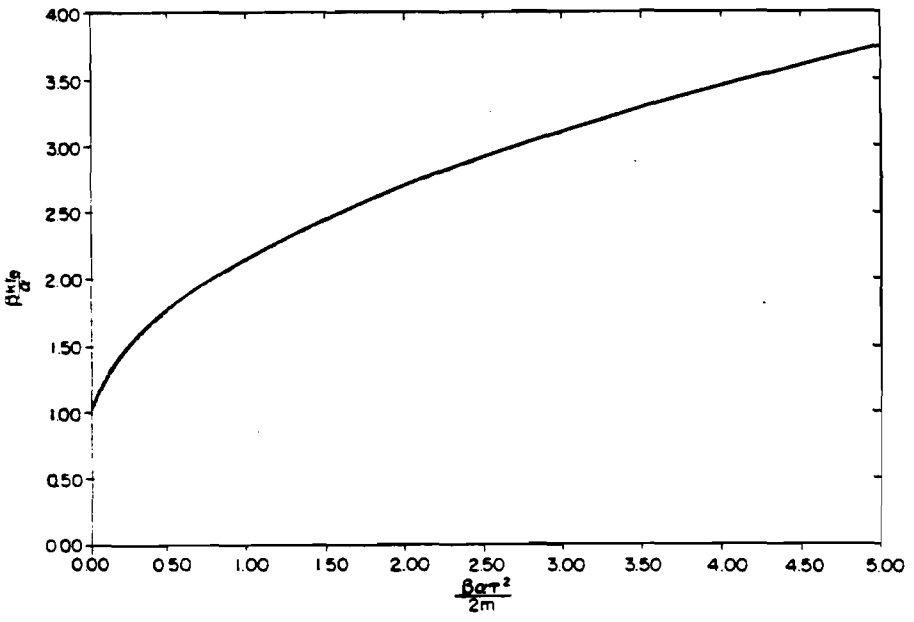

FIG. 4. Constant collision frequency presheath rise with cold neutrals.

25

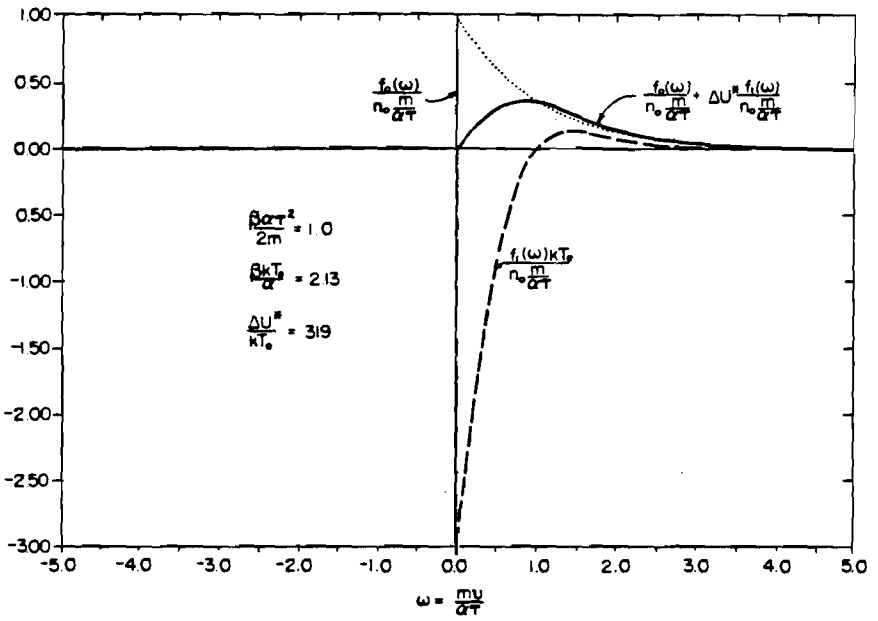

FIG. 5. Constant collision frequency ion distribution with cold neutrals.

This collision term is not really constant cross section because it is a one-dimensional representation which does not take into account average velocities in the other two dimensions. However, this collision term corresponds to that commonly called constant cross section. The application of this term leads to a set of integro-differential equations which can be at least approximately solved, and in the cold neutral case it leads to readily soluble first-order differential equations. The cold neutral case presented here corresponds to that which can be solved exactly (Riemann[4]). Unfortunately, though, the exact solution method is not extensible to noncold neutrals. The cold neutral collision term is

$$\left(\frac{\partial f}{\partial t}\right)_c = \sigma n_n \delta(v) \int_{-\infty}^{\infty} f(u)|u|du - \sigma f(v) n_n |v| \tag{58}$$

and the zero-order Boltzmann equation term (7a) becomes

$$\frac{\alpha}{m}\frac{\partial f_0}{\partial v}(v) = \sigma n_n \delta(v) \int_{-\infty}^{\infty} f_0(u)|u|du - \sigma n_n |v| f_0(v), \tag{59}$$

for which the solution is

$$f_0(v) = \begin{cases} n_0 \sqrt{\frac{2}{\pi}} \sqrt{\frac{\sigma m n_n}{\alpha}} \exp\left(-\frac{\sigma m n_n}{2\alpha} v^2\right), & v > 0, \\ 0, & v < 0. \end{cases} \tag{60}$$

The first-order Boltzmann term is

$$v\beta f_1(v) + \frac{\beta}{m}\frac{\partial f_0}{\partial v}(v) + \frac{\alpha}{m}\frac{\partial f_1}{\partial v}(v) = \sigma n_n \delta(v) \int_{-\infty}^{\infty} f_1(u)|u|du - \sigma n_n |v| f_1(v), \tag{61}$$

for which the solution is

$$f_1(v) = \begin{cases} \exp\left[-\frac{1}{2}\left(\frac{\beta m}{\alpha} + \frac{\sigma m n_n}{\alpha}\right)v^2\right]\left\{\frac{n_0}{m}\sqrt{\frac{2}{\pi}}\left(\sqrt{\frac{\sigma m n_n}{\alpha}}\right)^3\left[\exp\left(\frac{\beta m v^2}{2\alpha}\right) - 1\right] + C^+\right\}, & v > 0, \\ \exp\left[-\frac{1}{2}\left(\frac{\beta m}{\alpha} - \frac{\sigma m n_n}{\alpha}\right)v^2\right](C^-), & v < 0. \end{cases} \tag{62}$$

The jump condition at $v = 0$ must be satisfied in (61):

$$C^+ - C^- = \frac{\delta m n_n}{\alpha} \int_{-\infty}^{\infty} f_1(u)|u|du - \frac{\beta}{\alpha} n_0 \sqrt{\frac{2}{\pi}} \sqrt{\frac{\sigma m n_n}{\alpha}}. \tag{63}$$

No returning ions, $C^- = 0$, and the application of (63) to (62) yields

$$C^+ = -n_0(\beta/\alpha)\sqrt{2/\pi}\sqrt{\sigma m n_n/\alpha}. \tag{64}$$

The collisional presheath–collisionless sheath boundary ΔU^* is again

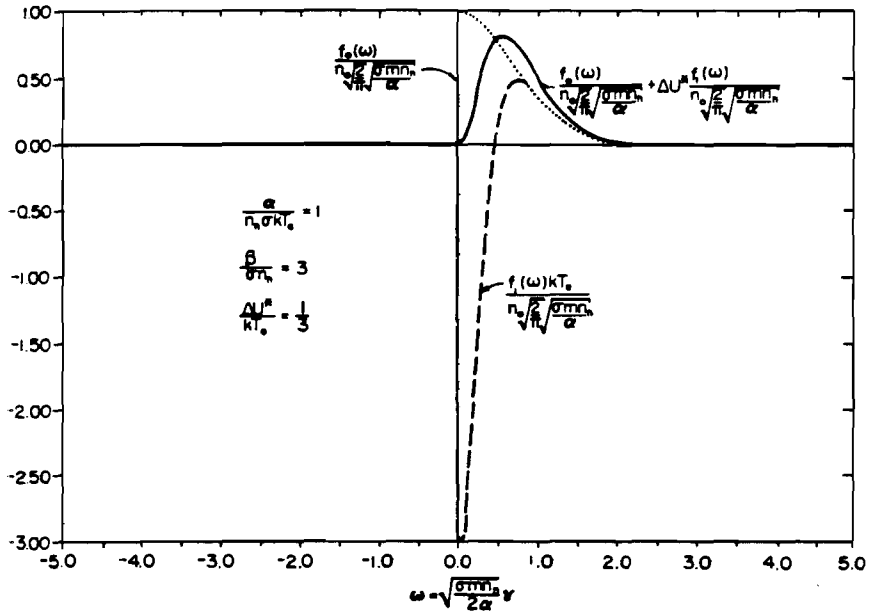

FIG. 6. Constant cross section ion distribution with cold neutrals.

$$0 = f(0^+) = f_0(0^+) + \Delta U^* f_1(0^+), \tag{65}$$

which yields

$$\Delta U^*/kT_e = \alpha/\beta kT_e. \tag{66}$$

Equation (62) is integrated to

$$n_1 = \int_{-\infty}^{\infty} f_1(v)dv = \frac{n_0 n_n \sigma}{\alpha}\left(1 - \sqrt{1 + \frac{\beta}{\sigma n_n}}\right) \tag{67}$$

and applied to the Poisson equation (8) to produce

$$\left(\frac{\beta}{\sigma n_n}\right)^2 = \left(\frac{4\pi q^2 n_0}{kT_e}\right)^2 \left(\frac{1}{\sigma n_n}\right)^2 \left[\frac{n_n \sigma kT_e}{\alpha}\left(1 - \sqrt{1 + \frac{\beta}{\sigma n_n}}\right) + 1\right]. \tag{68}$$

Under the assumption that the Debye length is short compared to the ion mean free path,

$$(4\pi q^2 n_0/kT_e)^2 (1/\sigma n_n)^2 \gg 1,$$

Eq. (68) results in

$$\beta/\sigma n_n = \alpha/n_n \sigma kT_e (2 + \alpha/n_n \sigma kT_e) \tag{69}$$

and

$$\Delta U^*/kT_e = 1/(2 + \alpha/n_n \sigma kT_e). \tag{70}$$

The Bohm criterion is satisfied at ΔU^* to the first order by virtue of (68). And interestingly, the presheath potential rise for $\alpha = 0$ is exactly that required by the cold ion Bohm criterion. Figure 6 presents the results for cold neutrals with $\alpha/n_n \sigma kT_e = 1$. From the ion distribution at ΔU^*, the mean ion velocity into the sheath can be determined to be $\bar{v} = 1.06\sqrt{kT_e/m_i}$, while the exact solution of Riemann gives $\bar{v} = 1.27\sqrt{kT_e/m_i}$; thus the first-order asymptotic result appears close.

V. CONCLUSIONS

It has been shown that approximate collisional presheath solutions can be obtained for a variety of collision terms. In particular the constant collision frequency case has been solved approximately, whereas previous attempts at exact solutions have found this case intractable. In addition, it has been shown that higher-order corrections can be made a regular and tractable fashion. Also the return of ions from the collisionless sheath can be treated.

ACKNOWLEDGMENTS

Thanks are due to Gregory Ridderbusch who produced the numerical results. This work was supported by the Air Force Office of Scientific Research Grant No. 85-0375.

APPENDIX: MULTIEXPONENTIAL FORMULATION

In the previous sections we have calculated only the first-order terms in the ion distribution and presheath potential rise. Also, we have implicitly made the same first-order approximation for electrons:

$$n_e = n_0(1 - \Delta U/kT_e). \tag{A1}$$

A complete multiexponential expansion can also be constructed that correctly calculates the second- and higher-order terms. Potential in the presheath is

$$U = U_0 + \Delta U + a_2\Delta U^2 + a_3\Delta U^3 + \cdots, \tag{A2}$$

where $U_0 = \alpha x$ and $\Delta U = \exp(\beta x)$. Thus

$$\frac{dU}{dx} = \alpha + \beta\Delta U + 2\beta a_2\Delta U^2 + 3\beta a\Delta U^3 + \cdots \tag{A3}$$

and

$$\frac{d(\Delta U)}{dU} = \frac{\beta\Delta U}{a + \beta\Delta U + 2\beta a_2\Delta U^2 + 3\beta a_3\Delta U^3 + \cdots}, \tag{A4}$$

which transforms the Boltzmann equation

$$\frac{dU}{dx}\left(v\frac{\partial f}{\partial\Delta U}(v)\frac{\partial\Delta U}{\partial U} \pm \frac{1}{m}\frac{\partial f}{\partial v}(v)\right) = \left(\frac{\partial f}{\partial t}\right)_c \tag{A5}$$

into

$$v\beta\Delta U\frac{\partial f}{\partial\Delta U}(v) \pm \frac{1}{m}(\alpha + \beta\Delta U + 2\beta a_2\Delta U^2 + \cdots)\frac{\partial f}{\partial v}(v) = \left(\frac{\partial f}{\partial t}\right)_c, \tag{A6}$$

or

$$1: \quad \pm\frac{\alpha}{m}\frac{\partial f_0}{\partial v}(v) = \left[\left(\frac{\partial f}{\partial t}\right)_c\right]_1, \tag{A7a}$$

$$\Delta U: \quad v\beta f_1(v) \pm \frac{\beta}{m}\frac{\partial f_0}{\partial v}(v) \pm \frac{\alpha}{m}\frac{\partial f_1}{\partial v}(v) = \left[\left(\frac{\partial f}{\partial t}\right)_c\right]_{\Delta U}, \tag{A7b}$$

$$\Delta U^2: \quad 2v\beta f_2(v) \pm \frac{2\beta a_2}{m}\frac{\partial f_0}{\partial v}(v) \pm \frac{\beta}{m}\frac{\partial f_1}{\partial v}(v) \pm \frac{\alpha}{m}\frac{\partial f_2}{\partial v}(v) = \left[\left(\frac{\partial f}{\partial t}\right)_c\right]_{\Delta U^2}, \tag{A7c}$$

$$\vdots$$

$$\Delta U^n: \quad nv\beta f_n(v) \pm \frac{n\beta a_n}{m}\frac{\partial f_0}{\partial v}(v) \pm \frac{(n-1)\beta a_{n-1}}{m}\frac{\partial f_1}{\partial v}(v) \pm \cdots \pm \frac{\beta}{m}\frac{\partial f_{n-1}}{\partial v}(v) \pm \frac{\alpha}{m}\frac{\partial f_n}{\partial v}(v) = \left[\left(\frac{\partial f}{\partial t}\right)_c\right]_{\Delta U^n}. \tag{A7d}$$

The Poisson equation (8) becomes

$$\beta^2\Delta U + (2\beta)^2 a_2\Delta U^2 + (3\beta)^2 a_3\Delta U^3 + \cdots = 4\pi q^2\left[\Delta U\left(\int_{-\infty}^{\infty} f_{i1}(v)dv - \int_{-\infty}^{\infty} f_{e1}(v)dv\right) + \Delta U^2\left(\int_{-\infty}^{\infty} f_{i2}(v)dv - \int_{-\infty}^{\infty} f_{e2}(v)dv\right) + \cdots\right]. \tag{A8}$$

[1] D. Bohm, in *Characteristics of Electrical Discharges in Magnetic Fields*, edited by A. Guthrie and R. Wakering (McGraw-Hill, New York, 1949), p. 77.
[2] E. R. Harrison and W. B. Thompson, Proc. Phys. Soc. London 74, 145 (1959).
[3] G. Ecker and H. Kanne, Z. Naturforsch. Teil A 21, 2027 (1966).
[4] K. U. Riemann, Phys. Fluids 24, 2163 (1981).
[5] G. A. Emmert, R. M. Wieland, A. T. Mense, and J. N. Davidson, Phys. Fluids 23, 803 (1980).

THE TEC PROGRAM RESULTS

The TEC program results shown here incorporate the asymptotic presheath work and give good agreement except at low current density. This disagreement is still not understood.

Comparison of TEC Program Results to Experimental Data

Reference: Advanced Thermionic Technology Program, Vol. 4, Oct. 1984. Thermo Electron Corporation, DOE/ET/11292-2

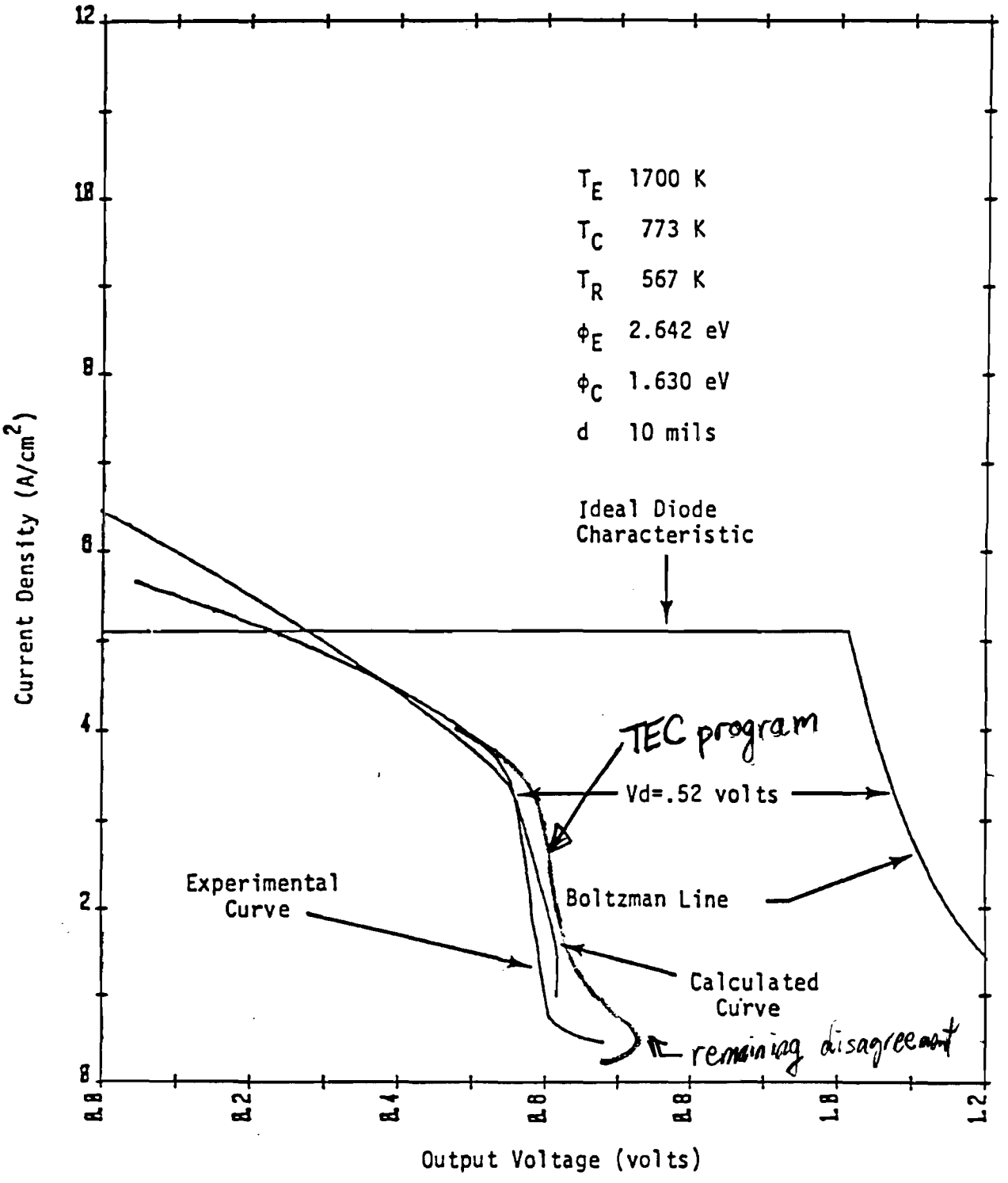

TEC INITIAL DATA SUMMARY

PHYSICAL OPERATING CONDITIONS-----

EMITTER TEMPERATURE	(TE) =	1700.0	KELVIN
COLLECTOR TEMPERATURE	(TC) =	773.0	KELVIN
EMITTER WORK FUNCTION	(EWF) =	2.642	EV
COLLECTOR WORK FUNCTION	(CWF) =	1.630	EV
CONVERTOR PRESSURE	(PN) =	1.541	TORR
GAP THICKNESS	(D) =	0.254	MM
OPERATING CURRENT	(J) =	2.000	AMPS/CM^2

TEC FUNCTION SETTINGS-----

DIAGNOSTIC LEVEL	(CHKDOT) =	1
RESTART SEQUENCE	(OFILE) =	0
POINT DENSITY	(N) =	11

PHYSICAL PARAMETERS EVALUATED-----

RICHARDSON CURRENT	(JRIC) =	0.51E+01	AMPS/CM^2
REFERENCE DENSITY	(NR) =	0.10E+15	1/CM^3
CHARACTERISTIC TIME	(TCHAR) =	0.0208	SECS*E-06
NONDIM CURRENT	(I) =	0.0196	
NONDIM EMISSION	(ENR) =	0.008	(NRIC/NR)
KNUDSEN NUMBER	(KN) =	0.0791	
SQRT(MASS RATIO)	(SMR) =	0.0020	
MEAN FREE PATH RATIO	(LAMDAR) =	0.3344	

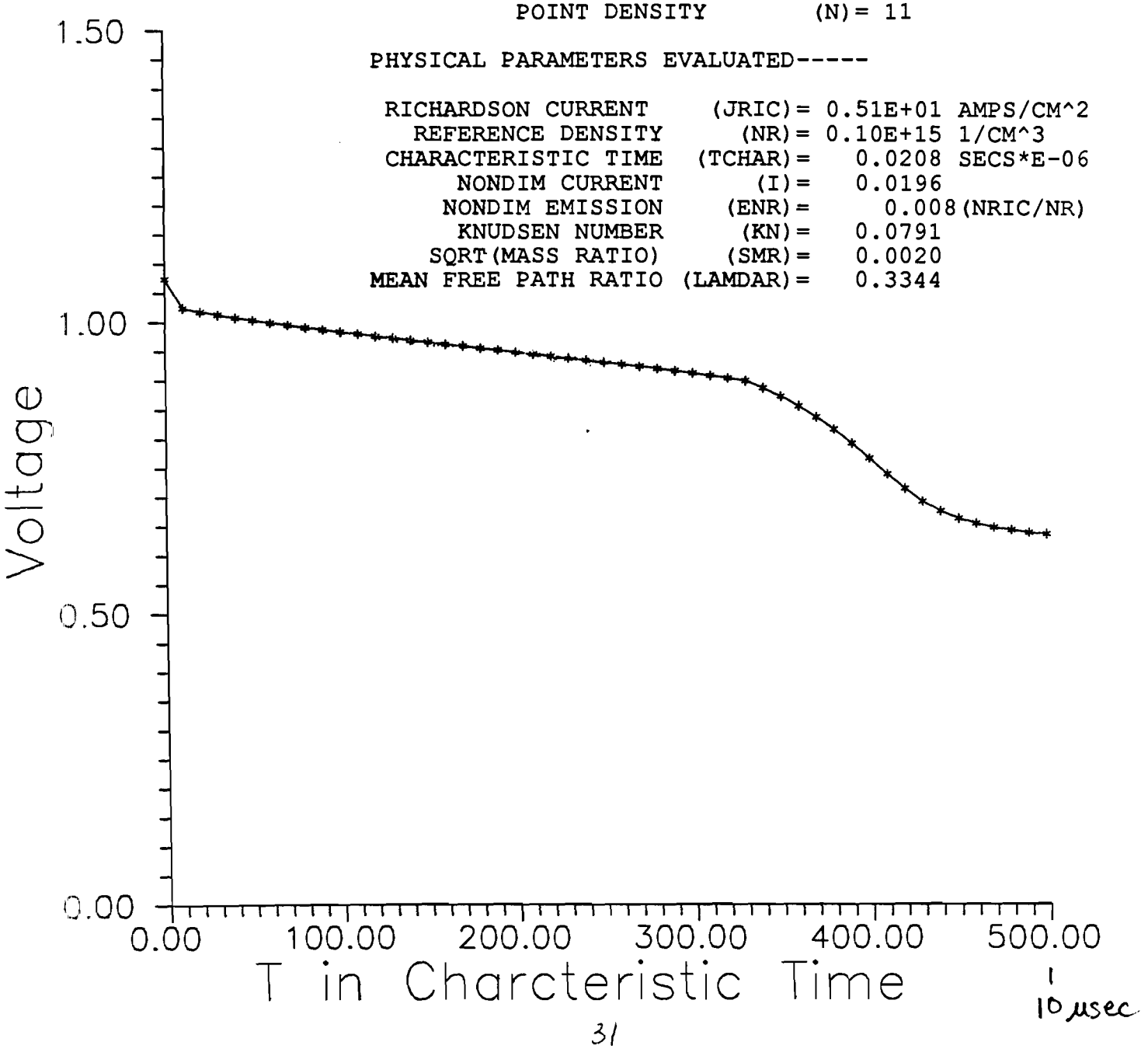

TEC INITIAL DATA SUMMARY

PHYSICAL OPERATING CONDITIONS-----

EMITTER TEMPERATURE	(TE) =	1700.0	KELVIN
COLLECTOR TEMPERATURE	(TC) =	773.0	KELVIN
EMITTER WORK FUNCTION	(EWF) =	2.642	EV
COLLECTOR WORK FUNCTION	(CWF) =	1.630	EV
CONVERTOR PRESSURE	(PN) =	1.541	TORR
GAP THICKNESS	(D) =	0.254	MM
OPERATING CURRENT	(J) =	2.000	AMPS/CM^2

TEC FUNCTION SETTINGS-----

DIAGNOSTIC LEVEL	(CHKDOT) =	1
RESTART SEQUENCE	(OFILE) =	0
POINT DENSITY	(N) =	11

PHYSICAL PARAMETERS EVALUATED-----

RICHARDSON CURRENT	(JRIC) =	0.51E+01	AMPS/CM^2
REFERENCE DENSITY	(NR) =	0.10E+15	1/CM^3
CHARACTERISTIC TIME	(TCHAR) =	0.0208	SECS*E-06
NONDIM CURRENT	(I) =	0.0196	
NONDIM EMISSION	(ENR) =	0.008	(NRIC/NR)
KNUDSEN NUMBER	(KN) =	0.0791	
SQRT(MASS RATIO)	(SMR) =	0.0020	
MEAN FREE PATH RATIO	(LAMDAR) =	0.3344	

TIME SETTINGS-----

NSTEPS=	1
T2=	500.0
DELTAT=	1.000
DTP=	1.000
LSF=	10

RESULTS AT TIME = 0.00 OPERATING VOLTAGE= 1.074

ENE =	0.027	ECHI=	6.241	EALPHA=	0.460
CNE =	0.000	CCHI=	6.734	CALPHA=	0.482
PHIB=	0.000	VD =	0.422	EMISS =	.268E-01

#	NDOT(#)	NEB(#)	TDOT(#)	TAU(#)
0	0.0015	-0.154	-0.0526	1.52
1	-0.0151	0.298	-0.0537	1.52
2	-0.0158	0.661	-0.0555	1.51
3	-0.0141	0.943	-0.0569	1.51
4	-0.0122	1.145	-0.0582	1.50
5	-0.0104	1.267	-0.0594	1.50
6	-0.0088	1.309	-0.0608	1.50
7	-0.0072	1.271	-0.0623	1.49
8	-0.0058	1.153	-0.0641	1.49
9	-0.0050	0.953	-0.0665	1.48
10	-0.0083	0.670	-0.0698	1.47
11	-0.0340	0.270	-0.0768	1.45

12	-0.0704	-0.551	-0.0807	1.43

RESULTS AT TIME = 100.00 OPERATING VOLTAGE= 0.982

ENE =	0.098	ECHI=	3.183	EALPHA=	0.617
CNE =	0.000	CCHI=	3.069	CALPHA=	0.719
PHIB=	0.000	VD =	-0.203	EMISS =	.981E-01

#	NDOT(#)	NEB(#)	TDOT(#)	TAU(#)
0	0.0003	-0.035	0.0001	1.14
1	-0.0007	0.081	0.0001	1.13
2	-0.0018	0.200	0.0000	1.11
3	-0.0028	0.316	-0.0001	1.10
4	-0.0037	0.419	-0.0001	1.09
5	-0.0043	0.501	-0.0002	1.08
6	-0.0047	0.552	-0.0003	1.07
7	-0.0046	0.562	-0.0003	1.06
8	-0.0043	0.524	-0.0004	1.05
9	-0.0035	0.431	-0.0005	1.03
10	-0.0022	0.281	-0.0006	1.01
11	-0.0006	0.074	-0.0008	0.97
12	0.0013	-0.170	-0.0009	0.95

RESULTS AT TIME = 200.00 OPERATING VOLTAGE= 0.946

ENE =	0.232	ECHI=	2.324	EALPHA=	0.587
CNE =	0.000	CCHI=	2.167	CALPHA=	0.750
PHIB=	0.000	VD =	-0.448	EMISS =	.232E+00

#	NDOT(#)	NEB(#)	TDOT(#)	TAU(#)
0	0.0001	-0.014	0.0006	1.19
1	-0.0003	0.034	0.0008	1.19
2	-0.0007	0.084	0.0008	1.17
3	-0.0011	0.134	0.0008	1.15
4	-0.0015	0.179	0.0007	1.13
5	-0.0018	0.216	0.0006	1.11
6	-0.0020	0.240	0.0005	1.09
7	-0.0020	0.247	0.0005	1.08
8	-0.0019	0.232	0.0004	1.06
9	-0.0016	0.193	0.0002	1.03
10	-0.0010	0.127	0.0001	1.00
11	-0.0003	0.033	-0.0002	0.93
12	0.0006	-0.081	-0.0003	0.90

RESULTS AT TIME = 300.00 OPERATING VOLTAGE= 0.910

ENE =	0.526	ECHI=	1.440	EALPHA=	0.551
CNE =	0.000	CCHI=	1.374	CALPHA=	0.754
PHIB=	0.000	VD =	-0.698	EMISS =	.526E+00

#	NDOT(#)	NEB(#)	TDOT(#)	TAU(#)
0	0.0001	-0.006	-0.0001	1.23
1	-0.0001	0.015	0.0007	1.27
2	-0.0003	0.036	0.0012	1.27

3	-0.0005	0.057	0.0013	1.25
4	-0.0007	0.077	0.0013	1.22
5	-0.0008	0.093	0.0012	1.20
6	-0.0009	0.104	0.0012	1.17
7	-0.0009	0.107	0.0011	1.15
8	-0.0009	0.101	0.0009	1.11
9	-0.0007	0.085	0.0008	1.07
10	-0.0005	0.056	0.0006	1.02
11	-0.0001	0.014	0.0003	0.93
12	0.0003	-0.038	0.0006	0.90

RESULTS AT TIME = 400.00 OPERATING VOLTAGE= 0.763

ENE = 0.879 ECHI= 1.392 EALPHA= 0.420
CNE = 0.000 CCHI= 0.914 CALPHA= 0.541
PHIB= 0.264 VD = -1.960 EMISS =.114E+01

#	NDOT(#)	NEB(#)	TDOT(#)	TAU(#)
0	0.0000	-0.002	0.0037	1.46
1	0.0000	0.007	0.0061	1.66
2	-0.0001	0.015	0.0077	1.76
3	-0.0002	0.024	0.0081	1.77
4	-0.0003	0.032	0.0082	1.75
5	-0.0003	0.038	0.0082	1.72
6	-0.0004	0.042	0.0081	1.68
7	-0.0004	0.043	0.0079	1.63
8	-0.0004	0.041	0.0076	1.58
9	-0.0003	0.034	0.0072	1.51
10	-0.0002	0.022	0.0068	1.42
11	-0.0001	0.006	0.0066	1.29
12	0.0002	-0.015	0.0086	1.35

RESULTS AT TIME = 500.00 OPERATING VOLTAGE= 0.632

ENE = 1.001 ECHI= 1.516 EALPHA= 0.371
CNE = 0.000 CCHI= 0.348 CALPHA= 0.433
PHIB= 0.352 VD = -2.945 EMISS =.142E+01

#	NDOT(#)	NEB(#)	TDOT(#)	TAU(#)
0	0.0000	-0.002	0.0001	1.59
1	0.0000	0.006	0.0002	1.88
2	0.0000	0.012	0.0003	2.04
3	0.0000	0.019	0.0003	2.06
4	0.0000	0.024	0.0003	2.05
5	0.0000	0.029	0.0003	2.02
6	0.0000	0.031	0.0003	1.98
7	0.0000	0.030	0.0003	1.93
8	0.0000	0.027	0.0003	1.87
9	0.0000	0.021	0.0004	1.79
10	0.0000	0.013	0.0004	1.69
11	0.0000	0.003	0.0008	1.61
12	0.0000	-0.007	0.0019	1.90

PAPERS AND PUBLICATIONS

1. The paper entitled "Asymptotically Correct Collisional Presheaths," by G L. Main, Phys. Fluids, June 1987, has been produced under this grant.

2 "Effects of Emitter Sheath Ion Reflection and Trapped Ions on Thermionic Convertor Performance Using an Isothermal Electron Model" by G. L. Main and S. H. Lam, IEEE Transactions on Plasma Science, June 1987.

3 "A Uniform Three Scale Asymptotic Solution for a Collisional Presheath and Collisionless Sheath with Ion Reflection," by G. L. Main and G. L. Ridderbusch is to appear in IEEE Trans. on Plasma Science, and has been produced under this grant.

APPENDIX A - Fokker Planck Collisions Presheath

This theory has been developed under this grant and is found to be applicable to fully ionized plasmas but was not incorporated into the Thermionic Convertor work due to its computational complexity.

[redacted]

AN ANALYTIC - NUMERICAL SCHEME FOR A COLLISIONAL FOKKER - PLANCK TIME DEPENDENT SHEATH - PRESHEATH STRUCTURE

A THESIS
Presented to
The Faculty of the Division of Graduate Studies
By

Jeffrey Paul Dansereau

In Partial Fulfillment
of the Requirements for the Degree
Master of Science in Mechanical Engineering

Georgia Institute of Technology
September, 1987

AN ANALYTIC - NUMERICAL SCHEME FOR A COLLISIONAL FOKKER - PLANCK TIME DEPENDENT SHEATH - PRESHEATH STRUCTURE

Approved:

Geoffrey L. Main, Chairman

J. Narl Davidson

Thomas L. Eddy

Date approved by chairman _____

ACKNOWLEDGMENTS

I would like to thank Geoffrey L. Main for all of his help and encouragement during the development of this project. This work was supported by the Air Force Office of Scientific Research grant 85-0375.

TABLE OF CONTENTS

LIST OF FIGURES

NOMENCLATURE

a - Inverse square of the particle thermal velocity

$a_1, a_2, \cdots$ - Coefficients of the potential structure

a, b - Integral limits

A - First derived Fokker Planck collision function

B - Second derived Fokker Planck collision function

$d_i(\tau)$ - An $m \times 1$ matrix

$D(\tau)$ - An $m \times 1$ solution matrix

e - Electron charge

E - Electric field strength

f - Particle distribution function in velocity space

F - Nondimensional particle distribution function in velocity space

g - Collision function

h - Grid spacing width

k - Boltzmann's constant

L - System dimension

m - Number of points in velocity space

m - Particle mass

M - Reduced mass

n - Plasma density

n_R - Reference density

q - Elementary charge

R - Radial velocity component

t - Time

T_i - Ion temperature

T_e - Electron temperature

$T(\tau)$ - An $m \times m$ matrix

U - Potential

v - Velocity vector

$v_i(\tau)$ - An $m \times 1$ matrix

$V(\tau)$ - An $m \times 1$ solution matrix

x - Position vector

x - Axial position component

z - Axial velocity component

Z - Ionization level

Z - Nondimensional axial velocity component

α - Potential gradient across the plasma

β - Exponential coefficient of the presheath rise

Γ - Fokker - Planck coefficient

ΔU - Potential expansion parameter

ϵ_0 - Permitivity of free space

ς, η, ξ - Variables of integration

θ - Velocity rotation angle in cylindrical coordinates

λ_D - Debye length

λ_i - Mean free path

Λ - Coulomb logarithm

τ - Nondimensional time

Φ - Electric potential

φ - Nondimensional coefficients of the potential structure

Subscripts:

c - Collision term

e - Electron

i - Ion

n - Order of expansion

Superscripts:

I - Particle species with which collisions occur

$*$ - Nondimensional

SUMMARY

The Maxwellian sources and charge exchange terms used to model particle interactions in current presheath models do not represent the Coulomb collisions taking place in fully ionized plasmas. These models approximate the collisional effects in the presheaths of partially ionized plasmas but are used to implicitly extrapolate the interesting case of fully ionized plasmas. The present study uses a Fokker - Planck collision term which models the limit of the small angle Coulomb collisions that occur in fully ionized plasmas. Normally these small angle collisions dominate the particle interactions of fully ionized plasmas. The Boltzmann equation coupled with the Fokker - Planck term, and the Poisson equation have been expanded using an exponential asymptotic technique. These equations have been solved numerically to determine the time dependent evolution of the presheath. The results presented show the presheath potential structure and particle distribution in velocity space. The model produces a self-consistent and accurate potential structure. The particle velocity distribution in the presheath has the correct acceleration of ions toward the wall but because the Fokker - Planck collision term only models the limit of small angle collisions it is unable to clear the particle distribution of returning ions. The collisional processes become dominated by the effects of the large angle collisions as the Debye sheath edge is approached. This study has found that a presheath model which describes the Coulomb collisions occurring in a fully ionized plasma must account for both the small angle and the large angle particle collisions to explain the clearing out of returning ions that must exist for the transition to an absorbing wall.

CHAPTER I

INTRODUCTION

The interaction of man and plasma, in some form, exists at almost all levels of society. A plasma is an ionized gas that has a collective behavior in an electromagnetic field. Plasmas exist in everyday devices like flourescent lights, neon signs, and electric arc welders. An understanding of the basic behavior and interaction of plasmas is essential to the advancement of all current plasma applications and to the discovery of new applications. This thesis involves the study of how a plasma interacts with the walls and surfaces with which it comes in contact.

Why is it important to understand plasma - wall interactions? Two basic reasons answer this question. First, a plasma has a strong effect on any surfaces it comes in contact with. The high temperature plasma can erode or destroy any surface quickly pitting and changing a wall which may need to maintain a particular profile or surface condition. Secondly, the wall affects the characteristics of the plasma. A surface can have a profound effect on the plasma depending on the amount and rate at which it can absorb energy. Examples of situations in which plasma - wall interactions are of importance include:

- Diverter plates in magnetic confinement fusion reactors.
- The rails in a plasma rail gun.
- Any body (like the space shuttle) upon reentry to the atmosphere.
- Plasma switches.
- Plasma etching.

- Almost every other use or occurrence of plasmas.

This study is primarily applicable to fully ionized plasmas. The hot temperatures necessary to produce fully ionized plasmas occur only in situations like on the surfaces of diverter plates in Tokamak fusion reactors.

The development of a mathematical model to represent the plasma - wall interaction region, or sheath, and a numerical solution to this model is the focus of this thesis. An understanding of the interaction between the plasma and the wall is achieved with a time dependent solution to the sheath region. If the potential structure and the particle velocity distributions are known for every location in the sheath then the energy going into the surface can be determined. In this way the results of this study can be used as a boundary condition for problems involving plasma characteristics and for problems invloving the surface physics of plasma devices.

CHAPTER II

BACKGROUND

A plasma will naturally maintain itself in a neutral and field free state. Application of forces and processes that try to alter the equilibrium are resisted by the plasma. A surface within a plasma that is not at the same potential as the plasma will be shielded from the remainder of the plasma by a sheath. The outer edge of this sheath is nearly at the plasma potential. Bohm[1] first came up with a criterion to determine the extent of the sheath. Bohm modeled the sheath region as completely collisionless. He also considered that the transition region from this collisionless sheath to the plasma was too small to be important.

More recent work has been done to describe this transition, or presheath, region. Self[2] has an exact solution to the sheath equation and has shown that the collisionless sheath makes a transition directly to the neutral plasma in the limit as $\frac{\lambda_D}{L} \rightarrow 0$, where λ_D is the Debye length and L is the plasma dimension. Emmert et al.[3] has determined a presheath structure based on the assumption of a Maxwellian source of ions to model the particle collisions. The solution to this model shows that the transition point from the sheath to the presheath has a finite electric field strength. Bissell and Johnson[4] have perfomed a similar solution using a Maxwellian source of ions. In contrast to Emmert et al., Bissell and Johnson have found that the electric field strength becomes infinite at the sheath edge. This solution agrees with the fluid and cold ion models. In a recent paper Bissell[5] shows that Emmert obtained a finite electric field strength because the Maxwellian source term used produced no ions at the point of zero velocity. Bissell and Johnson used a more realistic

Maxwellian source that produced ions at the zero point in velocity space for their solution.

Another approach to the problem involves the use of a charge exchange term to model the particle collisions. Riemann[6] has produced results using this technique. In a recent paper by Main[7] a charge exchange model is used to obtain a solution to the presheath potential structure and particle distribution. This model involves an asymptotic approximation of the plasma equations. The Boltzmann and Poisson equations are asymptotically expanded and then solved analytically when combined with a charge exchange model of the particle collisions.

All of these sheath and presheath solutions have modeled particle collisions by large instantaneous changes in particle velocity. These models do not represent the Coulomb collisions occurring in the presheath of a fully ionized plasma.

The current study extends the asymptotic solution presented by Main[7] to include a Fokker - Planck collision term instead of the charge exchange term. Unlike the previous collision terms used, the Fokker - Planck term describes the Coulomb collisions that exist within a fully ionized plasma. The addition of the Fokker - Planck term necessitates the use of numerical techniques, rather than analytical techniques, to obtain a solution. In using the Fokker - Planck term the collision processes are being modeled directly. The model developed obtains the time dependent evolution of the presheath for a fully ionized plasma.

CHAPTER III

MODEL FORMULATION

3.1 Concepts

In order to have a complete understanding of the problem at hand certain concepts need to be presented which will help in understanding the overall structure of the model.

1) Debye Length (λ_D) - The shielding distance beyond which the particle charge effect is weak. This is the natural charge separation distance. Negatively charged particles become surrounded by positively charged particles and vice versa, thus, balancing the overall charge at any point (see figure 3.1). There is a point beyond which a particle is not effected by the specific charge but responds to the influence of the entire plasma. The thermal effects in the plasma become dominant over the electric field strength.

2) Mean Free Path (λ_i) - The average distance a particle travels before its trajectory has been altered by ninety degrees. The mean free path is a function of the density of the plasma. The denser the plasma the shorter the mean free path. For the plasma under consideration in this study $\lambda_i >> \lambda_D$.

3) The coordinate system used to describe the plasma - The coordinate system used in the model is known phase space. In this system any point is described using three position coordinates and three velocity coordinates. Any orthogonal coordinate system, cartesian, cylindrical, spherical, can be used to describe both the position and the velocity components.

4) Distributions and Distribution Functions - Plasmas are studied in a collective sense. The motion of the entire plasma and not individual particles is described by the model. Therefore, the velocity of the plasma at any given location must be described by a distribution. The distibution function describes the overall particle velocity distibution.

5) Potential - In a plasma the wall potential is greater than the neutral plasma potential. The lighter, thus, faster electrons are absorbed by the wall faster than the heavier and slower ions. A net positive charge exists near the wall, increasing the potential (see figure 3.2). The potential at the physical interface between the wall and the plasma is dependent on the rate at which ions are absorbed by the surface. In this study $U = -e\Phi$ where e is the electron charge and Φ is electric potential in electron volts so that U has units of energy. The addition of the negative sign defines potential in the reverse of the usual sign convention so that increasing potential repels electrons.

6) Collision Possibilities using the Fokker - Planck Collision term - To describe the overall sturcture of the sheath the various collision possibilities must be included in a comprehensive model. The Fokker - Planck term describes the four major collision possibilities.

1) Ion - Ion

2) Ion - Electron

3) Electron - Ion

4) Electron - Electron

The collision model does not take into account three body collisions. Three body collisions are very rare, as such, the model is not hampered by the lack of

terms to describe these collisions.

3.2 Wall Region Model

The model of the Plasma - Wall region can be broken into three areas.

1) Neutral Plasma Region ($O(L)$) - The neutral plasma region represents the majority of the system and can be considered to have a physical width that is on the order of the overall dimension of the system, L. This region is considered to be fully collisional. The velocity distribution is near Maxwellian and as such can be modeled by fluid type equations (see figure 3.3).

2) Debye Sheath Region ($O(\lambda_D)$) - This region is a very thin area directly adjacent to the wall. Its width is considered to be on the order of a Debye length and since $\lambda_i >> \lambda_D$ no collisions are expected in this region. This collisionless sheath was first modeled by Langmuir[8] and Bohm[1] and is considered very well known and understood.

3) Collisional Presheath Region ($O(\lambda_i)$) - This is a transition region between the collisional neutral plasma and the collisionless Debye sheath region. It is considered to have a physical width on the order of a mean free path. Therefore, collisions are expected but at the same time the region cannot be considered fully collisional.

The potential must transition from a lower level in the neutral plasma to a higher level at the wall. The goal of this study has been to obtain a time dependent model of the evolution of the presheath region which asymptotically approaches the known potential in both the neutral plasma and in the Debye sheath region.

In order to show the validity of the three region model an example of Debye sheath width in relation to the overall wall region is appropriate. For this example

average hydrogen fusion plasma characteristics have been assumed:

$$T_i = 10^5 K$$

$$n_0 = 10^{20} m^{-3}$$

If the Debye length within this plasma is calculated an order of magnitude value for the Debye sheath width is determined. An appropriate equation for the Debye length in meters is:[9]

$$\lambda_D = 69\left(\frac{T_i}{n_0}\right)^{\frac{1}{2}} \tag{3.1}$$

From this equation:

$$\lambda_D = 2.18 \times 10^{-6} m$$

The overall sheath width is on the order of a mean free path. An appropriate equation for the mean free path in meters is:[10]

$$\lambda_i = 1.2 \times 10^{-4} \frac{1}{Z^4}\left(\frac{T_i}{e}\right)^2\left(\frac{n_i}{10^{20}}\right)^{-1} \tag{3.2}$$

For a singly ionized plasma $Z = 1$. Using this equation and the above example plasma characteristics the mean free path can be calculated.

$$\lambda_i = 1.14 \times 10^{-2} m$$

This is an order of magnitude estimate value for the width of the entire sheath region. Since the Debye sheath width is on the order of a Debye length it can be seen that the collisionless sheath is very thin in comparison with the entire wall region.

In order to obtain an idea of the importance of the electric field in the wall region an order of magnitude analysis is useful. The magnitude of the electric field is proportional to the thermal energy per length scale.

$$E \sim \frac{kT_i}{x} \tag{3.3}$$

In the sheath region the length scale is the Debye length.

$$E \sim \frac{kT_i}{\lambda_D} \tag{3.4}$$

Therefore, in this region the electric field is very significant since λ_D is very small. The collisional effects are small in comparison, and can be neglected.

In the presheath region the length scale is the mean free path.

$$E \sim \frac{kT_i}{\lambda_i} \tag{3.5}$$

Therefore, the electric field strength is on the order of the collisional effects making both important factors within this region.

In the neutral plasma region the length scale is the overall system dimension.

$$E \sim \frac{kT_i}{L} \tag{3.6}$$

Therefore, the electric field is very weak and can be neglected in comparison with the collisional effects.

3.3 Presheath Model

3.3.1 Equations Describing the Collective Behavior of a Plasma

The primary equation used to describe the behavior of a plasma is the Boltzmann equation. The Boltzmann equation represents the collective motion of many charged particles moving in an electromagnetic field[11].

$$\frac{\partial f}{\partial t} + v\frac{\partial f}{\partial x} \pm \frac{1}{m}\frac{\partial U}{\partial x}\frac{\partial f}{\partial v} = \{\frac{\partial f}{\partial t}\}_c \tag{3.7}$$

Where the + sign is for ion particles and the – sign is for electrons. In the Boltzmann equation f is the particle distribution function, and is defined such that $n = \int_{-\infty}^{\infty} f dv$.

The quantity t is time, v is a velocity vector, x is a position vector, m is the particle mass, and U is the potential. The term on the right hand side represents particle collisions and can take on various forms depending on the model being used.

Another important equation in describing the bahavior of a plasma is the Poisson equation. The Poisson equation is the elementary definition of potential as the collective effect of charged particles on a point[7].

$$\frac{d^2U}{dx^2} = 4\pi q^2\left[\int_{-\infty}^{\infty} f_i(v,\Delta U)\,dv - \int_{-\infty}^{\infty} f_e(v,\Delta U)\,dv\right] \tag{3.8}$$

Where q is the elementary charge, the subscript i refers to ions and the subscript e refers to electrons. The term in brackets is the ion - electron density difference. The potential is the driving force in the Boltzmann equation. The Poisson equation relates the potential to the particle distribution.

To complete the set of equations necessary for a full description of the presheath a collision term must be chosen to model the particle interactions. This study uses the Fokker - Planck collision term to model the particle collisions. The Fokker - Planck term represents the right hand side of the Boltzmann equation[11].

$$\left\{\frac{\partial f}{\partial t}\right\}_c = \Gamma\left[-\frac{\partial}{\partial v_i}\left(f\frac{m}{2M}\frac{\partial}{\partial v_i}\nabla^2 g\right) + \frac{1}{2}\frac{\partial^2}{\partial v_i \partial v_k}\left(f\frac{\partial^2 g}{\partial v_i \partial v_k}\right)\right] \tag{3.9}$$

Where,

$$\Gamma = \frac{q^2 q'^2 \ln\Lambda}{4\pi\epsilon_0^2 m^2} \tag{3.10}$$

$$g(v) = \int f(v') \mid v - v' \mid dv' \tag{3.11}$$

$$M = \frac{mm'}{m+m'} \tag{3.12}$$

Where M is called the reduced mass. No superscript refers to the particle species undergoing the collisions and the superscript $'$ refers to the particle species with which the collision occurs.

The Fokker - Planck equation describes the Coulomb collision between two charged particles. Certain restrictions and assumptions are made when using the Fokker - Planck collision term. First, it best describes fully ionized plasmas. The collision term models charged particle interaction and is most accurate for plasmas with few neutrals. This situation occurs only on the hottest of plasma surfaces like the diverter plates in Tokamak fusion reactors.

The second restriction involves the type of collisions that the Fokker - Planck term models. The overwhelming majority of particle collisions lead to only small deflections in the particle trajectories. The Fokker - Planck term describes the limit of these small angle deflections. Finally, the model does not take into account three body, and higher order, collisions.

3.3.2 Solution Conditions

The three equations presented in the previous section in conjunction with the asymptotic forms of potential and velocity distribution provide the necessary information to determine the presheath structure if two additional conditions are met.

First, if the equations are written in cylindrical coordinates the particle velocity distribution is axially symmetric. There is no theta, θ, dependence of the velocity distribution. Cylindrical coordinates are used for both the velocity and the position. The 'z' direction is perpendicular to the wall (see Figure 3.4) with the positive direction being defined into the wall. The coordinates R, θ, z have been used in velocity space for convenience.

The second condition for a solution to these equations involves an assumption of the particle velocity distribution parallel to the surface. For this model the radial velocity distribution has been assumed to take the form of a Maxwellian distribution. In addition, the temperature in the radial direction has been assumed

to be uniform and constant at all 'x' locations. Thus, the radial velocity distribution is constant for any position. Figure 3.5 is a schematic of these conditions. Note that at any 'x' location and rotation angle, θ, the radial velocity distribution is constant and follows a Maxwellian distribution. This represents the conditions of uniform temperature and axial symmetry, throughout the wall region. Figure 3.5 also shows a representation of the point of no returning ions. This is the point where the presheath transitions to the collisionless sheath.

The conditions of uniform temperature and radial Maxwellian distribution although good approximations are not exact models of the real situation.

The overall problem reduces to one dimension, the z direction, with the above conditions. The θ dependence having been removed by the axial symmetry and the radial dependence having been removed by the Maxwellian assumption. This one dimensional problem can be solved by staight forward numerical techniques.

3.3.3 Expansion of the Boltzmann Equation

The presheath model involves the expansion of the potential and velocity into asymptotic approximations. The potential is assumed to follow an exponential asymptotic form.

$$U = U_0 + a_1 \Delta U + a_2 \Delta U^2 + \cdots \tag{3.13}$$

where

$$U_0 = \alpha x \qquad \text{and} \qquad \Delta U = e^{\beta x} \tag{3.14}$$

$a_1, a_2 \cdots$ are parameters which describe the potential structure. Alpha, α, is non-zero for a non-zero potential gradient in the neutral plasma. ΔU is called the potential expansion parameter.

The particle distribution in velocity space is a function of potential and can be

similarly expanded.

$$f(v,\Delta U) = f_0(v) + \Delta U f_1(v) + \Delta U^2 f_2(v) + \cdots \tag{3.15}$$

The Boltzmann equation can be written as

$$\frac{\partial f}{\partial t} + v\frac{\partial f}{\partial(\Delta U)}\frac{\partial(\Delta U)}{\partial x} \pm \frac{1}{m}\frac{\partial U}{\partial x}\frac{\partial f}{\partial v} = \{\frac{\partial f}{\partial t}\}_c \tag{3.16}$$

where $\pm$ sign is respectively positive for ion particles and negative for electrons. The potential U has units of energy and is defined as shown in figure 3.3 such that $U = -e\Phi$ where Φ is electric potential. The Boltzmann equation can be expanded using equations 3.13 and 3.14. In addition since the solution is one dimensional in velocity space the velocity derivatives reflect only the 'z' direction. The following expansions are used.

$$\frac{\partial f}{\partial t} = \frac{\partial f_0}{\partial t} + \Delta U\frac{\partial f_1}{\partial t} + \Delta U^2\frac{\partial f_2}{\partial t} + \cdots \tag{3.17}$$

$$\frac{\partial f}{\partial(\Delta U)} = f_1 + 2\Delta U f_2 + 3\Delta U^2 f_3 + \cdots \tag{3.18}$$

$$\frac{\partial(\Delta U)}{\partial x} = \beta\Delta U \tag{3.19}$$

$$\frac{\partial U}{\partial x} = \alpha + \beta a_1\Delta U + 2\beta a_2\Delta U^2 + 3\beta a_3\Delta U^3 + \cdots \tag{3.20}$$

$$\frac{\partial f}{\partial z} = \frac{\partial f_0}{\partial z} + \Delta U\frac{\partial f_1}{\partial z} + \Delta U^2\frac{\partial f_2}{\partial z} + \cdots \tag{3.21}$$

Using these expansions the Boltzmann equation can be broken down by order in ΔU assuming the collision term can be likewise broken down:

$$1: \quad \frac{\partial f_0}{\partial t} \pm \frac{\alpha}{m}\frac{\partial f_0}{\partial z} = \left[\{\frac{\partial f}{\partial t}\}_c\right]_1 \tag{3.22a}$$

$$\Delta U: \quad \frac{\partial f_1}{\partial t} + \beta z f_1 \pm \frac{\alpha}{m}\frac{\partial f_1}{\partial z} \pm \frac{\beta a_1}{m}\frac{\partial f_0}{\partial z} = \left[\{\frac{\partial f}{\partial t}\}_c\right]_{\Delta U} \tag{3.22b}$$

$$\Delta U^2: \quad \frac{\partial f_2}{\partial t} + 2\beta z f_2 \pm \frac{\alpha}{m}\frac{\partial f_2}{\partial z} \pm \frac{\beta a_1}{m}\frac{\partial f_1}{\partial z} \pm \frac{2\beta a_2}{m}\frac{\partial f_0}{\partial z} = \left[\{\frac{\partial f}{\partial t}\}_c\right]_{\Delta U^2} \tag{3.22c}$$

$$\vdots$$

$$\Delta U^n: \quad \frac{\partial f_n}{\partial t} + n\beta z f_n \pm \frac{\alpha}{m}\frac{\partial f_n}{\partial z} \pm \frac{\beta a_1}{m}\frac{\partial f_{n-1}}{\partial z} \pm \frac{2\beta a_2}{m}\frac{\partial f_{n-2}}{\partial z} \pm \cdots \pm \frac{(n-1)\beta a_{n-1}}{m}\frac{\partial f_1}{\partial z} \pm \frac{n\beta a_n}{m}\frac{\partial f_0}{\partial z} = \left[\{\frac{\partial f}{\partial t}\}_c\right]_{\Delta U^n} \tag{3.22d}$$

The above exponential expansion is the only known way to break apart the Boltzmann equation. To complete the expansion the Poisson and Fokker - Planck terms must be similarly broken down.

At this point it is appropriate to nondimensionalize the expansion of the Boltzmann equation. The following nondimensional quantities have been used.

$$F_i = \frac{f_i}{n_R a^{3/2}} \quad \text{for} \quad 0 \le i \le n \tag{3.23a}$$

$$\tau = \frac{n_R \Gamma}{a^{1/2}} t \tag{3.23b}$$

$$Z = \sqrt{a'} z \tag{3.23c}$$

$$\varphi_{-1} = \frac{\alpha a}{m n_R \Gamma} \tag{3.23d}$$

$$\varphi_0 = \frac{\beta}{n_R \Gamma} \tag{3.23e}$$

$$\varphi_i = \frac{\beta a_i a}{m n_R \Gamma} \quad \text{for} \quad 1 \le i \le n \tag{3.23f}$$

Where n_R is a reference density, a and a' are the inverse square of the thermal velocities of the colliding particles, $a = \frac{m}{2kT}$ and $a' = \frac{m'}{2kT'}$. The quantities φ_{-1} through φ_n represent the potential structure of the presheath. F_i is nondimensionalized such that $1 = \int_{-\infty}^{\infty} F dZ$. Using these nondimensionalizations, the expansion of the Boltzmann equations becomes

$$1: \quad \frac{\partial F_0}{\partial \tau} \pm \varphi_{-1} \frac{\partial F_0}{\partial Z} = \left[\left\{ \frac{\partial F}{\partial \tau} \right\}_c \right]_1 \tag{3.24a}$$

$$\Delta U: \quad \frac{\partial F_1}{\partial \tau} + \varphi_0 Z F_1 \pm \varphi_{-1} \frac{\partial F_1}{\partial Z} \pm \varphi_1 \frac{\partial F_0}{\partial Z} = \left[\left\{ \frac{\partial F}{\partial \tau} \right\}_c \right]_{\Delta U} \tag{3.24b}$$

$$\Delta U^2: \quad \frac{\partial F_2}{\partial \tau} + 2\varphi_0 Z F_2 \pm \varphi_{-1} \frac{\partial F_2}{\partial Z} \pm \varphi_1 \frac{\partial F_1}{\partial Z} \pm 2\varphi_2 \frac{\partial F_0}{\partial Z} = \left[\left\{ \frac{\partial F}{\partial \tau} \right\}_c \right]_{\Delta U^2} \tag{3.24c}$$

$$\vdots$$

$$\Delta U^n: \quad \frac{\partial F_n}{\partial \tau} + n\varphi_0 Z F_n \pm \varphi_{-1} \frac{\partial F_n}{\partial Z} \pm \varphi_1 \frac{\partial F_{n-1}}{\partial Z} \pm 2\varphi_2 \frac{\partial F_{n-2}}{\partial Z} \pm \cdots \pm (n-1)\varphi_{n-1} \frac{\partial F_1}{\partial Z} \pm n\varphi_n \frac{\partial F_0}{\partial Z} = \left[\left\{ \frac{\partial F}{\partial \tau} \right\}_c \right]_{\Delta U^n} \tag{3.24d}$$

3.3.4 Expansion of the Poisson Equation

The Poisson equation,

$$\frac{d^2U}{dx^2} = 4\pi q^2\left[\int_{-\infty}^{\infty} f_i(v,\Delta U)\,dv - \int_{-\infty}^{\infty} f_e(v,\Delta U)\,dv\right] \tag{3.8}$$

is broken down using the same technique as the Boltzmann equation. Since:

$$\frac{\partial^2 U}{\partial x^2} = \beta^2 a_1 \Delta U + 4\beta^2 a_2 \Delta U^2 + 9\beta^2 a_3 \Delta U^3 + \cdots \tag{3.25}$$

$$\int_{-\infty}^{\infty} f(v,\Delta U)\,dv = \int_{-\infty}^{\infty} f_0(v)\,dv + \Delta U \int_{-\infty}^{\infty} f_1(v)\,dv + \Delta U^2 \int_{-\infty}^{\infty} f_2(v)\,dv + \cdots \tag{3.26}$$

Using these expansions the Poisson equation can be broken down by order in ΔU.

$$1: \quad 0 = 4\pi q^2\left[\int_{-\infty}^{\infty} f_{i0}\,dv - \int_{-\infty}^{\infty} f_{e0}(v)\,dv\right] \tag{3.27a}$$

$$\Delta U: \quad \beta^2 a_1 = 4\pi q^2\left[\int_{-\infty}^{\infty} f_{i1}(v)\,dv - \int_{-\infty}^{\infty} f_{e1}(v)\,dv\right] \tag{3.27b}$$

$$\Delta U^2: \quad 4\beta^2 a_2 = 4\pi q^2\left[\int_{-\infty}^{\infty} f_{i2}(v)\,dv - \int_{-\infty}^{\infty} f_{e2}(v)\,dv\right] \tag{3.27c}$$

$$\vdots$$

$$\Delta U^n: \quad n^2\beta^2 a_n = 4\pi q^2\left[\int_{-\infty}^{\infty} f_{in}(v)\,dv - \int_{-\infty}^{\infty} f_{en}(v)\,dv\right] \tag{3.27d}$$

The assumption of Boltzmann electrons is made to enable the numerical calculations to proceed with time steps on the order of an ion characteristic time. In the asymptotic presheath the Boltzmann electron assumption becomes

$$n_e = n_0 e^{-[a_1\Delta U + a_2\Delta U^2 + \cdots + a_n\Delta U^n]\frac{1}{kT_e}} \tag{3.28}$$

where n_e is the electron density, T_e is the electron temperature, and n_0 is the electron density in the asymptotic presheath at $\Delta U = 0$. Expansion of (3.28) in terms of ΔU yields

$$n_e = \left[n_0\right] + \Delta U\left[-\frac{a_1}{kT_e}n_0\right] + \Delta U^2\left[\left(-\frac{a_2}{kT_e} + \frac{1}{2}\frac{a_1^2}{(kT_e)^2}\right)n_0\right] + \Delta U^3\left[\left(-\frac{a_3}{kT_e} + \frac{a_1 a_2}{(kT_e)^2} - \frac{1}{6}\frac{a_1^3}{(kT_e)^3}\right)n_0\right] + \cdots \tag{3.29}$$

With the assumption that $\lambda_D \ll \lambda_i$ the Poisson equation reduces to equating electron and ion densities in order of ΔU. The Poisson and Boltzmann electron equations are nondimensionalized in the same manner as the Boltzmann equation. The nondimensionalized Poisson equation (3.27a-d) is combined with the Boltzmann electron equation (3.28) to become

$$\int_{-\infty}^{\infty} F_0\, dZ = \eta e^{[\varphi_1+\cdots+\varphi_n]\frac{1}{\varphi_0}\left(\frac{2T_i}{T_e}\right)} \tag{3.30a}$$

$$\int_{-\infty}^{\infty} F_1\, dZ = \eta e^{[\varphi_1+\cdots+\varphi_n]\frac{1}{\varphi_0}\left(\frac{2T_i}{T_e}\right)}\left[-\frac{\varphi_1}{\varphi_0}\left(\frac{2T_i}{T_e}\right)\right] \tag{3.30b}$$

$$\int_{-\infty}^{\infty} F_2\, dZ = \eta e^{[\varphi_1+\cdots+\varphi_n]\frac{1}{\varphi_0}\left(\frac{2T_i}{T_e}\right)}\left[-\frac{\varphi_2}{\varphi_0}\left(\frac{2T_i}{T_e}\right)+\frac{1}{2}\left(\frac{\varphi_1}{\varphi_0}\right)^2\left(\frac{2T_i}{T_e}\right)^2\right] \tag{3.30c}$$

$$\int_{-\infty}^{\infty} F_3\, dZ = \eta e^{[\varphi_1+\cdots+\varphi_n]\frac{1}{\varphi_0}\left(\frac{2T_i}{T_e}\right)}\left[-\frac{\varphi_3}{\varphi_0}\left(\frac{2T_i}{T_e}\right)+\frac{\varphi_1}{\varphi_0}\frac{\varphi_2}{\varphi_0}\left(\frac{2T_i}{T_e}\right)^2-\frac{1}{6}\left(\frac{\varphi_1}{\varphi_0}\right)^3\left(\frac{2T_i}{T_e}\right)^3\right] \tag{3.30d}$$

$$\vdots$$

where $\eta = \frac{n}{n_R}$ and may be specified as a function of time. This equation can be used to solve for the potential structure at each time step. T_i is the ion temperature and T_e is the electron temperature.

3.3.5 Expansion of the Fokker - Planck Term

The Fokker - Planck term must also be expanded in order of ΔU but first must be put into cylindrical coordinates. In addition, the assumption of axial symmetry must be accounted for in the term. This can be accomplished by expanding each term in the general Fokker - Planck term.

$$\left\{\frac{\partial f}{\partial t}\right\}_c = \Gamma\left[-\frac{\partial}{\partial v_i}\left(f\frac{m}{2M}\frac{\partial}{\partial v_i}\nabla^2 g\right)+\frac{1}{2}\frac{\partial^2}{\partial v_i \partial v_k}\left(f\frac{\partial^2 g}{\partial v_i \partial v_k}\right)\right] \tag{3.9}$$

The first term can be rewritten:

$$-\frac{m}{2M}\left(\nabla \cdot f\nabla(\nabla^2 g)\right) \tag{3.31}$$

$$\nabla^2 g = \frac{1}{R}\frac{\partial}{\partial R}\left(R\frac{\partial g}{\partial R}\right)+\frac{1}{R^2}\frac{\partial^2 g}{\partial \theta^2}+\frac{\partial^2 g}{\partial z^2} \tag{3.32}$$

Axial symmetry eliminates all θ dependence, eliminating the middle term. In addition, with the assumption of a Maxwellian radial velocity distribution the problem has been reduced to one dimension. Thus,

$$\nabla(\nabla^2 g) = \frac{\partial^3 g}{\partial z^3} \tag{3.33}$$

and the first term reduces to:

$$-\frac{\partial}{\partial z}\left(f\frac{m}{2M}\frac{\partial^3 g}{\partial z^3}\right) \tag{3.34}$$

The second term in the Fokker - Planck equation,

$$\frac{1}{2}\frac{\partial^2}{\partial v_i \partial v_k}\left(f\frac{\partial^2 g}{\partial v_i \partial v_k}\right),$$

can be reduced directly to the one dimensional case.

$$\frac{1}{2}\frac{\partial^2}{\partial z^2}\left(f\frac{\partial^2 g}{\partial z^2}\right) \tag{3.35}$$

Therefore, the Fokker - Planck term in one dimensional cylindrical coordinates is:

$$\frac{1}{\Gamma}\left\{\frac{\partial f}{\partial t}\right\}_c = \frac{1}{2}\frac{\partial^2}{\partial z^2}\left(f\frac{\partial^2 g}{\partial z^2}\right) - \frac{\partial}{\partial z}\left(f\frac{m}{2M}\frac{\partial^3 g}{\partial z^3}\right) \tag{3.36}$$

In order to get a complete collision model the function g must also be converted to the appropriate coordinate system.

$$g(v) = \int_{-\infty}^{\infty} f(v') \mid v - v' \mid dv'$$

This definition can be reduced for the one dimensional case.

$$g(z) = \int_{-\infty}^{\infty} f(\eta) \mid z - \eta \mid d\eta \tag{3.37}$$

or, written another way

$$g(z) = \int_{-\infty}^{\infty} f(z + \xi) \mid \xi \mid d\xi \tag{3.38}$$

With this definition the Fokker - Planck term becomes:

$$\frac{1}{\Gamma}\left\{\frac{\partial f}{\partial t}\right\}_c = \frac{1}{2}\frac{\partial^2}{\partial z^2}\left(f\int_{-\infty}^{\infty}\frac{\partial^2}{\partial z^2}(f(z+\xi))\mid\xi\mid d\xi\right) - \frac{\partial}{\partial z}\left(f\frac{m}{2M}\int_{-\infty}^{\infty}\frac{\partial^3}{\partial z^3}(f(z+\xi))\mid\xi\mid d\xi\right) \quad (3.39)$$

For brevity let $'$ denote a derivative with respect to z. Using this notation the Fokker - Planck term becomes:

$$\frac{1}{\Gamma}\left\{\frac{\partial f}{\partial t}\right\}_c = \frac{1}{2}\frac{\partial^2}{\partial z^2}\left(f\int_{-\infty}^{\infty}f''(z+\xi)\mid\xi\mid d\xi\right) - \frac{\partial}{\partial z}\left(f\frac{m}{2M}\int_{-\infty}^{\infty}f'''(z+\xi)\mid\xi\mid d\xi\right) \quad (3.40)$$

The Fokker - Planck term is nondimensionalized using the same variables as the Boltzmann equation.

$$\left\{\frac{\partial F}{\partial \tau}\right\}_c = \frac{\partial^2}{\partial Z^2}\left(F\frac{1}{2}\frac{a}{a'}\int_{-\infty}^{\infty}F''(Z+\varsigma)\mid\varsigma\mid d\varsigma\right) + \frac{\partial}{\partial Z}\left(F\frac{-m}{2M}\frac{a}{a'}\int_{-\infty}^{\infty}F'''(Z+\varsigma)\mid\varsigma\mid d\varsigma\right) \quad (3.41)$$

Let:

$$A(F) = \frac{1}{2}\frac{a}{a'}\int_{-\infty}^{\infty}F''(Z+\varsigma)\mid\varsigma\mid d\varsigma \quad (3.42)$$

$$B(F) = \frac{-m}{2M}\frac{a}{a'}\int_{-\infty}^{\infty}F'''(Z+\varsigma)\mid\varsigma\mid d\varsigma \quad (3.43)$$

The Fokker - Planck term can be written in a compact form using these defined functions.

$$\left\{\frac{\partial F}{\partial \tau}\right\}_c = \frac{\partial^2}{\partial Z^2}\Big(FA(F)\Big) + \frac{\partial}{\partial Z}\Big(FB(F)\Big) \quad (3.44)$$

The Fokker - Planck term can be expanded by order in ΔU using the same technique as the Boltzmann equation.

$$\begin{aligned}\left\{\frac{\partial F}{\partial \tau}\right\}_c = \quad & \left[\frac{\partial^2}{\partial Z^2}\Big(F_0A(F_0)\Big) + \frac{\partial}{\partial Z}\Big(F_0B(F_0)\Big)\right] \\ & + \Delta U\left[\frac{\partial^2}{\partial Z^2}\Big(F_1A(F_0)\Big) + \frac{\partial}{\partial Z}\Big(F_1B(F_0)\Big) + \frac{\partial^2}{\partial Z^2}\Big(F_0A(F_1)\Big) + \frac{\partial}{\partial Z}\Big(F_0B(F_1)\Big)\right] \\ & + \cdots \\ & + \Delta U^n\left[\sum_{m=0}^{n}\left(\frac{\partial^2}{\partial Z^2}\Big(F_{n-m}A(F_m)\Big) + \frac{\partial}{\partial Z}\Big(F_{n-m}B(F_m)\Big)\right)\right]\end{aligned} \quad (3.45)$$

This expansion can be combined directly with the expansion of the Boltzmann equation.

3.3.6 Solution Approach

To obtain a time dependent solution to the Boltzmann equation with the Fokker - Planck collision term a numerical technique is necessary. The solution presented has been limited to ion - ion collisions because these collisions represent the majority of the collisional energy and momentum transfer within the presheath. The positive signs in the Boltzmann equation must be applied for ion - ion collisions. The ratio of particle mass to reduced mass, $\frac{m}{M}$, must be equal to two for like particles. The ratio of the inverse squares of the particle thermal velocities, $\frac{a}{a'}$, must be one for like particle collisions. The nondimensional Boltzmann equation reduces to the following form.

$$\begin{aligned}&\frac{\partial F_i}{\partial \tau} - \frac{\partial^2}{\partial Z^2}\left(F_i A(F_0)\right) - \frac{\partial}{\partial Z}\left(F_i B(F_0)\right) + \varphi_0 i Z F_i + \varphi_{-1}\frac{\partial F_i}{\partial Z} \\ &= -\sum_{m=1}^{i} \varphi_m m \frac{\partial F_{i-m}}{\partial Z} + \sum_{m=1}^{i}\left(\frac{\partial^2}{\partial Z^2}\left(F_{i-m}A(F_m)\right) + \frac{\partial}{\partial Z}\left(F_{i-m}B(F_m)\right)\right)\end{aligned} \tag{3.46}$$

where the summations are taken to be zero if $i = 0$. The functions $A(F_m)$ and $B(F_m)$ can be written:

$$A(F) = \frac{1}{2}\int_{-\infty}^{\infty} F''(Z+\varsigma)\,|\,\varsigma\,|\,d\varsigma \tag{3.47}$$

$$B(F) = -\int_{-\infty}^{\infty} F'''(Z+\varsigma)\,|\,\varsigma\,|\,d\varsigma \tag{3.48}$$

The 'i' equations in the expansion are solved to obtain the time dependent particle velocity distribution. The Poisson equation is employed at each time step to obtain the potential structure. The ratio of the higher order equations with respect to the first order equation eliminates the $\eta e^{|\varphi_1+\cdots+\varphi_n|\frac{1}{\varphi_0}(\frac{2T_i}{T_e})}$ term from the Poisson equation. Using this technique each successive component of the potential

structure can be determined from the previous components.

$$\frac{\int_{-\infty}^{\infty} F_1\, dZ}{\int_{-\infty}^{\infty} F_0\, dZ} = -\frac{\varphi_1}{\varphi_0}\left(\frac{2T_i}{T_e}\right) \tag{3.49a}$$

$$\frac{\int_{-\infty}^{\infty} F_2\, dZ}{\int_{-\infty}^{\infty} F_0\, dZ} = -\frac{\varphi_2}{\varphi_0}\left(\frac{2T_i}{T_e}\right) + \frac{1}{2}\left(\frac{\varphi_1}{\varphi_0}\right)^2\left(\frac{2T_i}{T_e}\right)^2 \tag{3.49b}$$

$$\frac{\int_{-\infty}^{\infty} F_3\, dZ}{\int_{-\infty}^{\infty} F_0\, dZ} = -\frac{\varphi_3}{\varphi_0}\left(\frac{2T_i}{T_e}\right) + \frac{\varphi_1}{\varphi_0}\frac{\varphi_2}{\varphi_0}\left(\frac{2T_i}{T_e}\right)^2 - \frac{1}{6}\left(\frac{\varphi_1}{\varphi_0}\right)^3\left(\frac{2T_i}{T_e}\right)^3 \tag{3.49c}$$

$$\vdots$$

Using these equations the particle velocity distribution and the potential structure of the presheath are determined as a function of time.

Of interest in this study is the point at which there are no returning ions. This is the presheath - sheath interface. This occurs when the net ion flux away from the wall is zero. To calculate this point in the presheath it is necessary to obtain a value for the potential expansion parameter ΔU such that when the overall particle distribution is reconstructed from the various terms in the expansion no returning ions are present. Thus, at the critical point of no returning ions the model determines the total particle velocity distribution, the potential structure, and a value for the potential expansion parameter. From the potential structure and the potential expansion parameter the presheath height at the point of no returning ions can be determined (see figure 3.5).

CHAPTER IV

NUMERICAL TECHNIQUE

4.1 Problem Approach

The solution of the Boltzmann equation, as written in equation 3.46, coupled with the Poisson equation (3.49) is the goal of the numerical procedure.

The general approach is to solve the Boltzmann equation for the particle velocity distribution using a partially implicit, partially explicit scheme. Each step in time the Boltzmann equation is solved using some results from the previous time step. In equation 3.46 the left hand side is solved implicitly while the right hand side is solved explicitly.

$$\begin{aligned}&\frac{\partial F_i}{\partial \tau} - \frac{\partial^2}{\partial Z^2}\left(F_i A(F_0)\right) - \frac{\partial}{\partial Z}\left(F_i B(F_0)\right) + \varphi_0 i Z F_i + \varphi_{-1}\frac{\partial F_i}{\partial Z} \\ &= -\sum_{m=1}^{i} \varphi_m m \frac{\partial F_{i-m}}{\partial Z} + \sum_{m=1}^{i}\left(\frac{\partial^2}{\partial Z^2}\left(F_{i-m}A(F_m)\right) + \frac{\partial}{\partial Z}\left(F_{i-m}B(F_m)\right)\right)\end{aligned} \tag{3.46}$$

The left hand side of this equation can be put in a matrix form.

$$\begin{bmatrix} & T(\tau) & \end{bmatrix}\begin{bmatrix} F_i(\tau+\Delta\tau) \end{bmatrix} \tag{4.1}$$

In this form the matrix $T(\tau)$ is an $m \times m$ matrix created from the left hand side of the Boltzmann equation. The quantity m is the number of divisions in the velocity space Z chosen for the numerical scheme. The matrix $T(\tau)$ is computed from $A(F_0(\tau))$ and $B(F_0(\tau))$. The values of these derived functions are taken from the solution to the particle velocity distribution at the previous time step, τ. Numerical derivatives are used to represent the partial derivatives in the equation. This procedure produces a diagonal matrix where all elements except those on an odd number of centered

diagonals are zero. The number of diagonals reflects the order of accuracy in the solution. Diagonal matrices of this form are easily and quickly inverted. The $F_i(\tau+\Delta\tau)$ matrix is an $m\times 1$ matrix of unknowns that represents the particle velocity distribution at the current time step. 'i' equations of this form can be written corresponding to the number of terms in the expansion.

The right hand side of the Boltzmann equation can also be put in a matrix form.

$$\varphi_1\left[v_i^1(\tau)\right]+\cdots+\varphi_n\left[v_i^n(\tau)\right]+\left[d_i(\tau)\right] \tag{4.2}$$

The scalar φ_n values are unknowns and represent the nondimensional coefficients in the asymptotic potential structure of the presheath.

The $v_i^n(\tau)$ matrices are $m\times 1$ matrices which are comprised of the partial derivatives of the velocity distribution at the previous time step, τ. They represent the first summation on the right hand side of the Boltzmann equation.

$$\sum_{m=1}^{i}\varphi_m\left(-m\frac{\partial F_{i-m}}{\partial Z}\right)$$

The d_i matrix is an $m\times 1$ matrix comprised of the second summation on the right hand side of the Boltzmann equation.

$$\sum_{m=1}^{i}\left(\frac{\partial^2}{\partial Z^2}\left(F_{i-m}A(F_m)\right)+\frac{\partial}{\partial Z}\left(F_{i-m}B(F_m)\right)\right)$$

All values of the distribution and the functions $A(F_m)$ and $B(F_m)$ are taken at the previous time step, τ.

Putting together equations 4.1 and 4.2 a matrix form of the Boltzmann equation is created that can be solved for the particle velocity distribution.

$$\left[\quad T(\tau)\quad\right]\left[F_i(\tau+\Delta\tau)\right]=\varphi_1\left[v_i^1(\tau)\right]+\cdots+\varphi_n\left[v_i^n(\tau)\right]+\left[d_i(\tau)\right] \tag{4.3}$$

'i' equations of this form can be written corresponding to the number of terms in the asymptoic expansion being used.

These equations are quickly inverted to obtain the particle velocity distribution at the current time step.

$$\left[F_i(\tau+\Delta\tau)\right] = \varphi_1\left[V_i^1(\tau)\right] + \cdots + \varphi_n\left[V_i^n(\tau)\right] + \left[D_i(\tau)\right] \tag{4.4}$$

Where the V_n and D matrices represent the $m \times 1$ solution matrix to the inversion of the $T(\tau)$ matrix with the corresponding v_n or d matrix.

The particle velocity distribution is obtained from this equation using the φ_n values from the previous time step.

Equation 3.49 is employed to obtain the φ_n values at the current time step.

$$\frac{\int_{-\infty}^{\infty} F_1\,dZ}{\int_{-\infty}^{\infty} F_0\,dZ} = -\frac{\varphi_1}{\varphi_0}\left(\frac{2T_i}{T_e}\right) \tag{3.49a}$$

$$\frac{\int_{-\infty}^{\infty} F_2\,dZ}{\int_{-\infty}^{\infty} F_0\,dZ} = -\frac{\varphi_2}{\varphi_0}\left(\frac{2T_i}{T_e}\right) + \frac{1}{2}\left(\frac{\varphi_1}{\varphi_0}\right)^2\left(\frac{2T_i}{T_e}\right)^2 \tag{3.49b}$$

$$\frac{\int_{-\infty}^{\infty} F_3\,dZ}{\int_{-\infty}^{\infty} F_0\,dZ} = -\frac{\varphi_3}{\varphi_0}\left(\frac{2T_i}{T_e}\right) + \frac{\varphi_1}{\varphi_0}\frac{\varphi_2}{\varphi_0}\left(\frac{2T_i}{T_e}\right)^2 - \frac{1}{6}\left(\frac{\varphi_1}{\varphi_0}\right)^3\left(\frac{2T_i}{T_e}\right)^3 \tag{3.49c}$$

$$\vdots$$

The new distributions are integrated numerically and the φ_1 through φ_n scalars are determined consecutively. The value of φ_0 is input and is a nondimensional representation of the coefficient β in the potential expansion parameter, ΔU.

For each time step, the overall particle velocity distribution can be determined at any location from the original expansion once it has been nondimensionalized.

$$F(Z,\Delta U^*) = F_0(Z) + \Delta U^* F_1(Z) + \Delta U^{*2} F_2(Z) + \cdots \tag{4.5}$$

since,

$$\Delta U^* = e^{\varphi_0 x^*} \tag{4.6}$$

Where the * quantities are nondimensional. x has been nondimensionalized with respect to an ion mean free path.

$$x^* = \frac{x}{n_R \Gamma}$$

The potential structure of the presheath is detemined from the nondimensional form of the original expansion of potential.

$$U^* = U_0^* + \varphi_1 \Delta U^* + \varphi_2 \Delta U^{*2} + \cdots \tag{4.7}$$

Using this procedure the time dependent evolution of the presheath is obtained.

The point of no returning ions occurs where the integral of the left half plane of the total particle velocity distribution is zero.

$$0 = \int_{-\infty}^{0} F(Z) dZ \tag{4.8}$$

This equation can be rewritten using the expansion of the particle distribution.

$$0 = \int_{-\infty}^{0} F_0(Z) dZ + \Delta U^* \int_{-\infty}^{0} F_1(Z) dZ + \Delta U^{*2} \int_{-\infty}^{0} F_2(Z) dZ + \cdots \tag{4.9}$$

Equation 4.9 can be solved for ΔU^* Since the particle distributions are now known as a function of time and velocity. The entire solution at the point of no returning ions is known with this last piece of information.

4.2 Numerical Integration, Differentiation, and Matrix Inversion

In order to obtain a solution to the potential structure and particle distribution in the presheath it is necessary to develope the applicable mathematical tools. The primary techniques needed are integration, differentiation, and matrix inversion.

4.2.1 Numerical Integration

Throughout the solution integration is computed using a Simpson's $\frac{1}{3}$ rule technique[12].

$$\int_a^b f(x)dx = \frac{h}{3}\left(f_1 + 4f_2 + 2f_3 + 4f_4 + 2f_5 + \cdots + 2f_{n-1} + 4f_n + f_{n+1}\right) \tag{4.10}$$

Where h is the spacing between the points and f_1 through f_{n+1} represent the function values at each point. This procedure has a global error of $O(h^4)$. If the step size is chosen appropriately this procedure is very accurate.

4.2.2 Numerical Differentiation

The technique for determining numerical differentiation is a second order accurate scheme. This reduces the number of computations while maintaining high accuracy. Second order accurate numerical differentiation requires that only three points be known. Thus, the '$T(\tau)$' matrix contains only three diagonals. If third order accuracy was used the '$T(\tau)$' matrix would require five diagonals to represent the five points needed for the differentiation. In addition, to maintain uniformity a central difference technique is desirable on as many points as possible. The greater the number of points needed for each derivative the more points that require forward or backward difference techniques (rather than the central difference technique). Below is a list of the techniques used to obtain derivatives[12].

Central Difference

$$\frac{\partial F}{\partial x} = \frac{F(x+1) - F(x-1)}{2h} \tag{4.11a}$$

$$\frac{\partial^2 F}{\partial x^2} = \frac{F(x+1) - 2F(x) + F(x-1)}{h^2} \tag{4.11b}$$

$$\frac{\partial^3 F}{\partial x^3} = \frac{F(x+2) - 2F(x+1) + 2F(x-1) - F(x-2)}{2h^3} \tag{4.11c}$$

Forward Difference

$$\frac{\partial F}{\partial x} = \frac{-F(x+2) + 4F(x+1) - 3F(x)}{2h} \tag{4.12a}$$

$$\frac{\partial^2 F}{\partial x^2} = \frac{F(x+2) - 2F(x+1) + F(x)}{h^2} \tag{4.12b}$$

$$\frac{\partial^3 F}{\partial x^3} = \frac{F(x+3) - 3F(x+2) + 3F(x+1) - F(x)}{h^3} \tag{4.12c}$$

Backward Difference

$$\frac{\partial F}{\partial x} = \frac{3F(x) - 4F(x-1) + 3F(x-2)}{2h} \tag{4.13a}$$

$$\frac{\partial^2 F}{\partial x^2} = \frac{F(x) - 2F(x-1) + F(x-2)}{h^2} \tag{4.13b}$$

$$\frac{\partial^3 F}{\partial x^3} = \frac{F(x) - 3F(x-1) + 3F(x-2) - F(x-3)}{h^3} \tag{4.13c}$$

Where h is the grid spacing. The derivatives are being taken about point x.

It is worth noting that the third derivative equations require up to five points. There is no second order accurate numerical third derivative representation. These equations are third order accurate. This does not effect the '$T(\tau)$' matrix in that it contains no third derivatives. The solution procedure requires third derivatives only in the determination of the function $B(F_i(\tau))$.

These equations are used throughout the solution for derivatives with respect to velocity, Z, and time, τ.

4.2.3 Matrix Inversion

In order to obtain a solution a procedure for inverting a diagonal matrix is necessary. The procedure used will invert any centered diagonal matrix. For the second order accurate case the matrix in question is tridiagonal. The procedure uses Guassian elimination on all terms below the center diagonal and then through back substitution determines the solution vector. This technique can quickly invert a 200×200 tridiagonal matrix.

4.3 Obtaining a Solution

As in any numerical model certain restraints and conditions must be met to obtain an accurate solution. This model requires some form of input distribution function and in order to obtain higher order terms must also have a perturbation applied to the potential structure. In addition, certain numerical techniques have been used to remove instabilities in the model.

4.3.1 Initial Distribution

To model the presheath region an initial particle velocity distribution that conforms to a Maxwellian profile has been used. This profile represents the distribution that naturally occurs in the neutral plasma region. The idea is that the time dependent evolution of the distribution will change from a Maxwellian at time zero to a shifted new form as the presheath is entered. The Maxwellian profile is initially given to the zero order term having set the initial conditions of all higher order terms to zero.

If the potential structure of the presheath is not perturbed in some manner then the model represents the neutral plasma region and the particle velocity distribution remains Maxwellian (as it should). If, however, a small perturbation in the potential stucture is added (ie. a nonzero $a_1, a_2 \cdots$) then the model readjusts to describe the presheath region. In this manner the model is used to give the time dependent evolution of the presheath.

4.3.2 Instability Damping

By the nature of the implicit - explicit technique being employed certain numerical problems are expected to appear. This model is no exception. Two techniques have been used to remove these instabilities.

The most important thing to do to avoid numerical problems in a scheme of this nature is to ensure that as much as possible of the solution is computed implicitly. In addition, once some new data has been calculated it should be applied to any new calculations immediately.

In this model each term in the expansion of the particle distribution function uses the new data already determined in calculating all of the lower order terms. Once F_0 is determined that information is used in calculating F_1. This idea is repeated for the higher order terms.

A second method applied to the model to eliminate oscilliatory instabilities that start on a very small scale and grow is the application of a very weak averaging scheme to the particle distribution functions. Each point in the distribution is weakly averaged with the points on either side.

$$F(Z) = \frac{0.025F(Z+1) + F(Z) + 0.025F(Z-1)}{1.05} \tag{4.14}$$

This technique, although necessary, has the negative effect of falsely increasing the energy in the system by spreading the distribution slightly (see figure 5.1). The change is very small and can be considered insignificant with respect to the overall solution.

4.4 Program Structure

The entire program has been written in FORTRAN and can be run on either an IBM PC AT or on the CYBER mainframe. The code has been written in a segmented manner that easily allows one section to be altered without having to alter other sections. The overall structure of the program consists of three initialization programs, three input data files, the main program, and three output data files. The main program contains a driver and seventeen subroutines. Several of the sub-

routines perform operations that are used throughout the main code. Figure 4.1 is a diagram of the structure of the program. The flexibility of the code is derived from the generalized subroutine structure and the ability to enter a variety of input variables. The driver keeps track of time and maintains the overall operating structure of the solution while the subroutines perform the necessary manipulations. Below is a list of the function of each program, data file and subroutine.

AVE - Subroutine to smooth distributions by averaging.

CONSERV - Subroutine to determine conservation of energy, momentum, and particles.

CONSOUT - Conservation output data file.

CRF - Particle distribution initialization program.

CRPHI - Potential structure initialization program.

DENSITY - Subroutine to solve for a new presheath structure.

FDATA - Initial particle distribution data file.

FD1 - Subroutine to find first derivatives.

FD2 - Subroutine to find second derivatives.

FD3 - Subroutine to find third derivatives.

FINDA - Subroutine to determine 'A' function.

FINDB - Subroutine to determine 'B' function.

FPINIT - Primary initialization program.

FPOUT - Output particle distribution data file.

FPSHETH - Main program driver.

GETAB - Subroutine to make A and B function vectors.

INITDAT - Initialization data file.

MAKED - Subroutine to make d matrix.

MAKEF - Subroutine to read initial particle distribution.

MAKEPHI - Subroutine to read initial potential structure.

MAKET - Subroutine to make T matrix.

MAKEV - Subroutine to make v matrix.

MODIAG - Subroutine to invert diagonal matices.

PHIDAT - Initial potential structure data file.

PHIDOUT - Output potential structure data file.

SIMPS - Subroutine to perform Simpson's rule integration.

TOT - Subroutine to obtain total distribution at point of no returning ions.

CHAPTER V

RESULTS

The ratio of ion temperature to electron temperature, $\frac{T}{T_e}$, has been set to one half throughout these results. There is little effect on the particle distribution or potential structure if the temperature ratio is changed to other values. The electron temperature is expected to be higher than the ion temperature in the presheath since electrons absorb energy from electric and magnetic fields faster than ions and other large particles.

Through repeated test runs of the model it was found that fifty-one points in velocity space were enough to provide high accuracy and produce good results. The range of points in velocity space has been truncated to ± 5 nondimensional units. The results show that at ± 5 the distribution is near zero, substantiating the truncation.

A time step of 0.2 nondimensional times was found to keep the solution accurate. Three nondimensional units in time were sufficient to produce stable results.

It was found that the magnitude of the higher order terms in the particle velocity distribution drop off very rapidly. Thus, the higher order terms have very little impact on the shape of the potential or of the particle distribution.

To understand the effects of a quiescent plasma interacting with a surface the potential gradient in the neutral plasma has been set to zero. To accomplish this the α term in the expansion of potential has been set to zero.

$$U = U_0 + a_1 \Delta U + a_2 \Delta U^2 + \cdots \tag{3.13}$$

where

$$U_0 = \alpha x \qquad \text{and} \qquad \Delta U = e^{\beta x} \tag{3.14}$$

A stable solution exists only for a specific critical value of the exponential coeficient, β, which represents the scale of the presheath. The quantitiy β is nondimensionalized as $\varphi_0 = \frac{\beta}{n_R \Gamma}$, where $n_R \Gamma$ is an ion mean free path. It is expected, as shown in section 3.2, that the critical value should be on the order of a mean free path. It was found that $\frac{\beta}{n_R \Gamma} = 0.4$ produces the most nearly stable results. The distributions become unstable for values greater or less than 0.4. The small remaining instability at $\frac{\beta}{n_R \Gamma} = 0.4$ can be attributed to the inexact nature of the numerical solution.

The results presented here are first order and produce a complete picture of the structure of the presheath because the higher order terms collective contribution is more than an order of magnitude smaller. Figures 5.1 and 5.2 are plots of the zeroth and first order expansions of the particle distribution in velocity space. The zero order term remains Maxwellian because the potential gradient in the neutral plasma is zero. The first order term of the distribution obtains a profile that has roughly the shape (but not magnitude) of the negative first derivative of the zeroth order solution. The potential expansion parameter at the point of no returning ions is determined for each time step. Using the particle distribution functions and the known potential expansion parameter together produce the overall particle velocity distribution at the point of no returning ions, the presheath - sheath interface. Figure 5.3 shows this distribution.

The positive shift in the total distribution is as expected for the presheath. The ions are being pulled into the wall. The particle distribution for velocities away from the wall is zero for the case of no returning ions. The point of no returning ions exists where the particle distribution for velocities away from the wall integrates

to zero. Figure 5.3 shows that the ion distribution becomes negative for velocities away from the wall. A negative particle distribution cannot exist physically. The addition of higher order terms does not correct the problem because the expansion drops off so quickly that any higher order terms have no impact on the shape of the distribution. The problem is fundamental to the type of collision term being applied in the model. The Fokker - Planck term only models the limit of small angle collisions. However, large angle collisions become important in the presheath.

The first term of the nondimensionalized potential structure, φ_1, has been initially perturbed to 1.0×10^{-4} to obtain the results presented in figures 5.1, 5.2 and 5.3. Perturbing the potential structure provides the model with the nonequilibrium condition necessary to initiate the time dependent development of the presheath. The strength of the initial perturbation is not significant to obtaining an accurate particle distribution and potential structure of the presheath. Figures 5.4, 5.5, and 5.6 are the result of an initial perturbation of 1.0×10^{-3} and figures 5.7, 5.8 and 5.9 are the result of an initial perturbation of 1.0×10^{-5}. Comparing these results show that the magnitude of the initial perturbation only affects the scale of the first order term and has no effect on the overall particle distribution in velocity space.

Figure 5.10 is a plot of the position of the point of no returning ions, the presheath - sheath interface, as a function of time for the three solutions. Since no source of ions exists in the model the relative position of the plasma with respect to the surface changes as a function of time. The wall is moving into the plasma, or the plasma is moving into the wall, at the rate at which the wall is absorbing ions. The three solutions have different magnitudes but follow the same profile. The strength of the perturbation controls the relative position of the zero point.

Figure 5.11 is a plot of the potential structure of the presheath obtained from

the three solutions as a function of position. The data for the potential structure has been taken from the solution at a nondimensional time of two. Note that the affect of the different initial perturbation values is to cause a shift in the relative position of the potential but has no effect on the shape of the potential or on the strength of the potential at the point of no returning ions. Changing the perturbation strength alters the location of the zero point but not its shape. The stronger the perturbation the further the zero point is moved from the surface. The horizontal line in the plot depicts the presheath height at the point of no returning ions. The vertical lines show the position of the point of no returning ions.

A time dependent plot of the presheath height at the point of no returning ions is presented in figure 5.12. This plot shows that the time evolution of the sheath height approaches smoothly to a nearly constant value of 0.16. All three solutions fall on the same curve. This shows that the strength of the perturbation does not affect the results obtained.

CHAPTER VI

CONCLUSIONS

The solution obtained is an accurate representation of the time dependent development of the Fokker - Planck presheath. The model produces a precise potential structure, however, the distribution of returning ions breaks down in the presheath. An oscillation developes in the negative tail of the distribution, as seen in figures 5.3, 5.6, and 5.9. This oscillation cannot be removed by including additional terms to the expansion. In addition, the sheath height of 0.16 determined at the point of no returning ions is roughly an order of magnitude smaller than expected. Both of these conditions lead to the conclusion that the Fokker - Planck collision term does not represent the type of collisions that remove the returning ions in the presheath. This breakdown is do to the failure of the Fokker - Planck collision term to model the large angle collisions that take place within the presheath. The Fokker - Planck term is effective at modeling the collisions present in the center of the plasma but breaks down in the presheath. The primary mechanism behind clearing out the returning ions from within the presheath is not particle diffusion as represented by small angle deflections but rather the large velocity changes caused by large angle collisions. Since the Fokker - Planck term models particle collisions that represent the limit of small angle collisions it is inadequate at describing the mechanisms controlling the ion velocity distribution moving away from the wall. The solutions obtained using a Maxwellian distribution by Bissell and Johnson[4] and Emmert et al.[3] and those obtained using a charge exchange collision model by Riemann[6] and Main[7] effectively include the large angle collisions since they model the collisions

by instantaneous changes in particle velocity and position. These collision models do not represent the Coulomb collisions taking place in a fully ionized plasma. They do not represent the collision processes but only approximate the collisional effects.

This Fokker - Planck presheath model produces a self-consistent and precise potential structure. The particle velocity distribution in the presheath has the correct acceleration of ions toward the wall but because the Fokker - Planck collision term only models the limit of small angle collisions it is unable to clear the particle distribution of returning ions. The effect of not modeling the large angle collisions is that the particle distribution for returning ions is accurate only in the initial section of the presheath where the collisional processes are dominated by particle diffusion. The collisional processes become dominated by the effects of the large angle collisions as the interface between the presheath and the Debye sheath is approached. Only by including a collision term which accounts for these large angle collisions can a presheath model produce a particle velocity distribution that accurately models the condition of no returning ions. This study has found that a presheath model which describes the Coulomb collisions occurring in a fully ionized plasma must account for both the small angle collisions and the large angle collisions.

REFERENCES

[1] D. Bohm, in Characteristics of Electrical Discharges in Magnetic Fields,edited by A. Guthrie and R. Wakering, McGraw - Hill, New York, 1949, p. 77

[2] S. A. Self, "Exact Solution of the Coliisionless Plasma - Sheath Equation", The Physics of Fluids, Vol. 6, No. 12, Dec. 1963

[3] G. A. Emmert, R. M. Wieland, A. T. Mense, and J. N. Davidson, "Electric Sheath and Presheath in a Collisionless Finite Ion Temperature Plasma", The Physics of Fluids, Vol. 23, No. 4, April 1980

[4] R. C. Bissell and P. C. Johnson, "The Solution of the Plasma Equation in a Plane Parallel Geometry with a Maxwellian Source", The Physics of Fluids, Vol. 30, No. 3, March 1987

[5] R. C. Bissell, "The Application of the Generalized Bohm Criterion to Emmert's Solution of the warm ion Collisionless Plasma Equatuion", The Physics of Fluids, Vol. 30, No. 7, July 1987

[6] K. -U. Riemann, "Kinetic Theory of the Plasma Sheath Transition in a Weakly Ionized Plasma", The Physics of Fluids, Vol. 24, No. 12, March 1987

[7] G. L. Main, "Asymptotically Correct Collisional Presheaths", The Physics of Fluids, Vol. 30, No. 6, June 1987

[8] I. Langmuir, Phys. Rev.,34: 876 (1929)

[9] F. F. Chen, Introduction to Plasma Physics and Controled Fusion, vol. 1, Plenum, New York, 1984, p. 10

[10] K. Miyamoto, Plasma Physics for Nuclear Fusion, The MIT Press, Cambridge, Mass., 1980, p. 602

[11] G. Schmidt, Physics of High Temperature Plasmas, Academic Press, New York, 1979

[12] C. F. Gerald and P. O Wheatley, Applied Numerical Analysis, Addison - Wesley, Reading, Mass., 1984

[13] C. M. Bender and S. A. Orszag, Advanced Mathematical Methods for Scientists and Engineers, McGraw - Hill, New York, 1978

FIGURES

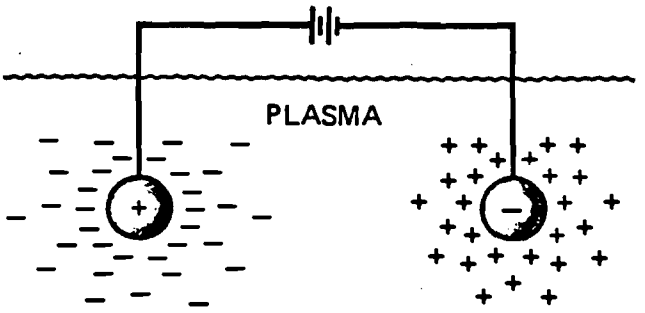

Figure 3.1 Debye Shielding

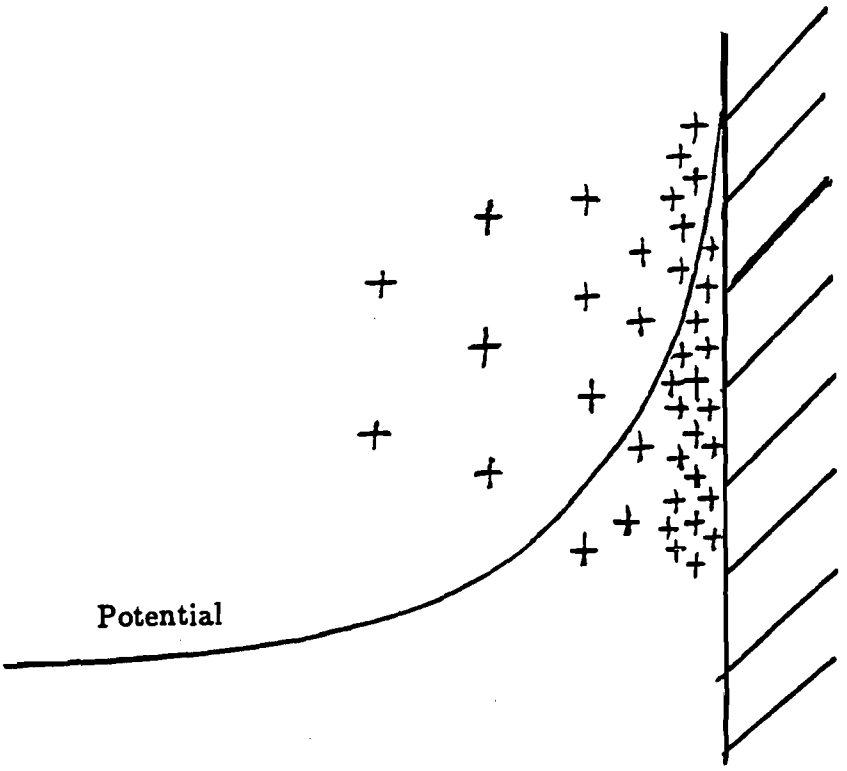

Figure 3.2 Wall Potential

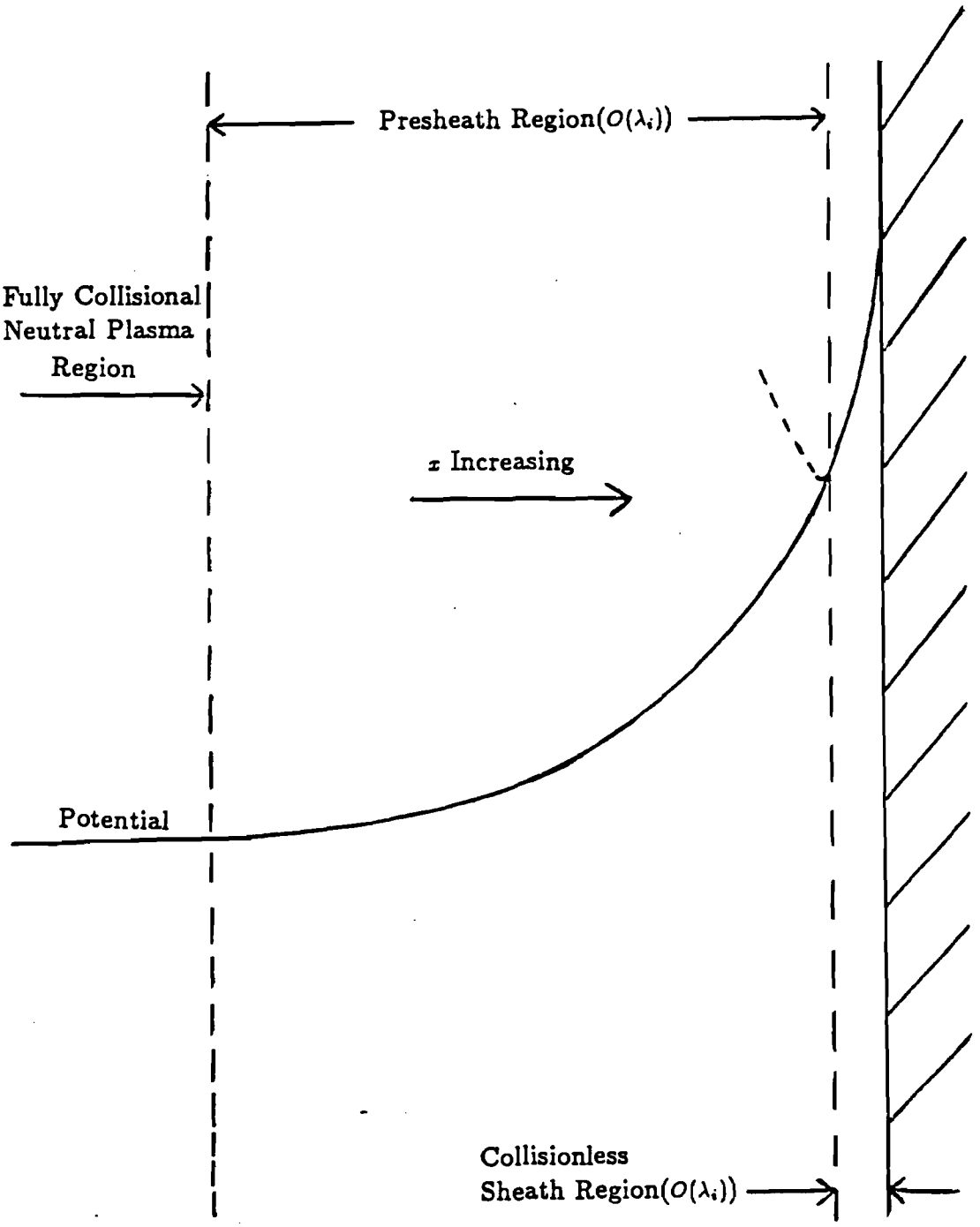

Figure 3.3 Wall Region Model

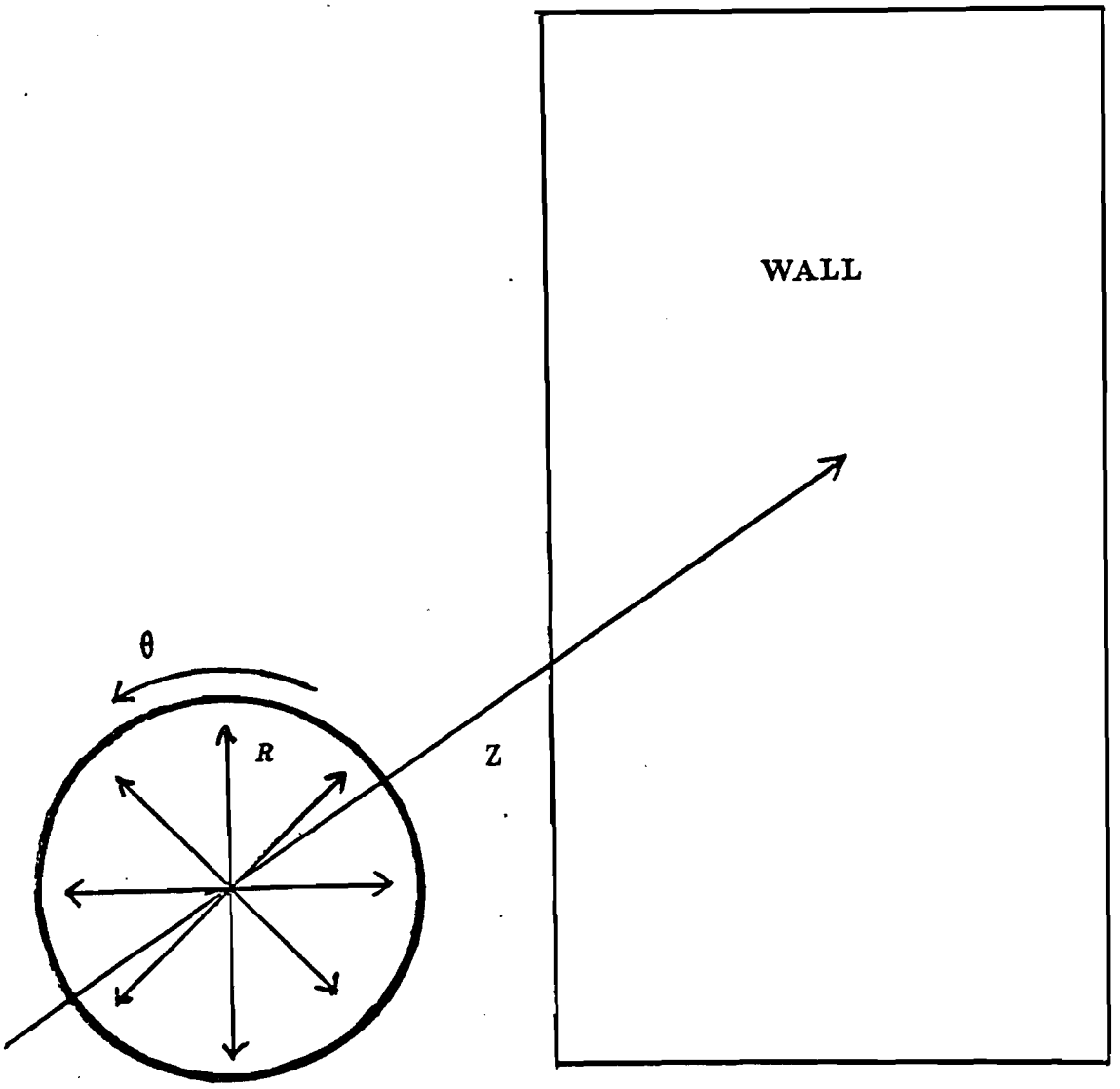

Figure 3.4 Coordinate System in Velocity Space

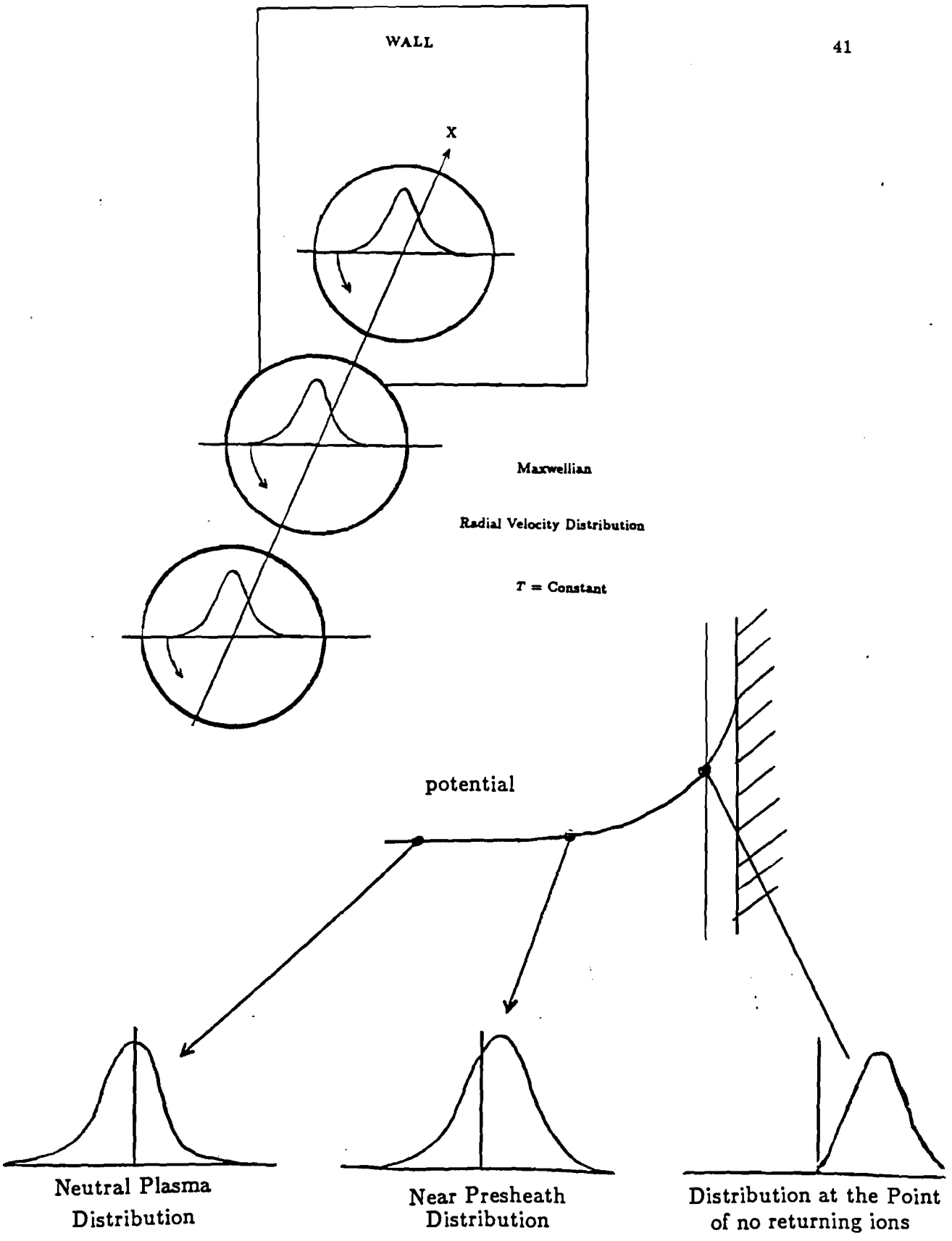

Figure 3.5 Radial, Symmetric, and No Returning Ions Conditions

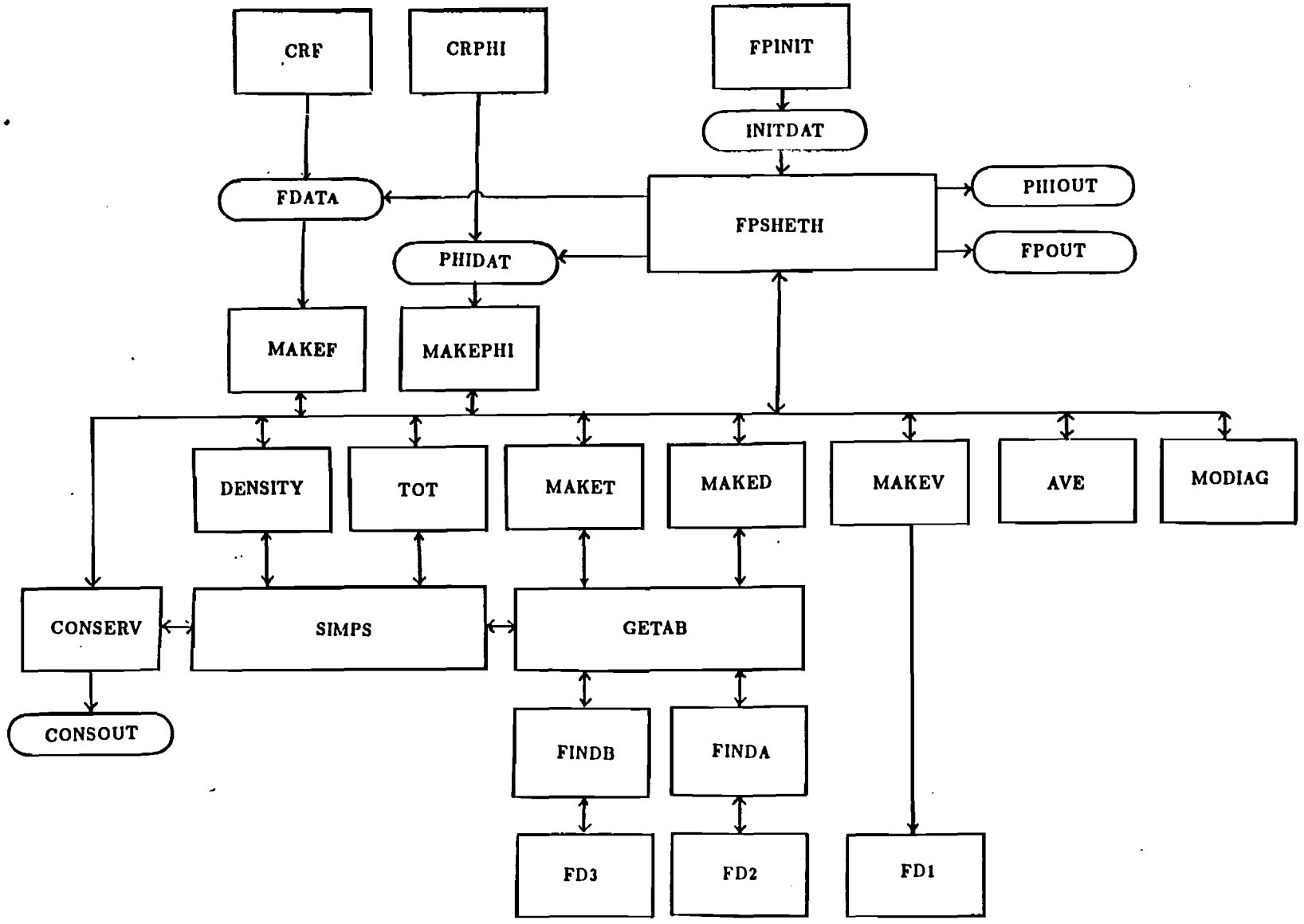

Figure 4.1 Program Diagram

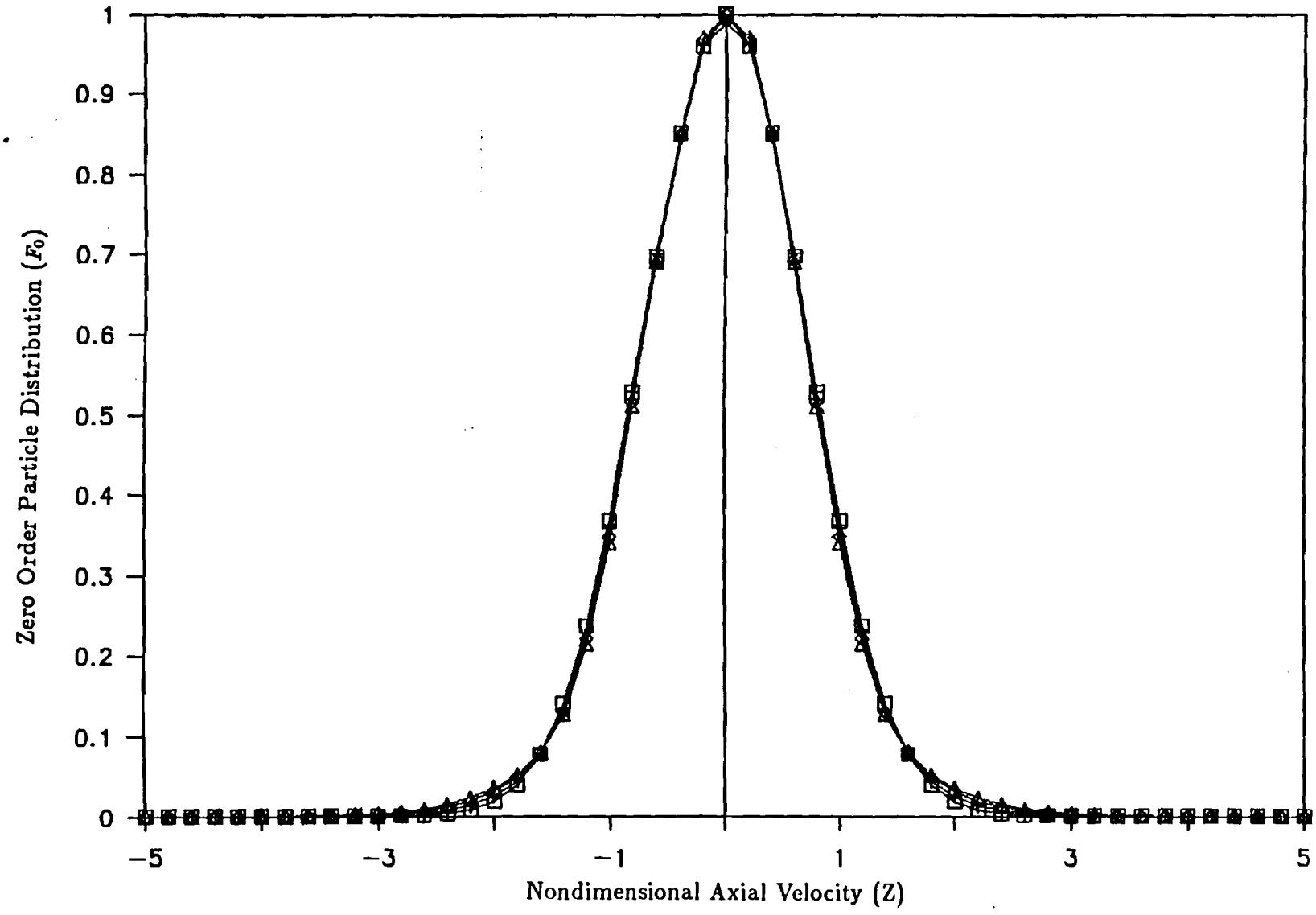

Figure 5.1 Zero Order Particle Velocity Distribution, $\omega_1 = 1.0 \times 10^{-4}$

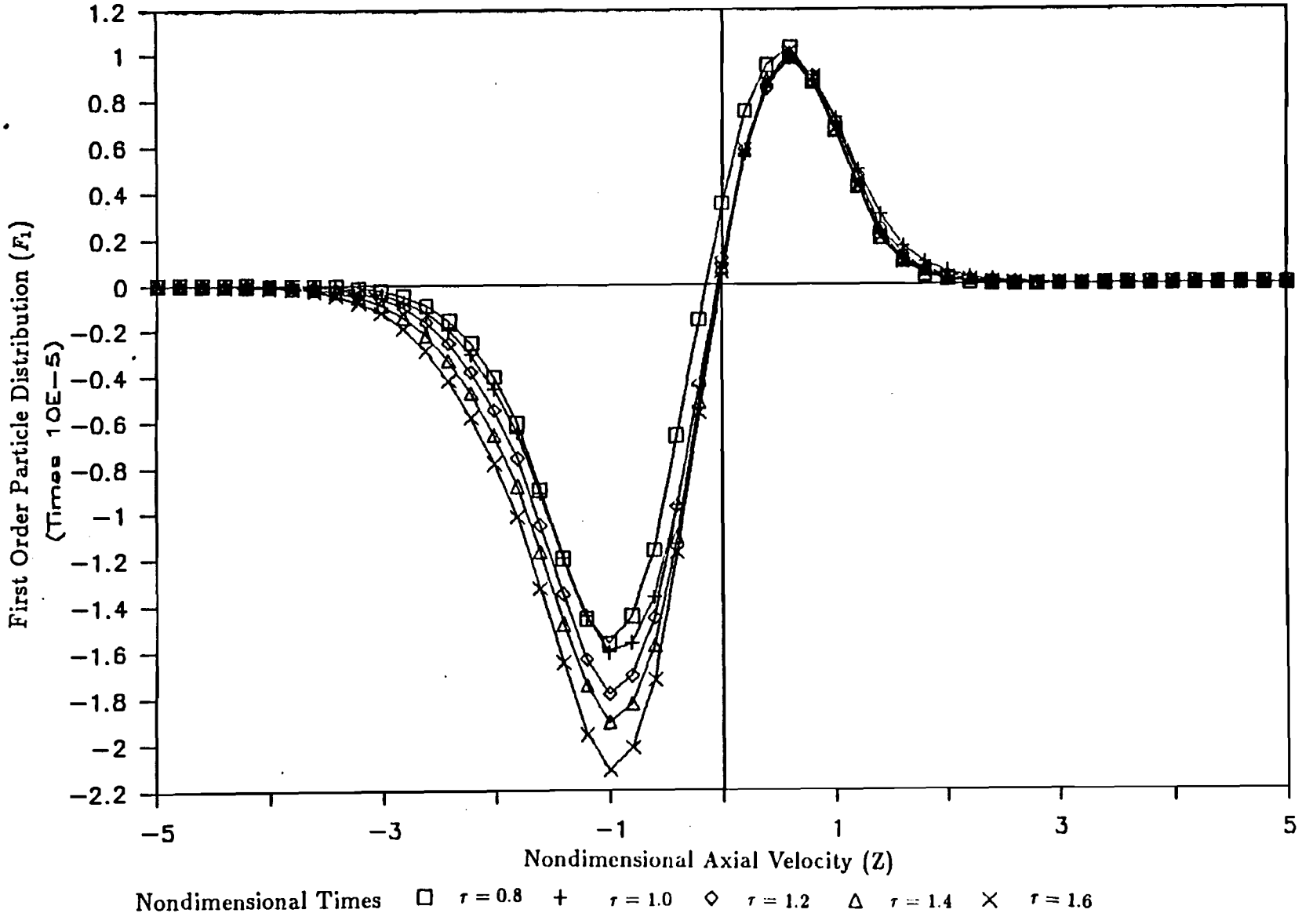

Figure 5.2 First Order Particle Velocity Distribution, $\varphi_1 = 1.0 \times 10^{-4}$

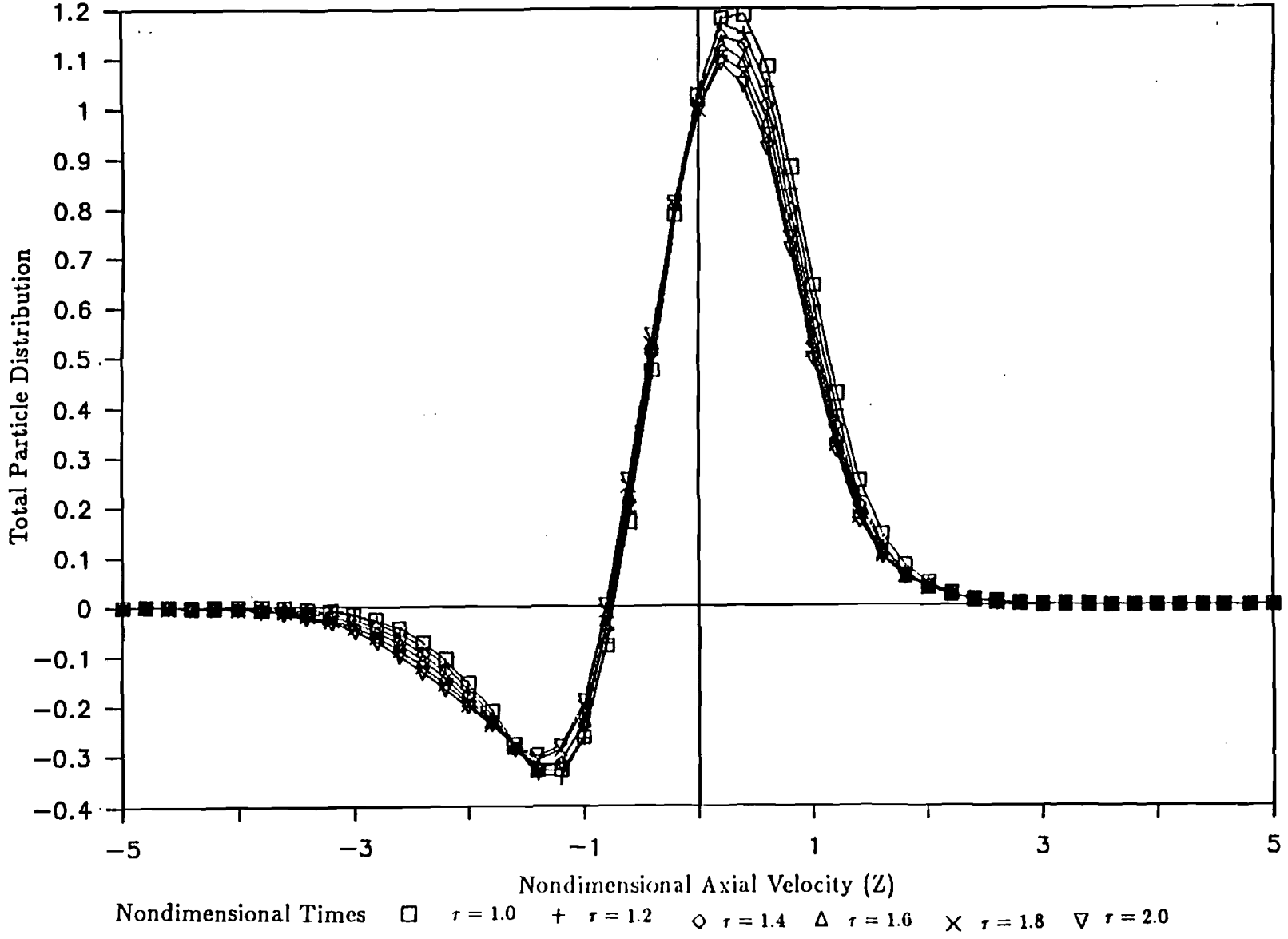

Figure 5.3 Total Particle Velocity Distribution, $\varphi_1 = 1.0 \times 10^{-4}$

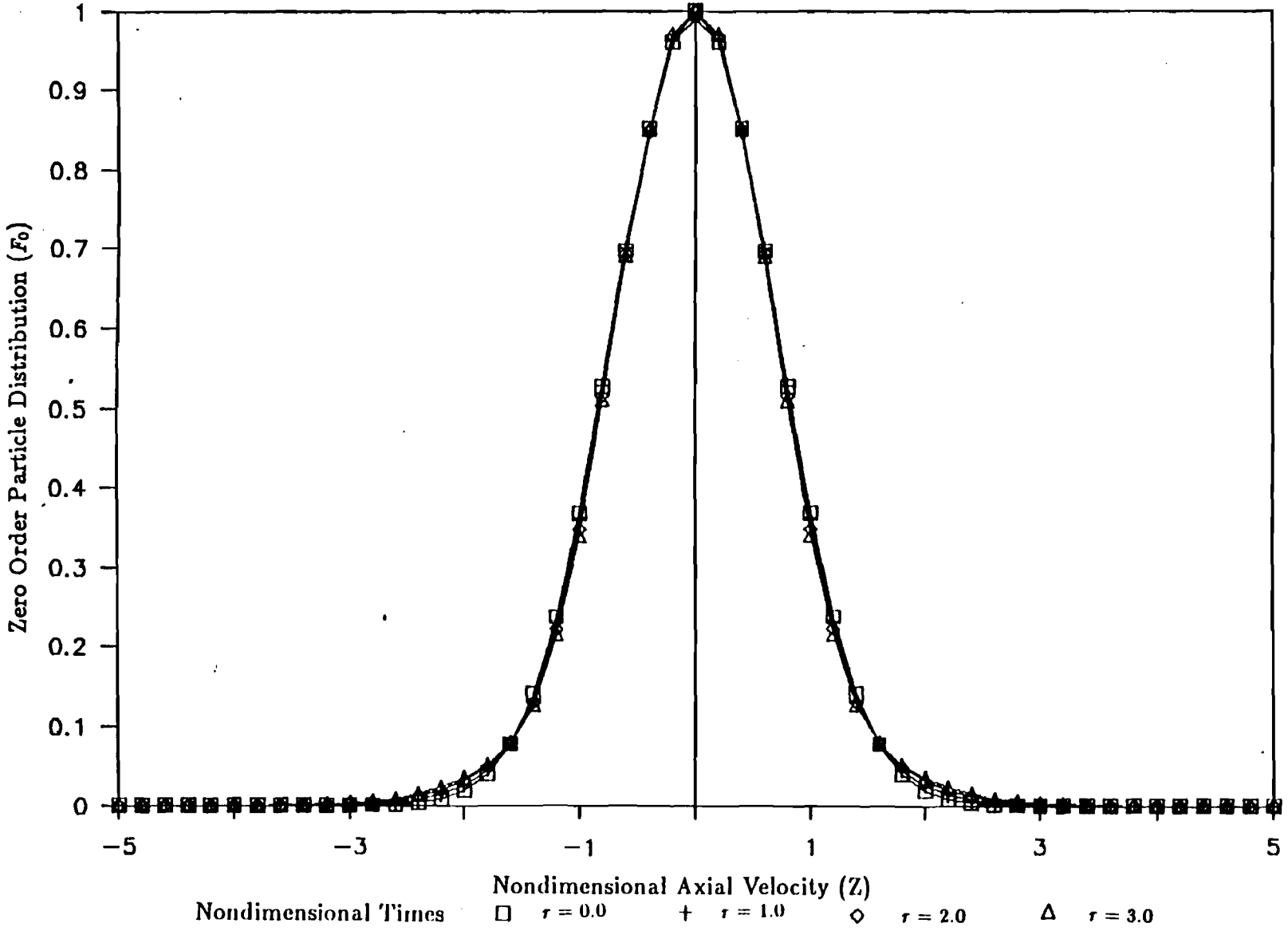

Figure 5.4 Zero Order Particle Velocity Distribution, $\varphi_1 = 1.0 \times 10^{-3}$

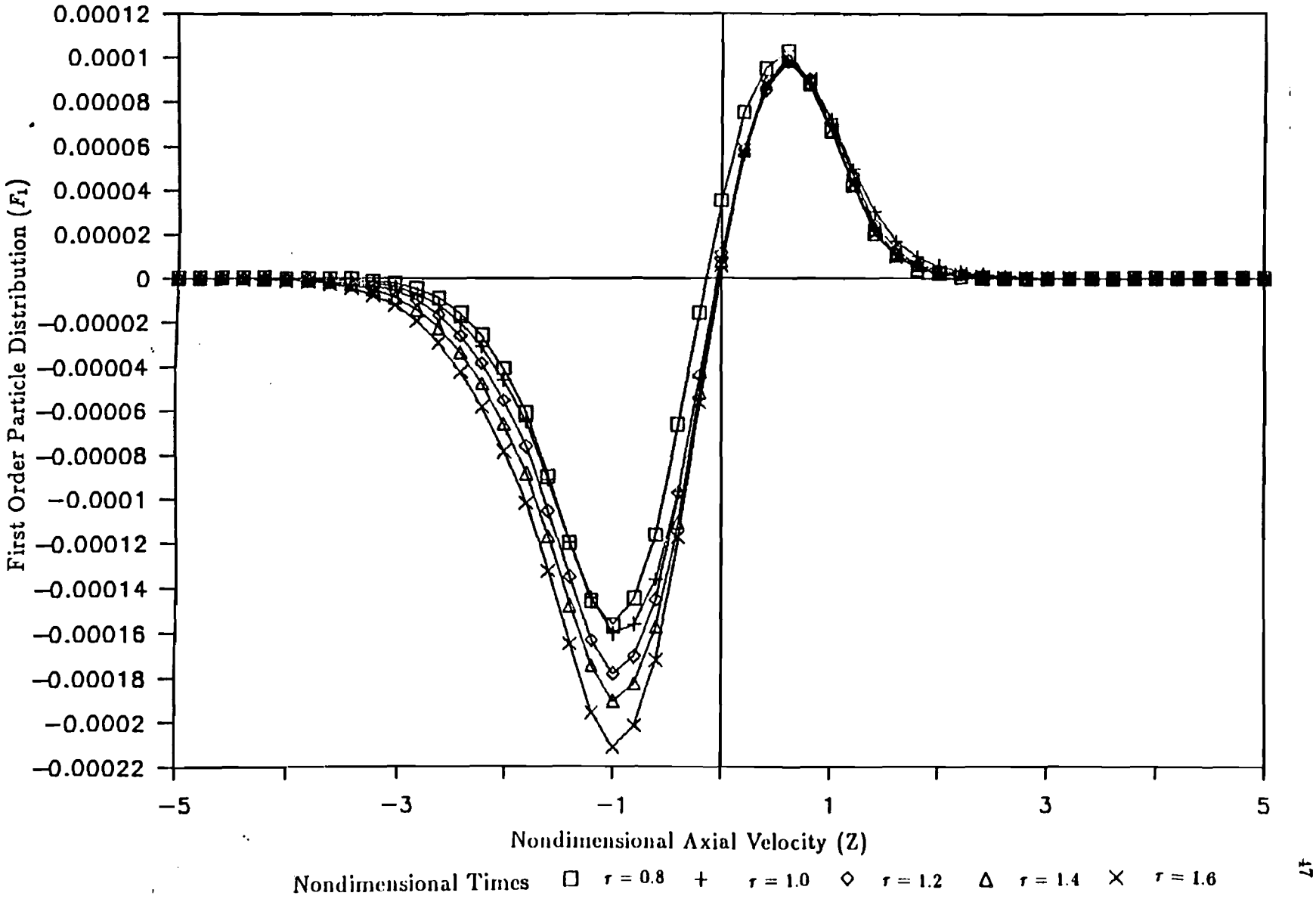

Figure 5.5 First Order Particle Velocity Distribution, $\varphi_1 = 1.0 \times 10^{-3}$

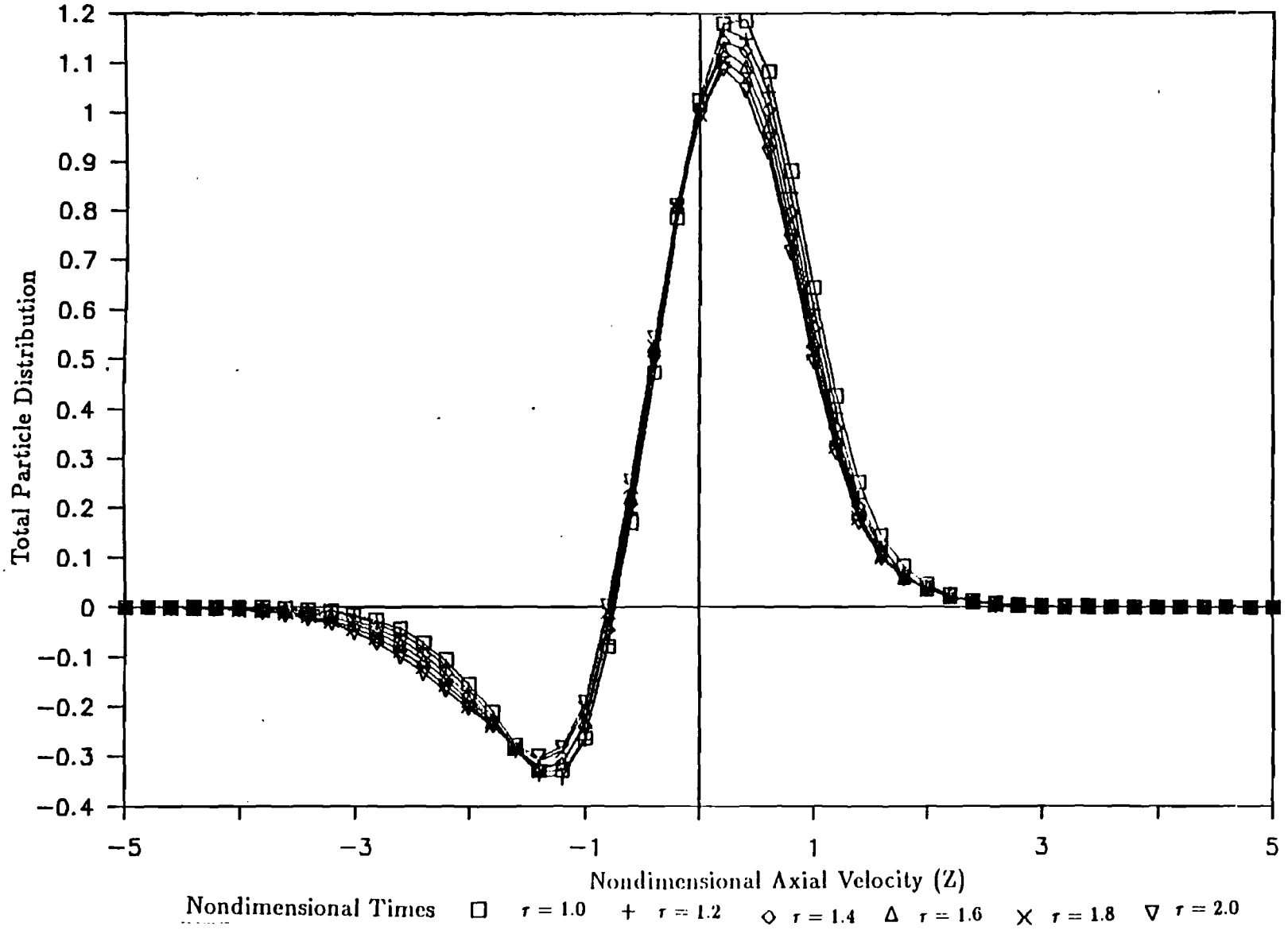

Figure 5.6 Total Particle Velocity Distribution, $\varphi_1 = 1.0 \times 10^{-3}$

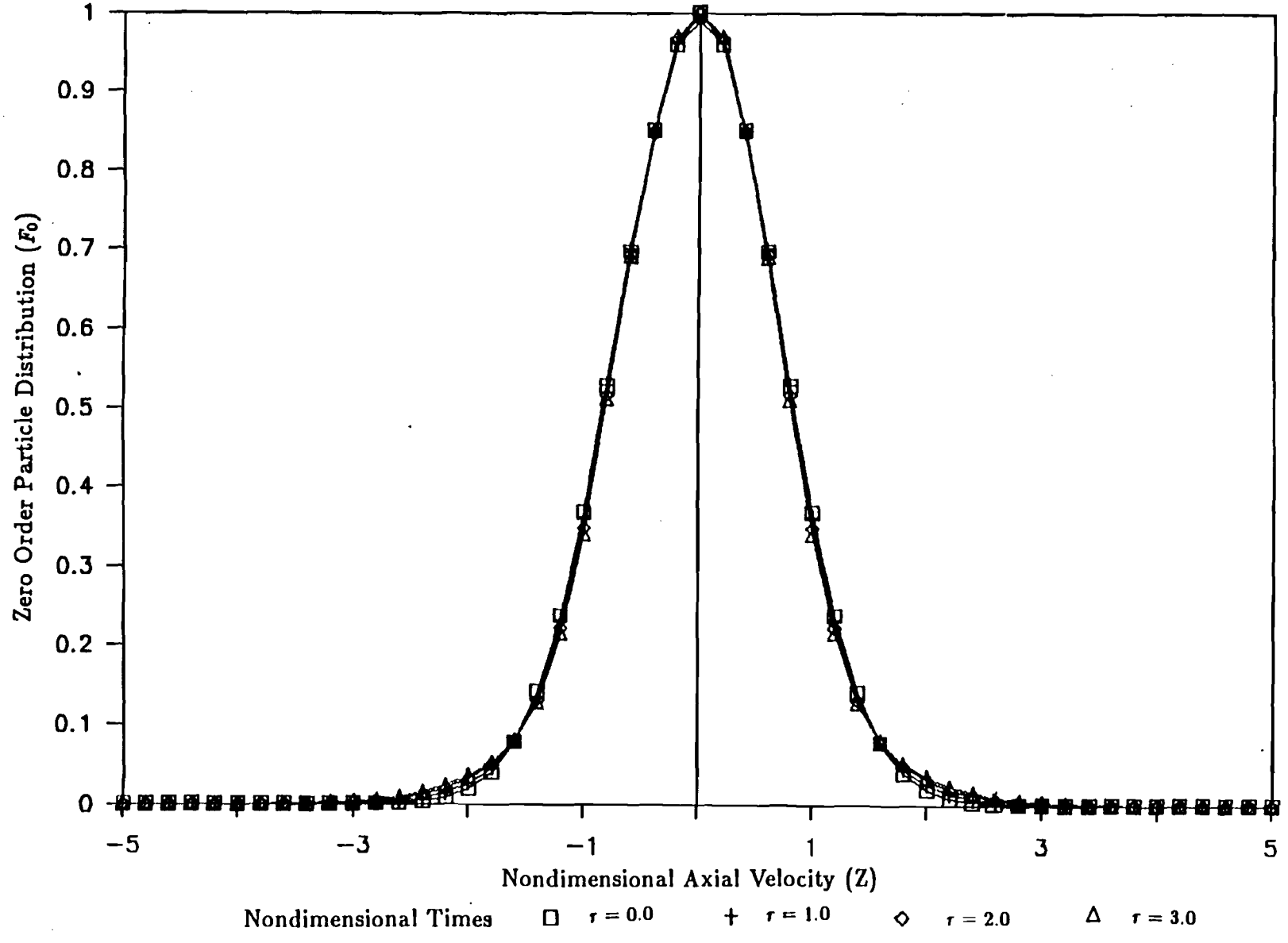

Figure 5.7 Zero Order Particle Velocity Distribution, $\varphi_1 = 1.0 \times 10^{-5}$

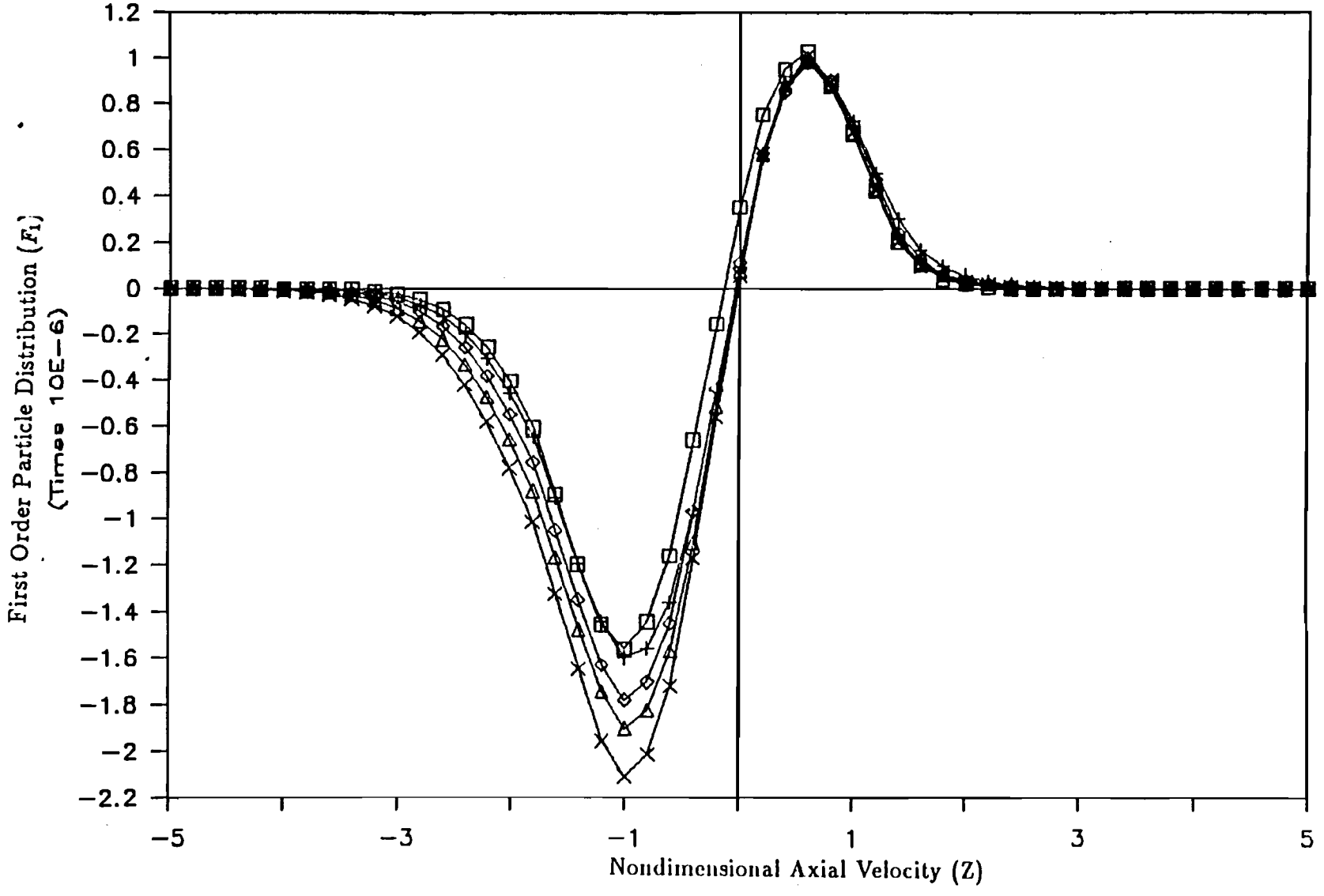

Figure 5.8 First Order Particle Velocity Distribution, $\varphi_1 = 1.0 \times 10^{-6}$

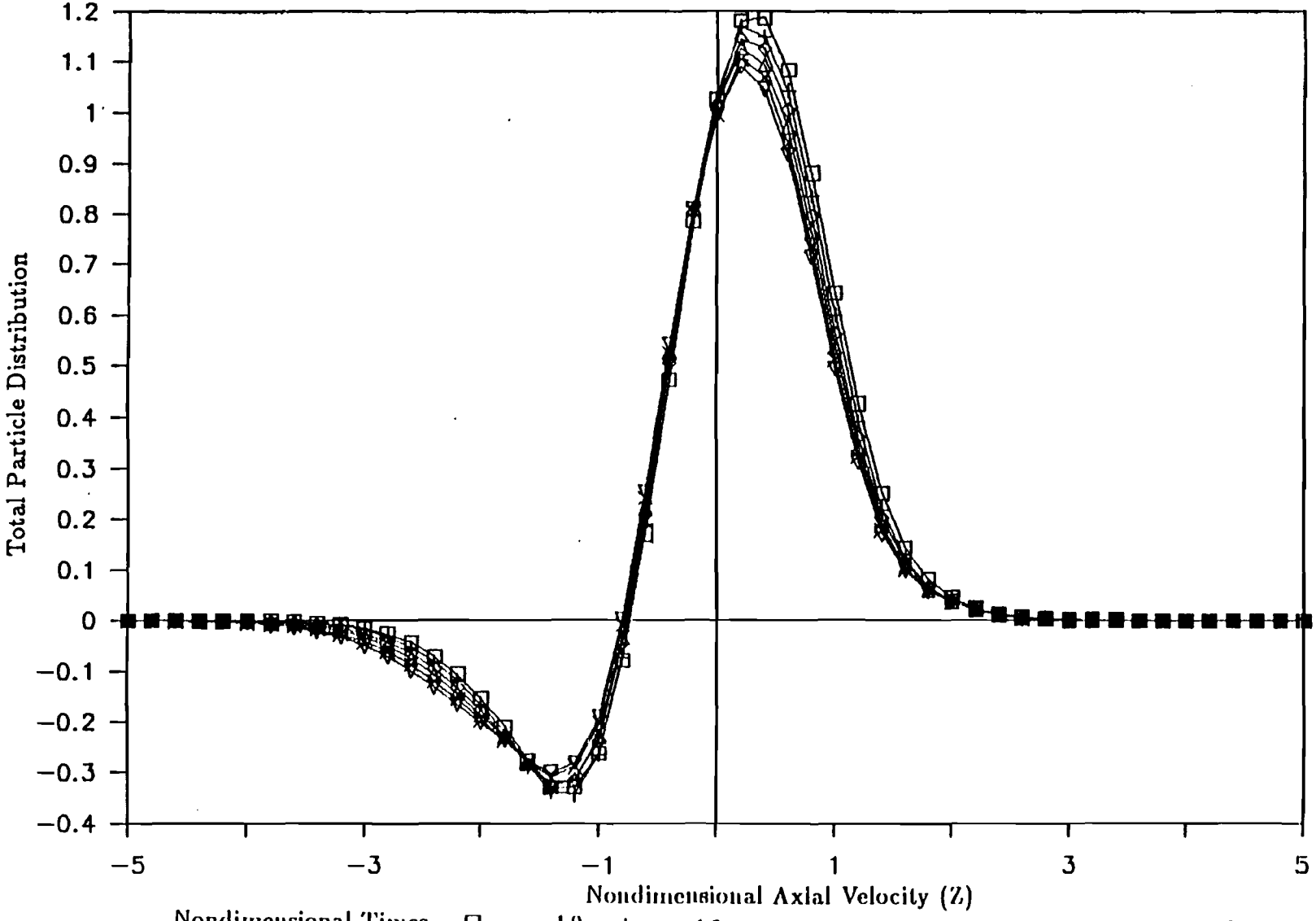

Figure 5.9 Total Particle Velocity Distribution, $\varphi_1 = 1.0 \times 10^{-5}$

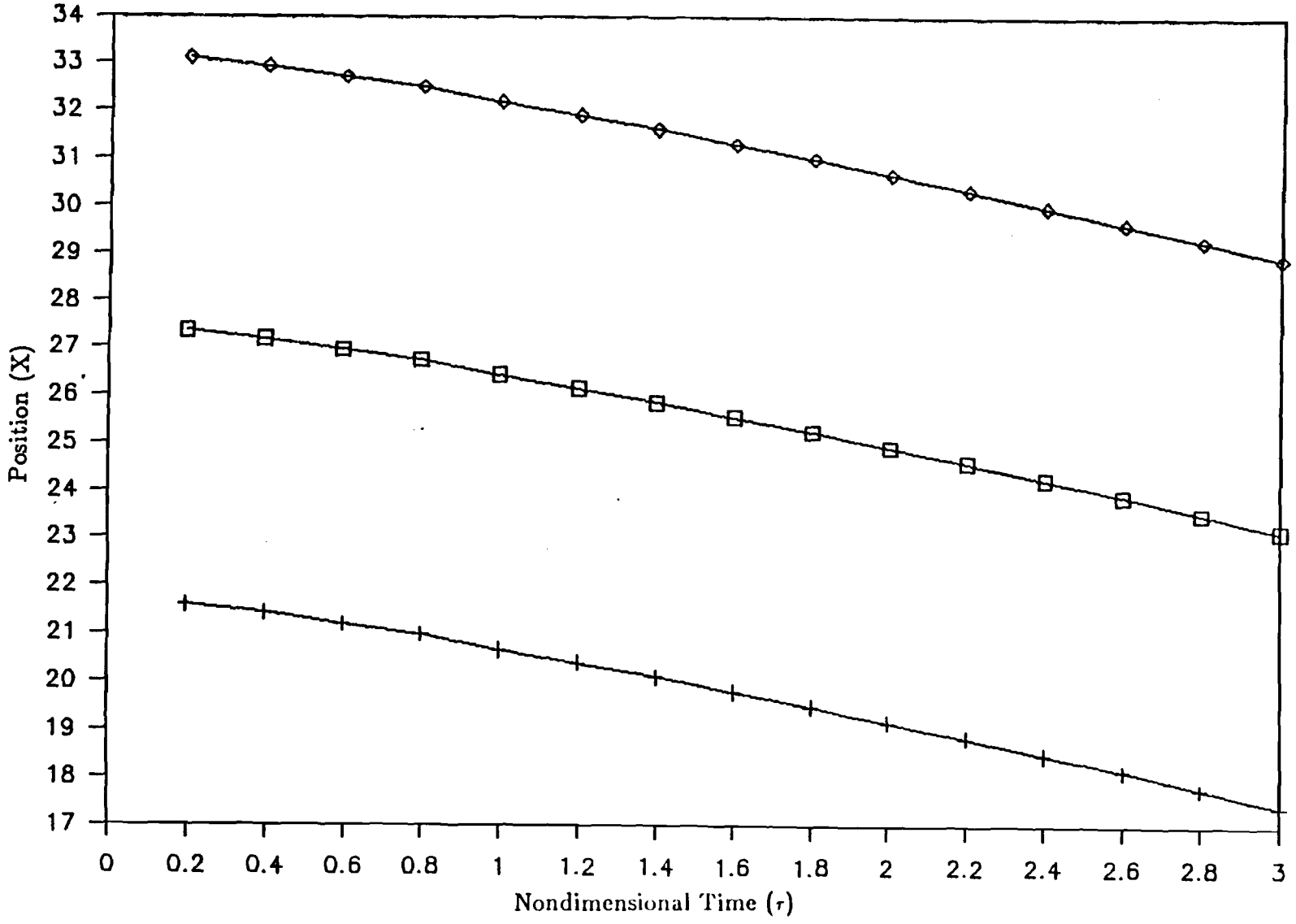

Figure 5.10 Time Dependent Position of the Potential

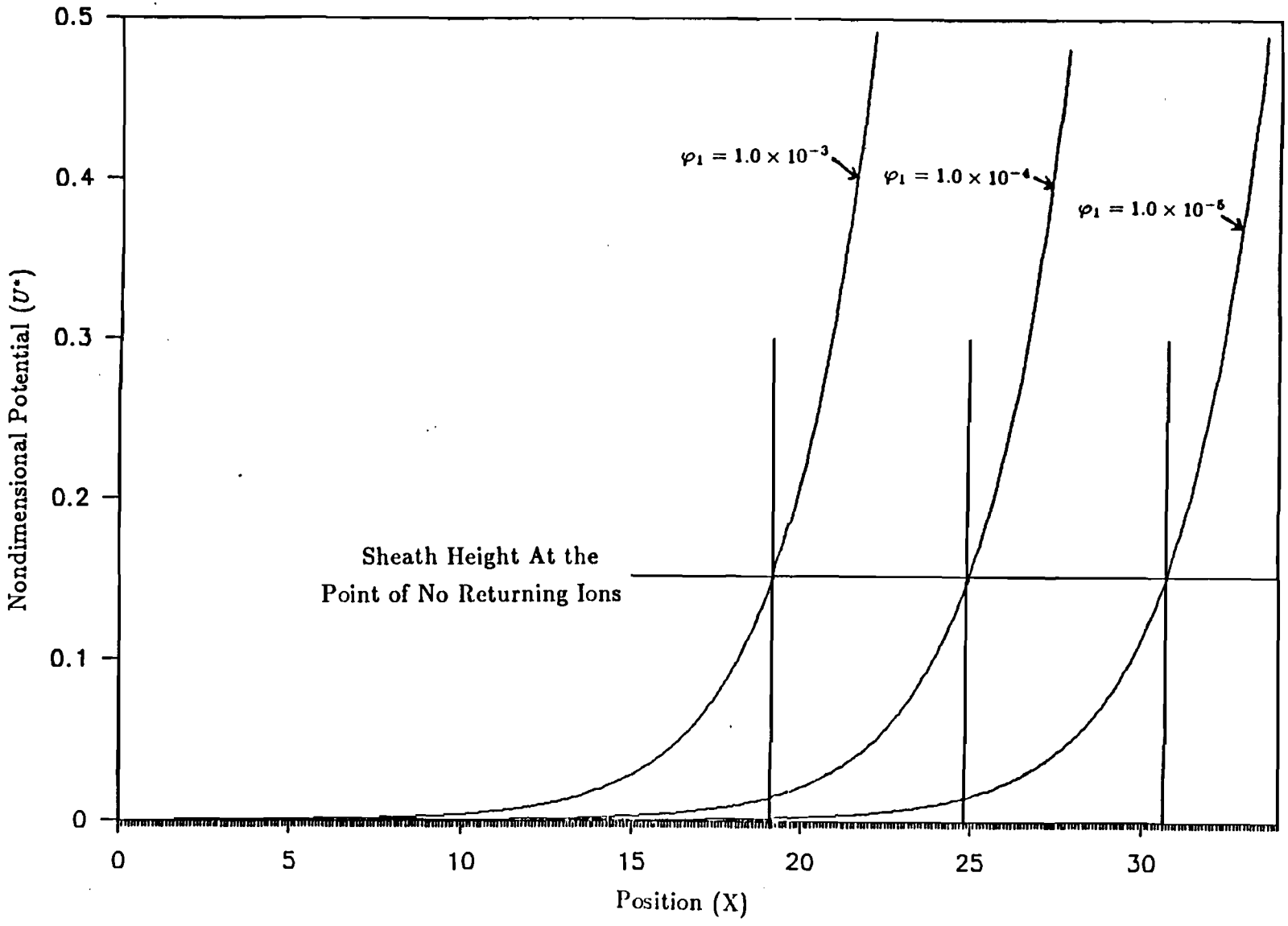

Figure 5.11 Potential Structure of the Presheath

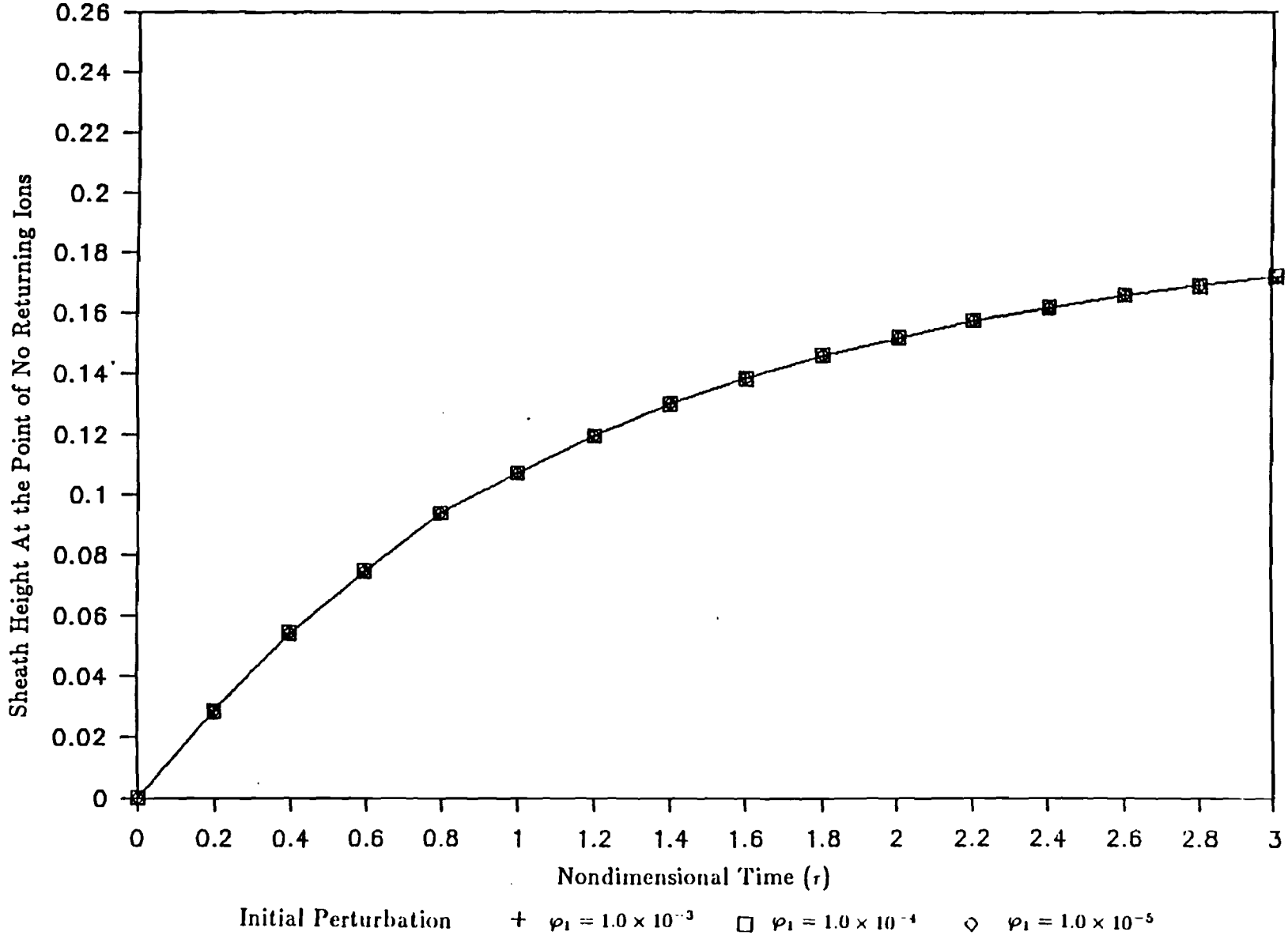

Figure 5.12 Time Dependent Structure of the Sheath Height

APPENDIX: PROGRAM LISTING

```
**********************************************************************
*     THIS PROGRAM WAS WRITTEN BY JEFFREY P. DANSEREAU
*
*       THIS VERSION WAS LAST UPDATED ON 7/17/87
**********************************************************************
C
C     THIS PROGRAM IS A TIME DEPENDENT MODEL OF THE SHEATH -
C     PRESHEATH OF A PLASMA.  IT USES A FOKKER-PLANCK COLLISION
C     TERM WITH ONLY COULOMB COLLISIONS.  BELOW IS A LIST OF
C     THE VARIABLES AND THEIR MEANING
C
C       T - DIAGONAL REPRESENTATION OF T MATRIX.1ST IS DIAGONALS.
C           2ND IS M VEL POS.
C       V - 3-D MATRIX OF V COMPONENTS. 1ST POS. IS F'S, 2ND IS
C           N PHI POS., 3RD IS M VEL. POS.
C       VV - 3-D MATRIX OF V VALUES AFTER INVERSION WITH T MATRIX.
C           POS. ARE SAME AS V MATRIX WITH ADDITIONAL ROW FOR BC'S.
C       D - 2-D MATRIX OF D VALUES. 1ST POS. IS F'S, 2ND IS M VEL POS.
C       DD - 2-D MATRIX OF D VALUES AFTER INVERSION WITH T MATRIX
C       PHI- VECTOR OF PHI VALUES
C       F - 2-D MATRIX OF DENSITY FUNCTIONS, 1ST POS. IS THE n F'S
C           THAT ARE BEING USED.  (n=N-1).  F(1,X)= F0 ECT...  THE
C           2ND POS IS THE M VEL POS.
C       TSTEP - VALUE OF DELTA T AS TIME IS STEPPED THROUGH
C       VSTEP - VALUE OF DELTA V AS VEL. SPACE IS STEPPED THROUGH
C       RTIME - CURRENT VALUE OF NON-DIM. TIME
C       ETA   - CURRENT VEL.
C       NETA  - ETA PARAMETER IN POISSON EQN
C       TOTE  - RATIO OF T TO Te(T OVER Te)
C       SM    - SMALL M(m) IN F-P EQN
C       BM    - BIG M(M) IN F-P EQN
C       AA    - a IN F-P EQN
C       AP    - a' IN F-P EQN
C       M     - NUMBER OF DIV. IN VEL. SPACE
C       N     - NUMBER OF PHI VALUES
C       ND    - NUMBER OF DIAGONALS IN T MATRIX
```

```
C       TIME  - INTEGER VALUE IN TIME LOOP
C       TEND  - RTIME TO FINISH SIMULATION
C       L     - INTEGER TIME VALUE TO END SIMULATION
C       FLAG1 - FLAG TO PRINT OR NOT PRINT MATRICES(99 TO PRINT)
C       FLAG2 - FLAG TO PRINT OR NOT PRINT INTERMEDIATE MATRICES
C             (99 TO PRINT)
C       TRBLE - FLAG TO PRINT TROUBLE STATEMENT IF MATRIX IS NOT
C             INVERTABLE
C       B,SOLN - INTERMEDIATE VALUES OF VARIOUS FUNCTIONS
C       X,Y,Z  - INTEGER COUNTERS
C
C     THIS PROGRAM STEPS THROUGH TIME SOLVING THE BOLTZMANN EQN FOR
C      VALUES OF THE EXPANDED DENSITY FUNCTION
C
      REAL T(6,8,202),V(6,6,202),B(202),SOLN(202),TEND
      REAL VV(6,6,202),D(6,202),DD(6,202),PHI(6),L
      REAL F(6,202),TSTEP,RTIME,SM,BM,AA,AP,VSTEP,ETA,NETA,TOTE
      REAL FTOTAL(202),S0,DU,DUPHI1
      INTEGER X,Y,Z,M,N,ND,TIME,TRBLE,FLAG1,FLAG2,FLAG3,P,PSTEP,SKIP
C
C     READ IN PARAMETERS AND PRINT THEM
C
      OPEN(UNIT=2,FILE='INITDAT.DAT',STATUS='OLD')
      READ(2,705) M,NETA,TOTE,AA,AP,SM,FLAG3,SKIP,S0
      READ(2,707) BM,VSTEP,N,ND,TEND,TSTEP,FLAG1,FLAG2
      CLOSE(UNIT=2)
705   FORMAT(I4,1X,F6.4,1X,F6.4,1X,F6.4,1X,F6.4,1X,F6.4,1X,I3,1X,
     +       I3,1X,F9.4,/)
707   FORMAT(1X,F6.4,1X,F6.4,1X,I4,1X,I4,1X,F8.5,1X,F7.5,1X,I3,1X,I3)
      OPEN(UNIT=1,FILE='PHI.OUT',STATUS='UNKNOWN')
      OPEN(UNIT=3,FILE='FPSHETH.OUT',STATUS='UNKNOWN')
      WRITE(3,717) '************************************************
     +         ,'**********'
717   FORMAT(A,A)
      WRITE(3,711) 'FOKKER - PLANCK SIMULATION OUTPUT'
      WRITE(3,717) '************************************************
     +         ,'**********'
      WRITE(3,710) 'INPUT PARAMETERS'
      WRITE(3,715) 'NUMBER OF VEL. STEPS - M',M
      WRITE(3,715) 'NUMBER OF PHI VALUES - N',N
```

```
      WRITE(3,715) 'NUMBER OF DIAGONALS IN T MATRIX - ND',ND
      WRITE(3,720) 'VALUE OF ETA IN POISSON EQN - NETA',NETA
      WRITE(3,720) 'VALUE OF T OVER TE - TOTE',TOTE
      WRITE(3,720) 'SIZE OF EACH VEL. STEP - VSTEP',VSTEP
      WRITE(3,720) 'SIZE OF EACH TIME STEP - TSTEP',TSTEP
      WRITE(3,720) 'VALUE OF ENDING TIME FOR SIMULATION',TEND
      WRITE(3,720) 'VALUE OF A PARAMETER IN F-P EQN - AA',AA
      WRITE(3,720) 'VALUE OF A PRIME PARAMETER IN F-P EQN - AP',AP
      WRITE(3,720) 'VALUE OF SMALL M IN F-P EQN - SM',SM
      WRITE(3,720) 'VALUE OF BIG M IN F-P EQN - BM',BM
      WRITE(3,716) 'FLAG TO PRINT PRIMARY MATRICES(99 TO PRINT)',
     +       ' - FLAG1',FLAG1
      WRITE(3,716) 'FLAG MAKE FDATA AND PHIDAT NEW FINAL VALUES',
     +       '(99 = YES) - FLAG3',FLAG3
      WRITE(3,715) 'TIME SKIP FOR PRINT OF F FILE - SKIP',SKIP
  716 FORMAT(5X,A,A,2X,I3)
      WRITE(3,710) ' '
  710 FORMAT(15X,A,//)
  711 FORMAT(8X,A,/)
  715 FORMAT(5X,A,2X,I3)
  720 FORMAT(5X,A,2X,F9.5)
C
C     MAKE NON TIME DEPENDENT QUANTITIES AND INITIAL APPROXIMATIONS
C     TO F'S, PHI'S, AN  THE BC
C
      DU=0.0
      DUPHI1=0.0
      CALL MAKEF(M,F)
      CALL MAKEPHI(N,RTIME,PHI)
      CALL TOT(F,FTOTAL,PHI,N,M,VSTEP,DU,DUPHI1)
      TT=0.0
      CALL CONSERV(F,VSTEP,TT,M)
C
C     ************************************
C
C     START MAIN TIME LOOP
C
C     ************************************
C
C
```

```
C     COMPUTE END LOOP TIME L
C
      L=TEND/TSTEP
      PSTEP=0
C
      DO 40 TIME=1,INT(L)+1
C        PRINT RESULTS OF CURRENT TIME STEP
C
          PSTEP=PSTEP+1
          IF (TIME.LE.3) GOTO 1000
          IF (PSTEP.GE.SKIP) THEN
              PSTEP=0
              GOTO 1000
          ENDIF
          GOTO 1001
1000      WRITE(3,350) 'TIME = ',RTIME,'TSTEP = ',TIME-1
          DO 210 Z=1,N
              WRITE(3,250) 'PHI(',Z-2,') = ',PHI(Z)
210       CONTINUE
          WRITE(3,351) 'DU = ',DU,'DU*PHI(1) = ',DUPHI1
          WRITE(3,711) ' '
          WRITE(3,275) 'M','ETA','F0','F1','F2','F3','FTOTAL'
          ETA=-5.0
          DO 220 X=1,M
              WRITE(3,300) X,ETA,F(1,X),F(2,X),F(3,X),FTOTAL(X)
              ETA=ETA+VSTEP
220       CONTINUE
1001      WRITE(3,710) ' '
          WRITE(1,813) TIME,RTIME,PHI(1),PHI(2),PHI(3),DU,DUPHI1
813       FORMAT(I3,1X,F7.4,1X,E13.6,1X,E13.6,1X,E13.6,1X,E13.6,
     +       1X,E13.6)
          IF (TIME.GT.INT(L)) GOTO 40
          WRITE(*,946) 'CURRENTLY IN TIME STEP',TIME,'OF',INT(L)
946       FORMAT(5X,A,I4,2X,A,I4)
C
C         MAKE TIME DEPENDENT QUANTITIES T MATRIX, V MATRIX, D MATRIX
C
          DO 445 JJ=1,2
          CALL MAKET(ND,M,F,VSTEP,SM,BM,AA,AP,TSTEP,S0,PHI,N,T)
          CALL MAKEV(N,M,F,VSTEP,V)
```

```
      CALL MAKED(M,F,VSTEP,TSTEP,SM,BM,AA,AP,N,PHI,D)
C
C     INVERT T MATRIX WITH V VECTORS, MAKING VV MATRIX
C
      DO 50 X=1,N-1
         DO 60 Y=3,N
            DO 70 Z=1,M
               B(Z)=V(X,Y,Z)
70          CONTINUE
            CALL MODIAG(M,ND,T,B,SOLN,TRBLE,X)
            IF (TRBLE.EQ.999) THEN
               WRITE(3,*) 'MATRIX HAS NO SOLUTION'
               TRBLE=0
            ENDIF
            DO 80 Z=1,M
               VV(X,Y,Z)=SOLN(Z)
80          CONTINUE
60       CONTINUE
50    CONTINUE
C
C     INVERT T MATRIX WITH D VECTORS, MAKING DD MATRIX
C
      DO 90 X=1,N-1
         DO 100 Y=1,M
            B(Y)=D(X,Y)
100      CONTINUE
         CALL MODIAG(M,ND,T,B,SOLN,TRBLE,X)
         IF (TRBLE.EQ.999) THEN
            WRITE(3,*) 'MATRIX HAS NO SOLUTION'
            TRBLE=0
         ENDIF
         DO 110 Y=1,M
            DD(X,Y)=SOLN(Y)
110      CONTINUE
90    CONTINUE
C
C     GET NEW F VALUES FROM NEW PHI VALUES
C
      DO 160 X=1,N-1
         IF ((JJ.EQ.1).AND.(X.EQ.2)) GOTO 160
```

```
            IF ((JJ.EQ.2).AND.(X.EQ.1)) GOTO 160
            DO 165 Z=1,M
                F(X,Z)=0.0
165         CONTINUE
            DO 170 Y=3,N
                DO 180 Z=1,M
                    F(X,Z)=F(X,Z)+PHI(Y)*VV(X,Y,Z)
180             CONTINUE
170         CONTINUE
            DO 190 Z=1,M
                F(X,Z)=F(X,Z)+DD(X,Z)
190         CONTINUE
160     CONTINUE
        CALL AVE(F,M,N,JJ)
C
445     CONTINUE
C
C       GET NEW PHI VALUES
C
        CALL DENSITY(N,M,PHI,F,TOTE,VSTEP)
C
C       MAKE TOTAL DENSITY
C
        CALL TOT(F,FTOTAL,PHI,N,M,VSTEP,DU,DUPHI1)
C
        TT=RTIME+TSTEP
        CALL CONSERV(F,VSTEP,TT,M)
C
C       INCREASE REAL TIME TO NEXT POSITION
C
        RTIME=RTIME+TSTEP
C
C       CONTINUE TIME LOOP
C
40  CONTINUE
C   ************************************
C
C    END TIME LOOP
C
C   ************************************
```

```
C
C     FORMAT STATEMENTS FOR PRINTS
C
250   FORMAT(5X,A,I4,A,1X,E13.6)
275   FORMAT(2X,A,2X,A,9X,A,12X,A,12X,A,12X,A,10X,A)
300   FORMAT(I3,1X,F5.2,1X,E13.6,1X,E13.6,1X,E13.6,1X,E13.6,1X,E12.5)
350   FORMAT(5X,A,F7.4,10X,A,I5,/)
351   FORMAT(5X,A,E13.6,5X,A,E13.6)
      CLOSE(UNIT=3)
      IF (FLAG3.EQ.99) THEN
          OPEN(UNIT=4,FILE='FDATA.DAT',STATUS='UNKNOWN')
          DO 265 X=1,M
              WRITE(4,266) F(1,X),F(2,X),F(3,X),F(4,X)
266           FORMAT(E13.6,1X,E13.6,1X,E13.6,1X,E13.6)
265       CONTINUE
          CLOSE(UNIT=1)
          OPEN(UNIT=8,FILE='PHIDAT.DAT',STATUS='UNKNOWN')
          DO 267 X=1,N
              WRITE(8,268) RTIME
              WRITE(8,268) PHI(X)
268           FORMAT(E13.6)
267       CONTINUE
      ENDIF
      STOP
      END


      REAL F(6,202),ETA,VSTEP,NETA,TOTE,B,PI,C
      INTEGER X,M,Z
      OPEN(UNIT=3,FILE='FDATA.DAT',STATUS='UNKNOWN')
      ETA=-5.0
      PRINT*,'INPUT M,VSTEP'
      READ(*,*) M,VSTEP
      N=M-(M-1)/2
      DO 10 X=1,N
          F(1,X)=EXP(-(ETA**2))
          F(2,X)=0.0
          F(3,X)=0.0
          F(4,X)=0.0
          ETA=ETA+VSTEP
```

```
10    CONTINUE
      Z=1
      DO 30 X=M,N+1,-1
          DO 40 Y=1,4
              F(1,X)=F(1,Z)
40        CONTINUE
          Z=Z+1
30    CONTINUE
      DO 20 X=1,M
          WRITE(3,100) F(1,X),F(2,X),F(3,X),F(4,X)
100       FORMAT(E13.6,1X,E13.6,1X,E13.6,1X,E13.6)
20    CONTINUE
      STOP
      END


      REAL PHI(6),RTIME
      INTEGER N,X
      N=5
      RTIME=0.0
      WRITE(*,*) 'INPUT PHI(-1)'
      READ(*,200) PHI(1)
      WRITE(*,*) 'INPUT PHI(0)'
      READ(*,200) PHI(2)
200   FORMAT(F10.5)
      WRITE(*,*) 'INPUT PHI(1)'
      READ(*,200) PHI(3)
      DO 10 X=4,N
          PHI(X)=0.0
10    CONTINUE
      OPEN(UNIT=9,FILE='PHIDAT.DAT',STATUS='UNKNOWN')
      WRITE(9,120) RTIME
      DO 20 X=1,N
          WRITE(9,120) PHI(X)
120       FORMAT(E13.6)
20    CONTINUE
      RETURN
      END
```

```
      SUBROUTINE CONSERV(F,VSTEP,T,M)
      REAL F(6,202),F0(202),VSTEP,ZF(202),Z2F(202),ENER,MOM,DEN,T,ETA
      INTEGER X,M
      ETA=-5.0
      DO 10 X=1,M
          F0(X)=F(1,X)
          ZF(X)=F(1,X)*ETA
          Z2F(X)=ZF(X)*ETA
          ETA=ETA+VSTEP
10     CONTINUE
      CALL SIMPS(F0,M,VSTEP,DEN)
      CALL SIMPS(ZF,M,VSTEP,MOM)
      CALL SIMPS(Z2F,M,VSTEP,ENER)
      OPEN(UNIT=9,FILE='CONSERV.OUT',STATUS='UNKNOWN')
      WRITE(9,100) T,DEN,MOM,ENER
100    FORMAT(2X,F8.5,1X,E13.6,1X,E13.6,1X,E13.6)
      RETURN
      END


      SUBROUTINE DENSITY(N,M,PHI,F,TOTE,VSTEP)
      REAL F(6,202),PHI(6),TOTE,VSTEP,G(202),R(4),NO(6)
      INTEGER M,N,X,Y
      DO 10 X=1,N-1
          DO 20 Y=1,M
              G(Y)=F(X,Y)
20        CONTINUE
          CALL SIMPS(G,M,VSTEP,NO(X))
10     CONTINUE
      R(1)=NO(2)/NO(1)
      R(2)=NO(3)/NO(1)
      R(3)=NO(4)/NO(1)
      PHI(3)=-PHI(2)*R(1)/(2.0*TOTE)
      PHI(4)=PHI(2)*((((PHI(3)/PHI(2))**2)*((2.0*TOTE)**2)/2.0)-R(2))
     +       /(2.0*TOTE)
      PHI(5)=PHI(2)*((((2.0*TOTE)**2)*PHI(3)*PHI(4)/(PHI(2)**2))
     + -(((2.0*TOTE)**3)*((PHI(3)/PHI(2))**3)/6.0)-R(3))/(2.0*TOTE)
      RETURN
      END
```

```
      SUBROUTINE MAKEF(M,F)
      REAL F(6,202)
      INTEGER X,M
      OPEN(UNIT=8,FILE='FDATA.DAT',STATUS='UNKNOWN')
      DO 10 X=1,M
          READ(8,100) F(1,X),F(2,X),F(3,X),F(4,X)
100        FORMAT(E13.6,1X,E13.6,1X,E13.6,1X,E13.6)
10    CONTINUE
      RETURN
      END


      SUBROUTINE MAKEPHI(N,RTIME,PHI)
      REAL PHI(6),RTIME
      INTEGER N,X
      OPEN(UNIT=9,FILE='PHIDAT.DAT',STATUS='UNKNOWN')
      READ(9,120) RTIME
      DO 20 X=1,N
          READ(9,120) PHI(X)
120       FORMAT(E13.6)
20    CONTINUE
      RETURN
      END


      SUBROUTINE MAKEV(N,M,F,VSTEP,V)
      REAL F(6,202),V(6,6,202),VSTEP,FD1(6),Z,ETA
      INTEGER N,M,X,Y,R,S
      ETA=-5.0
      DO 10 X=1,M
          CALL FD1(F,N,M,X,VSTEP,FD1)
          IF ((X.EQ.1).OR.(X.EQ.M)) THEN
              DO 15 Y=1,N-1
                  DO 17 R=3,N
                      V(Y,R,X)=0.0
17                CONTINUE
15            CONTINUE
          ELSE
              DO 20 Y=1,N-1
```

```
                Z=1.0
                S=1
                DO 30 R=3,N
                    IF (S.GT.(Y-1)) THEN
                        V(Y,R,X)=0.0
                    ELSE
                        V(Y,R,X)=-Z*FD1(Y-R+2)
                    ENDIF
                    S=S+1
                    Z=Z+1.0
30              CONTINUE
20          CONTINUE
        ENDIF
        ETA=ETA+VSTEP
10   CONTINUE
    RETURN
    END


    SUBROUTINE MAKED(M,F,VSTEP,TSTEP,SM,BM,AA,AP,N,PHI,D)
    REAL VSTEP,TSTEP,SM,BM,AA,AP,F(6,202),D(6,202),A(6,202),PHI(6)
    REAL FD1(6),FD2(6),AH(202),BH(202),B(6,202)
    REAL ETA,GD1,GD2
    INTEGER N,M,X,Y,Z
    DO 10 X=1,N-1
        CALL GETAB(F,VSTEP,M,SM,BM,AA,AP,AH,BH,X)
        DO 15 Y=1,M
            A(X,Y)=AH(Y)
            B(X,Y)=BH(Y)
15      CONTINUE
10   CONTINUE
    DO 17 Y=1,N-1
        D(Y,M)=0.0
        D(Y,1)=0.0
17   CONTINUE
    ETA=-5.0+VSTEP
    DO 20 X=2,M-1
        DO 30 Y=1,N-1
            D(Y,X)=0.0
            DO 40 Z=1,Y
```

```
            IF (Z.LE.Y-1) THEN
                GD2=(A(Z+1,X+1)*F(Y-Z,X+1)-2.0*
     +        A(Z+1,X)*F(Y-Z,X)+A(Z+1,X-1)*F(Y-Z,X-1))/(VSTEP**2)
                GD1=(B(Z+1,X+1)*F(Y-Z,X+1)-B(Z+1
     +          ,X-1)*F(Y-Z,X-1))/(2.0*VSTEP)
                D(Y,X)=D(Y,X)+GD2+GD1
            ENDIF
40        CONTINUE
          D(Y,X)=D(Y,X)+F(Y,X)/TSTEP
30      CONTINUE
        ETA=ETA+VSTEP
20    CONTINUE
    RETURN
    END


    SUBROUTINE FD1(F,N,M,X,VSTEP,FD1)
    REAL F(6,202),FD1(6),VSTEP
    INTEGER Y,X,N,M
    DO 10 Y=1,N-1
        IF (X.LE.2) THEN
            FD1(Y)=(-F(Y,X+2)+4.0*F(Y,X+1)-3.0*F(Y,X))/(2.0*VSTEP)
        ELSE IF (X.GE.M-1) THEN
            FD1(Y)=(3.0*F(Y,X)-4.0*F(Y,X-1)+F(Y,X-2))/(2.0*VSTEP)
        ELSE
            FD1(Y)=(F(Y,X+1)-F(Y,X-1))/(2.0*VSTEP)
        ENDIF
10    CONTINUE
    RETURN
    END


    SUBROUTINE MAKET(ND,M,F,VSTEP,SM,BM,AA,AP,TSTEP,S0,PHI,N,T)
    REAL VSTEP,TSTEP,SM,BM,AA,AP,F(6,202),T(6,8,202),A(202)
    REAL ETA,B(202),PHI(6),P
    INTEGER ND,M,X,Y,N,Z
    CALL GETAB(F,VSTEP,M,SM,BM,AA,AP,A,B,1)
    P=0.0
    DO 5 Z=1,N-1
```

```
      ETA=-5.0
      DO 10 X=1,M
         IF ((X.EQ.M).OR.(X.EQ.1)) THEN
            T(Z,2,X)=0.0
            T(Z,3,X)=1.0
            T(Z,4,X)=0.0
         ELSE
            T(Z,2,X)=(((-A(X-1)/VSTEP)+B(X-1)/2.0)/VSTEP)
            T(Z,2,X)=T(Z,2,X)-PHI(1)/(2.0*VSTEP)
            T(Z,3,X)=1.0/TSTEP+(2.0*A(X)/(VSTEP**2))
            T(Z,3,X)=T(Z,3,X)+PHI(2)*P*ETA
            T(Z,4,X)=((-A(X+1)/VSTEP-B(X+1)/2.0)/VSTEP)
            T(Z,4,X)=T(Z,4,X)+PHI(1)/(2.0*VSTEP)
         ENDIF
         ETA=ETA+VSTEP
10    CONTINUE
           P=P+1.0
5     CONTINUE
      RETURN
      END


      SUBROUTINE GETAB(F,VSTEP,M,SM,BM,AA,AP,A,B,Y)
      REAL A(202),B(202),AA,AP,F(6,202),VSTEP,Z,SM,BM,E(202)
      REAL P(202),H(202),G(202),K(202),DB,DA,S1,S2,S3,S4,S5
      INTEGER M,X,Y,N
      Z=-5.0
      DO 10 X=1,M
         CALL FINDA(F,Z,VSTEP,AA,AP,M,A(X),Y)
         CALL FINDB(F,Z,VSTEP,AA,AP,SM,BM,M,B(X),Y)
         Z=Z+VSTEP
10    CONTINUE
      ETA=-5.0
      DO 20 X=1,M
         H(X)=B(X)*F(Y,X)
         G(X)=A(X)*F(Y,X)
         K(X)=ETA*B(X)*F(Y,X)
         P(X)=ETA*F(Y,X)
         E(X)=F(Y,X)
         ETA=ETA+VSTEP
```

```
20    CONTINUE
      CALL SIMPS(H,M,VSTEP,S1)
      CALL SIMPS(G,M,VSTEP,S2)
      CALL SIMPS(K,M,VSTEP,S3)
      CALL SIMPS(P,M,VSTEP,S4)
      CALL SIMPS(E,M,VSTEP,S5)
      IF (S5.EQ.0.0) RETURN
      DB=-S1/S5
      DA=-(S2-S3-DB*S4)/S5
      DO 30 X=1,M
          B(X)=B(X)+DB
          A(X)=A(X)+DA
30    CONTINUE
      RETURN
      END


      SUBROUTINE FINDA(F,Z,VSTEP,AA,AP,M,A,Y)
      REAL F(6,202),Z,VSTEP,AA,AP,A,ETA,SOLN,H(202),FD2
      INTEGER X,M,Y
      ETA=-5.0
      DO 10 X=1,M
          CALL FD2(F,M,X,VSTEP,FD2,Y)
          H(X)=FD2*ABS(ETA-Z)
          ETA=ETA+VSTEP
10    CONTINUE
      CALL SIMPS(H,M,VSTEP,SOLN)
      A=(SOLN*AA)/(2.0*AP)
      RETURN
      END


      SUBROUTINE FINDB(F,Z,VSTEP,AA,AP,SM,BM,M,B,Y)
      REAL F(6,202),Z,VSTEP,AA,AP,B,ETA,G2,SOLN
      REAL J(202),FD3,SM,BM
      INTEGER X,M,Y
      ETA=-5.0
      DO 10 X=1,M
          CALL FD3(F,M,X,VSTEP,FD3,Y)
```

```
      J(X)=FD3*ABS(ETA-Z)
      ETA=ETA+VSTEP
10    CONTINUE
      CALL SIMPS(J,M,VSTEP,SOLN)
      B=-(AA/AP)*(SM/(2.0*BM))*SOLN
      RETURN
      END


      SUBROUTINE SIMPS(F,N,H,RESULT)
      REAL F(202),H,RESULT
      INTEGER N,NPANEL,NHALF,NBEGIN,NEND
      NPANEL=N-1
      NHALF=NPANEL/2
      NBEGIN=1
      RESULT=0.0
      IF ((NPANEL-2*NHALF).NE.0) THEN
         RESULT=3.0*H/8.0*(F(1)+3.0*F(2)+3.0*F(3)+F(4))
         NBEGIN=4
         IF (N.EQ.4) RETURN
      ENDIF
      RESULT=RESULT+H/3.0*(F(NBEGIN)+4.0*F(NBEGIN+1)+F(N))
      NBEGIN=NBEGIN+2
      IF (NBEGIN.EQ.4) RETURN
      NEND=N-2
      DO 10 I=NBEGIN,NEND,2
         RESULT=RESULT+H/3.0*(2.0*F(I)+4.0*F(I+1))
10    CONTINUE
      RETURN
      END


      SUBROUTINE FD2(F,M,X,VSTEP,FD2,Y)
      REAL F(6,202),FD2,VSTEP
      INTEGER X,M,Y
      IF (X.LE.1) THEN
         FD2=(F(Y,X+2)-2.0*F(Y,X+1)+F(Y,X))/(VSTEP**2)
      ELSE IF (X.GE.M) THEN
         FD2=(F(Y,X)-2.0*F(Y,X-1)+F(Y,X-2))/(VSTEP**2)
```

```
      ELSE
          FD2=(F(Y,X+1)-2.0*F(Y,X)+F(Y,X-1))/(VSTEP**2)
      ENDIF
      RETURN
      END


      SUBROUTINE FD3(F,M,X,VSTEP,FD3,Y)
      REAL F(6,202),FD3,VSTEP
      INTEGER X,M,Y
      IF (X.LE.2) THEN
          FD3=(F(Y,X+3)-3.0*F(Y,X+2)+3.0*F(Y,X+1)-F(Y,X))/(VSTEP**3)
      ELSE IF (X.GE.M-1) THEN
          FD3=(F(Y,X)-3.0*F(Y,X-1)+3.0*F(Y,X-2)-F(Y,X-3))/(VSTEP**3)
      ELSE
          FD3=(F(Y,X+2)-2.0*F(Y,X+1)+2.0*F(Y,X-1)-F(Y,X-2))/
     +   (2.0*(VSTEP**3))
      ENDIF
      RETURN
      END


      SUBROUTINE MODIAG(M,D,MATRIX,C,SOLN,TRBLE,N)
      REAL A(8,202),B,SOLN(202),MATRIX(6,8,202),C(202)
      INTEGER M,D,W,X,Y,Z,TRBLE,N,I,MN1
      TRBLE=0
      DO 10 X=1,D+2
          DO 20 Y=1,M
              IF (X.EQ.D+2) THEN
                  A(X,Y)=C(Y)
              ELSE
                  A(X,Y)=MATRIX(N,X,Y)
              ENDIF
 20       CONTINUE
 10   CONTINUE
      DO 30 I=2,M
          A(2,I)=A(2,I)/A(3,I-1)
          A(3,I)=A(3,I)-A(2,I)*A(4,I-1)
          A(5,I)=A(5,I)-A(2,I)*A(5,I-1)
```

```
30    CONTINUE
      DO 80 X=1,M
         IF (A(3,X).EQ.0) THEN
            PRINT*,'MATRIX HAS NO SOLUTION'
            TRBLE=999
            GOTO 999
         ENDIF
80    CONTINUE
      MN1=M-1
      A(5,M)=A(5,M)/A(3,M)
      DO 40 I=MN1,1,-1
         A(5,I)=(A(5,I)-A(4,I)*A(5,I+1))/A(3,I)
40    CONTINUE
      DO 50 X=1,M
         SOLN(X)=A(5,X)
50    CONTINUE
999   RETURN
      END


      SUBROUTINE AVE(F,M,N,JJ)
      REAL F(6,202)
      INTEGER X,N,M,Z,JJ
      DO 443 Z=1,N-1
         IF ((JJ.EQ.1).AND.(Z.EQ.2)) GOTO 443
         IF ((JJ.EQ.2).AND.(Z.EQ.1)) GOTO 443
         DO 444 X=2,M-1
            F(Z,X)=(.025*F(Z,X-1)+F(Z,X)+.025*F(Z,X+1))/1.05
444      CONTINUE
443   CONTINUE
      RETURN
      END


      SUBROUTINE TOT(F,FTOTAL,PHI,N,M,VSTEP,DU,DUPHI1)
      REAL F(6,202),FTOTAL(202),PHI(6),VSTEP,G(202),NO(6),DU
      REAL X1,X2,TOL,F1,F2,XERR
      INTEGER M,N,X,Y,NLIM
      L=(M+1)/2
```

```
      DO 10 X=1,N-1
          DO 20 Y=1,L
              G(Y)=F(X,Y)
20        CONTINUE
          CALL SIMPS(G,L,VSTEP,NO(X))
10    CONTINUE
      X1=0.0
      X2=1.0E6
      TOL=.0001
      NLIM=50
30    CALL FCN(NO,X1,N,F1)
      CALL FCN(NO,X2,N,F2)
      IF (F1*F2.GT.0.0) THEN
          X2=X2*10.0
          IF (X2.GT.1.0E15) THEN
              WRITE(*,*) 'NO SIGN CHANGE UP TO 1E15'
              RETURN
          ENDIF
          GOTO 30
      ENDIF
      DO 40 J=1,NLIM
          DU=(X1+X2)/2.0
          CALL FCN(NO,DU,N,FR)
          XERR=ABS(X1-X2)/2.0
          IF (XERR.LE. TOL) GOTO 1000
          IF (ABS(FR).LE.TOL) GOTO 1000
          IF (FR*X1.GT.0.0) THEN
              X1=DU
              F1=FR
          ELSE
              X2=DU
              F2=FR
          ENDIF
40    CONTINUE
      WRITE(*,*) 'NLIM EXCEEDED'
      RETURN
1000  DO 50 X=1,M
          FTOTAL(X)=0.0
          DO 60 Y=1,N-1
              FTOTAL(X)=FTOTAL(X)+DU**(Y-1)*F(Y,X)
```

APPENDIX B - The TEC program

```
C                                                       DOS FILE TECINIT.FOR
C*************************************************************************
C        TEC DATA INITIALIZATION ACCESS CODE
C        WRITTEN BY GREGORY L RIDDERBUSCH
C                    AUGUST 1986
C*************************************************************************
      REAL ARRAY(9)
      INTEGER IPARAM(5)
      WRITE(*,103)
      OPEN(UNIT=2,FILE='PINDATA.DAT',STATUS='OLD')
      READ(2,101) (ARRAY(I),I=1,9)
      READ(2,102) (IPARAM(I),I=1,5)
   10 WRITE(*,104) (ARRAY(I),I=1,7)
      WRITE(*,105)
      READ(*,*) IVALUE
      IF (IVALUE .EQ. 0) THEN
         GOTO 20
      ELSE
         WRITE(*,106)
         READ(*,*) VALUE
         ARRAY(IVALUE)=VALUE
         GOTO 10
      ENDIF
   20 WRITE(*,107) (IPARAM(I),I=1,5)
      WRITE(*,110) ARRAY(8),ARRAY(9)
      WRITE(*,105)
      READ(*,*) IVALUE
      IF (IVALUE .EQ. 0) THEN
         GOTO 30
      ELSE
         WRITE(*,108)
         IF (IVALUE .EQ. 6 .OR. IVALUE .EQ. 7) THEN
            READ(*,*) VALUE
            ARRAY(IVALUE+2)=VALUE
            GOTO 20
         ELSE
            READ(*,*) INEW
           IPARAM(IVALUE)=INEW
            GOTO 20
         ENDIF
      ENDIF
   30 REWIND(2)
      WRITE(2,101) (ARRAY(I),I=1,9)
      WRITE(2,102) (IPARAM(I),I=1,5)
      CLOSE(2)
      WRITE(*,109)
      STOP
C
  101 FORMAT(F8.1/F8.1/F6.3/F6.3/F6.3/F6.3/F7.2/F5.2/F6.1)
  102 FORMAT(I1/I1/I3/I3/I3)
  103 FORMAT(1X,'*****************************************'/
     &'          TEC OPERATING CONDITIONS'/
     &1X,'*****************************************')
  104 FORMAT(//4X,'CURRENT CONVERTOR OPERATING SETTINGS:'//
     &7X,'1.     EMITTER TEMPERATURE: ',F8.1,' KELVIN',/
     &7X,'2.   COLLECTOR TEMPERATURE: ',F8.1,' KELVIN',/
     &7X,'3.   EMITTER WORK FUNCTION:   ',F6.2,' EV'/
     &7X,'4. COLLECTOR WORK FUNCTION:   ',F6.2,' EV'/
     &7X,'5.      CONVERTOR PRESSURE:   ',F6.2,' TORR'/
     &7X,'6.           GAP THICKNESS:   ',F6.2,' MM'/
```

```
   &7X,'7.       OPERATING CURRENT:  ',F7.2,' AMPS/CM^2')
105 FORMAT(/4X,'ENTER ID NUMBER OF VALUE TO BE CHANGED, 0=NONE: ')
106 FORMAT(4X,'ENTER NEW OPERATING SETTING: ')
107 FORMAT(//4X,'CURRENT TEC FUNCTION SETTINGS:'//
   &7X,'1. DIAGNOSTIC LEVEL: ',I3,'   (0-RESTRICTED OUTPUT)'/
   &7X,'                             (1-FULL OUTPUT)'/
   &7X,'                             (2-ENABLE SHEATH DIAGNOSTICS)'/
   &7X,'                             (3-ENABLE DOT DIAGNOSTICS)'/
   &7X,'2. RESTART SEQUENCE: ',I3,'   (0-DEFAULT STARTUP VALUES)'/
   &7X,'                             (1-RESTART WITH PREVIOUS VALUES)'/
   &7X,'3. STEPS BETWEEN PRINTS: ',I3/
   &7X,'4.    POINT DENSITY: ',I3,'   (11,21,31,...151)'/
   &7X,'5. LOTUS SKIP FACTOR: ',I3,'  (1..99)')
108 FORMAT(4X,'ENTER NEW FUNCTIONAL SETTING: ')
109 FORMAT(1X,'*****************************************'/
   &'                                     '/
   &1X,'*****************************************')
110 FORMAT(7X,'6.        TIME STEP:  ',F5.2,
   &'  (0.1,0.2,0.3,0.4,0.5)'/7X,'7.          END TIME: ',
   &F6.1,'  (1.0,2.0,...,10.0)')
    END
```

```
C                                                          DOS FILE PRED1.FOR
C*************************************************************************
C     PROGRAM TEC
C*************************************************************************
      REAL CNE,ENE,ECHI,CCHI,EALPHA,CALPHA,LAMNEB,LAMTAU
      REAL DTP,T2,AN,AT,CN,CT,BN,BT,RE,KN,TCHAR,PN,DT
      REAL SMR,LAMDAR,NR,TE,TC,ENR,I,ARECN,EGNDB,ELOSSB,NNR
      REAL TAU(0:150),NEB(0:150),DELTAT,SN,ST,PI,CA,CSAHA,DZ
      REAL DTAUNDZ,MUI(0:150),RMUR,TAUN(0:150),EMISS,TIME2,LCCHI
      REAL NDOT1(0:150),TDOT1(0:150),NNB(0:150),TIME1,JNET,CV(0:150)
      REAL FYEN,IVD,IKN,EGRADA,PHIB,EWF,CWF,D,ESOURCE(0:150)
      INTEGER N,IDEN,EFIX,CFIX,CHKDOT,ICOUNT,NSTEPS,C,PC,LS,LC,EO,EC
C
      COMMON /PRED/ CA,CSAHA,DT,DTAUNDZ,DZ,EGNDB,ELOSSB,ENR,I,IDEN,KN
      COMMON /PRED/ LAMDAR,LAMNEB,LAMTAU,MUI,N,NNB,NNR,NR,PI,RE,RMUR
      COMMON /PRED/ TAUN,EFIX,CFIX,CHKDOT,FYEN,ENE,ECHI,CCHI,CNE
      COMMON /PRED/ EALPHA,CALPHA,CV,ESOURCE,LCCHI
c
      data nsteps /1/
C
      OPEN (UNIT=2,FILE='PINDATA.DAT',STATUS='OLD')
      OPEN (UNIT=4,FILE='EXOUT.DAT',STATUS='UNKNOWN')
      OPEN (UNIT=7,FILE='LOTUS1.DAT',STATUS='UNKNOWN')
      OPEN (UNIT=8,FILE='PREDRES.DAT',STATUS='OLD')
      OPEN (UNIT=9,FILE='PRNTOUT.DAT',STATUS='UNKNOWN')
C....SET ABBREVIATED PRNTDAT SAMPLING POINTS WITH PC
C...SET LOTUS SKIP COUNTER WITH LC
C
      CALL INITIAL(TE,TC,EWF,CWF,PN,NSTEPS,DTP,T2,AN,AT,
     &CN,CT,BN,BT,TCHAR,SMR,ARECN,DELTAT,SN,ST,TAU,NEB,LS,pc)
      c=pc
      LC=LS
      EO=100*LS
      EC=EO
C
      IF (CHKDOT .EQ. 3)
     &   OPEN (UNIT=9,FILE='D:PDOTDIAG.DAT',STATUS='UNKNOWN')
      IF (CHKDOT .GT. 1)
     &   OPEN (UNIT=11,FILE='D:PSTHDIAG.DAT',STATUS='UNKNOWN')
C
C-------------------------------------------------------------------
      EGRADA=0.0
      ICALCS=INT(T2/DTP+0.001)
      WRITE(*,76)
      DO 30 ICOUNT=0,ICALCS
         WRITE(*,77) (icount),100*(icount)/ICALCS
         TIME1=(icount)*DTP
         TIME2=(icount+1)*DTP
         CALL PREDCOR(TIME1,TIME2,TAU,NEB,NSTEPS,TE,TC,TDOT1,NDOT1,
     &   PN,ARECN,TCHAR,AN,AT,BN,BT,CN,CT,IVD,SMR,EGRADA,PHIB,JNET)
         VOUT=EWF + (PHIB + IVD/I + LCCHI)*TE/11600 - CWF
         IF (C .EQ. PC) THEN
           WRITE (9,67) TIME1,VOUT
           IF (CHKDOT .EQ. 0) THEN
            WRITE (9,70)
            WRITE (9,71) (I1,NEB(I1),TAU(I1),I1=1,N)
           ELSE
            EMISS=ENR/NEB(1)
            WRITE(9,72) ENE,ECHI,EALPHA,CNE,LCCHI+CCHI,CALPHA,PHIB,
```

```
     &                    IVD/I,EMISS
            WRITE(9,73)  (I1,NDOT1(I1),NEB(I1),
     &                   TDOT1(I1),TAU(I1),I1=0,N+1)
          ENDIF
          IF (EFIX .EQ. 1) WRITE(9,74)
          IF (CFIX .EQ. 1) WRITE(9,75)
          C=0
        ENDIF
        c=c+1
        IF (LC .EQ. LS) THEN
          WRITE(7,78)TIME1,VOUT,ENE,JNET,ECHI,CCHI,EALPHA,CALPHA,
     &          PHIB,IVD/I,EMISS,NEB(1),NEB(11),TAU(1),TAU(11)
          LC=0
        ENDIF
        LC=LC+1
        IF (EC .EQ. EO) THEN
          WRITE(4,*) TIME1
          WRITE(4,71)  (I1,NEB(I1),TAU(I1),I1=1,N)
          EC=0
        ENDIF
        EC=EC+1
30      CONTINUE
C-----------------------------------------------------------------------
C*****OUTPUT STARTUP VALUES TO PREDRES.DAT
      WRITE(8,69) ENE,CNE,ECHI,CCHI,EALPHA,CALPHA,N
      WRITE(8,68)  (NEB(I1),TAU(I1),I1=0,N+1)
      REWIND(8)
      CLOSE(8)
      STOP
C
 67   FORMAT(//,'RESULTS AT TIME = ',F8.2,4X,'OPERATING VOLTAGE=',F6.3)
 68   FORMAT(2F8.3)
 69   FORMAT(F9.4/F9.4/F8.3/F8.3/F9.4/F9.4/I3)
 70   FORMAT(/3X,' #      NEB(#)        TAU(#)'/
     &3X,'---------------------------')
 71   FORMAT(3X,I3,4X,F6.3,7X,F5.2)
 72   FORMAT(/3X,'ENE =',F8.3,4X,'ECHI=',F8.3,4X,'EALPHA=',F8.3/
     &3X,'CNE =',F8.3,4X,'CCHI=',F8.3,4X,'CALPHA=',F8.3/
     &3X,'PHIB=',F8.3,4X,'VD  =',F8.3,4X,'EMISS =',E8.3/
     &/3X,' #      NDOT(#)    NEB(#)        TDOT(#)     TAU(#)',
     &/3X,'-----------------------------------------')
 73   FORMAT(3X,I3,4X,F7.4,4X,F6.3,7X,F7.4,4X,F5.2)
 74   FORMAT('***AT LEAST ONE UNPHYSICAL EMITTER BC WAS INVOKED.')
 75   FORMAT('***AT LEAST ONE UNPHYSICAL COLLECTOR BC WAS INVOKED.')
 76   FORMAT(/1X,'    TEC CALCULATIONS BEGIN...(WAIT)...')
 77   FORMAT(4X,'ITERATION #',I3,'    COMPLETION--',I3,' %')
 78   FORMAT(16E13.6)
      END
C*************************************************************************
      SUBROUTINE PREDCOR(T1,T2,TAU,NEB,NSTEPS,TE,TC,TDOT1,NDOT1,
     +   PN,ARECN,TCHAR,AN,AT,BN,BT,CN,CT,IVD,SMR,EGRADA,PHIB,JNET)
C*************************************************************************
      REAL T1,T2,DT,AN,AT,BN,BT,CN,CT,IVD,LAMTAU,LAMNEB,CNE
      REAL TAU(0:150),NEB(0:150),TDOT1(0:150),NDOT1(0:150),ENE
      REAL ECHI,CCHI,EALPHA,CALPHA,MUI(0:150),I,DZ,TCHAR,LCCHI
      REAL TE,TC,DTAUNDZ,PN,ENR,NR,EGNDB,ELOSSB,RE,SMR,LAMDAR
      REAL RMUR,KN,NNR,ARECN,PI,CA,CSAHA,NNB(0:150),TAUN(0:150)
      REAL MSOURCE(0:150),ESOURCE(0:150),CV(0:150),MUEA(0:150)
      REAL NDOT2(0:150),TDOT2(0:150),TTILDA(0:150),NTILDA(0:150)
      REAL J,IIVD,AVD,FYEN,EGRADA,PHIB,JNET
```

```
      INTEGER N,CFIX,EFIX,IDEN,CHKDOT,NSTEPS
C
      COMMON /PRED/ CA,CSAHA,DT,DTAUNDZ,DZ,EGNDB,ELOSSB,ENR,I,IDEN,KN
      COMMON /PRED/ LAMDAR,LAMNEB,LAMTAU,MUI,N,NNB,NNR,NR,PI,RE,RMUR
      COMMON /PRED/ TAUN,EFIX,CFIX,CHKDOT,FYEN,ENE,ECHI,CCHI,CNE
      COMMON /PRED/ EALPHA,CALPHA,CV,ESOURCE,LCCHI
C
C*****HANDLE EXCEPTIONAL CONDITIONS
      DZ=1.0/(N-1)
      DT=(T2-T1)/NSTEPS
      CFIX=0
      EFIX=0
C*****SET NEUTRAL TEMPERATURE AND DENSITY
      IF (TE.EQ.TC)THEN
         DO 10 I1=0,N+1
            TAUN(I1)=1.0
 10      CONTINUE
      ELSE
         DO 20 I1=0,N+1
            TAUN(I1)=1.0+(TC/TE-1.0)*(I1-1.0)/(N-1)
 20      CONTINUE
      ENDIF
      NNR=965.5E16*PN/TE
      DO 30 I1=0,N+1
         NNB(I1)=1.0/TAUN(I1)
 30   CONTINUE
      DTAUNDZ=TAUN(N)-TAUN(1)
C*****SET TRANSPORT PARAMETERS
      RMUR=LAMDAR*SMR
      DO 40 I1=0,N+1
         MUI(I1)=SQRT(TAUN(I1))
 40   CONTINUE
C*****SET IONIZATION AND SAHA PARAMETERS
      CA=0.41283*ARECN*TCHAR*(NR/1.0E14)**2*(TE/1500)**(-4.5)
      CSAHA=LOG((1.4027E20*NNR/NR/NR)*(TE/1500)**1.5)
C-----------------------------------------------------------------
      DO 70 ICOUNT=0,NSTEPS-1
C-----PREDICTOR STEP
         IF (CHKDOT.EQ.3) WRITE(9,81)
         CALL DOT(NDOT1,TDOT1,NEB,TAU,EGRADA,PHIB,JNET)
         DO 45 I1=0,N+1
            NTILDA(I1)=NEB(I1)+AN*DT*NDOT1(I1)
            TTILDA(I1)=TAU(I1)+AT*DT*TDOT1(I1)
 45      CONTINUE
C-----CORRECTOR STEP
         IF (AN.EQ.0.0.AND.AT.EQ.0.0) THEN
            DO 50 I1=0,N+1
               NDOT2(I1)=0.0
               TDOT2(I1)=0.0
 50         CONTINUE
            GOTO 55
         ELSE
            IF (CHKDOT.EQ.3) WRITE(9,82)
            CALL DOT(NDOT2,TDOT2,NTILDA,TTILDA,EGRADA,PHIB,JNET)
         ENDIF
 55      DO 60 I1=0,N+1
            NEB(I1)=NEB(I1)+DT*(BN*NDOT1(I1)+CN*NDOT2(I1))
            TAU(I1)=TAU(I1)+DT*(BT*TDOT1(I1)+CT*TDOT2(I1))
 60      CONTINUE
 70   CONTINUE
```

```
C-----------------------------------------------------------------------
C*****UPDATE TIME DERIV.S, IMAGE POINTS, AND FIND PLASMA POWER GAIN
      CV(0)=0.0
      CV(N+1)=0.0
      ESOURCE(0)=0.0
      ESOURCE(N+1)=0.0
      IF (CHKDOT.EQ.3) WRITE(9,83)
      CALL DOT(NDOT1,TDOT1,NEB,TAU,EGRADA,PHIB,JNET)
      IIVD=0.0
      DO 75 I1=2,(N-1)
         IIVD=IIVD+(ESOURCE(I1)-CV(I1)*TDOT1(I1))
 75   CONTINUE
      AVD=0.5*(ESOURCE(1)-CV(1)*TDOT1(1))+0.5*(ESOURCE(N)-CV(N)
     +        *TDOT1(N))
      IVD=(AVD+IIVD)*DZ+2.0*I*(TAU(1)-TAU(N))-(NEB(1)*ENE/KN)
     +        *(TAU(1)-1)
      RETURN
C
 81   FORMAT(//,'CALL DOT FOR FIRST TIME.',//)
 82   FORMAT(//,'CALL DOT FOR SECOND TIME.',//)
 83   FORMAT(//,'CALL DOT FOR LAST TIME.',//)
      END
c
```

```
C                                                          DOS FILE PRED2.FOR
C*****************************************************************************
      SUBROUTINE DOT(NEBDOT,TAUDOT,NEB,TAU,EGRADA,PHIB,JNET)
C*****************************************************************************
      REAL A,ALPHA(0:150),BETA(0:150),CA,CALPHA,CCHI,CDETA,CNE,SIGMA
      REAL CTETA,CTZ,CV(0:150),CONVECT,D21B,D32B,DT,DZ,DGDU,DELU
      REAL DETAP,DTAUNDZ,ESOURCE(0:150),ELOSSB,EGNDB,ETZ,ETETA,DELTAU
      REAL ENE,ECHI,ENR,F(15),FYEN,GAMMAP,GAMMAM,GU,I,IB,K(0:150)
      REAL LAMTAU,LAMDAR,LAMNEB,MUI(0:150),MSOURCE(0:150),MUISOLD
      REAL MURSOLD,MUIS,MURS,MUEA(0:150),NR,NNR,NEB(0:150),NBC0A
      REAL NBC1A,NBC1B,NBC1C,NES2,NNB(0:150),NUE,NA(0:150),NB(0:150)
      REAL NEBU(0:150),ND(0:150),NS(0:150),NEBDOT(0:150),NEBA(0:150)
      REAL NEBV(0:150),PC(0:150),PI,PB,PBP,POHMIC,P0,QKP,QKM,RE,RMUR
      REAL TAU(0:150),TAUN(0:150),TAUDOT(0:150),TA(0:150),TB(0:150)
      REAL TS(0:150),TAUA(0:150),TAUB(0:150),TAUC(0:150),TAUV(0:150)
      REAL TBC0B,TBC0C,TBC1A,TBC1B,TBC1C,U,CSAHA,DETA,EALPHA,KN,KDE
      REAL NEBB(0:150),TAUU(0:150),NEBC(0:150),NC(0:150),NBC0B,LCCHI
      REAL NBC0C,TC(0:150),TBC0A,JNET,SMR,EGRADA,PHIB,BIGU,JRC,CGRADA
      INTEGER CFIX,EFIX,CHKDOT,CFLAG
C
      COMMON /PRED/ CA,CSAHA,DT,DTAUNDZ,DZ,EGNDB,ELOSSB,ENR,I,IDEN,KN
      COMMON /PRED/ LAMDAR,LAMNEB,LAMTAU,MUI,N,NNB,NNR,NR,PI,RE,RMUR
      COMMON /PRED/ TAUN,EFIX,CFIX,CHKDOT,FYEN,ENE,ECHI,CCHI,CNE
      COMMON /PRED/ EALPHA,CALPHA,CV,ESOURCE,LCCHI
C
      F(1)=5.74E-3
      F(2)=1.40E-3
      F(3)=2.3
      F(4)=0.2
      F(5)=2.70E-2
      F(6)=5.74E-3
      F(7)=4.24E-2
      F(8)=2.82
      F(9)=0.0
      F(10)=11.607
      F(11)=0.0
      F(12)=27.04
C*****SET THERMAL & ELECTRICAL CONDUCTIVITIES AT 0+ (E) & 1- (C)
      IF(TAU(1).LT.0.1)THEN
         TAU(1)=0.1
         EFIX=1
      ENDIF
      IF(TAU(N).LT.0.1)THEN
         TAU(N)=0.1
         CFIX=1
      ENDIF
      IF(RE.EQ.0.5)THEN
         DO 10 I1=0,N+1
         MUEA(I1)=TAUN(I1)
 10      CONTINUE
      ENDIF
      IF(RE.EQ.0.0)THEN
         DO 20 I1=0,N+1
         MUEA(I1)=TAUN(I1)/SQRT(TAU(I1))
 20      CONTINUE
      ENDIF
      IF(RE.EQ.-0.5)THEN
         DO 30 I1=0,N+1
         MUEA(I1)=TAUN(I1)/TAU(I1)
```

```
 30       CONTINUE
      ELSE
         DO 40 I1=0,N+1
         MUEA(I1)=TAUN(I1)*(TAU(I1)**(RE-0.5))
 40       CONTINUE
      ENDIF
      DO 50 I1=0,N+1
         K(I1)=((RE+2.0)/FYEN)*MUEA(I1)*NEB(I1)*TAU(I1)
         PC(I1)=NEB(I1)*(TAU(I1)+TAUN(I1))
 50   CONTINUE
      DETA=ALOG(K(2)/K(1))*DZ/(K(2)-K(1))
      DETAP=ALOG(K(2)/K(1))*DZ/(K(2)-K(1))
C*****DETERMINE EMITTER SHEATH*****
      JNET=(I*KN*1.595769)/(SQRT(TAU(1))*NEB(1))
      CALL SHEATH(JNET,ENR/NEB(1),TAU(1),ECHI,PHIB,EALPHA,ENE)
C-----FIND EMITTER (0+) DERIVATIVES FROM B.C.
      IF(ECHI.LE.1E-5.OR.ECHI.GE.20) EFIX=1
      ETETA=(TAU(1)-1)*ENE*NEB(1)/KN-I*(ECHI-TAU(1)/2)
      ETZ=ETETA/K(1)
      EPCZ=(SQRT(PI/8/EALPHA)/LAMDAR/KN)*NEB(1)/MUI(1)-I/MUEA(1)
      ENZ=(EPCZ-NEB(1)*(ETZ+DTAUNDZ))/(TAU(1)+TAUN(1))
C*****SOLVE COLLECTOR SHEATH
      CFLAG=0
      CNE=0.0
      U=1.0
      GU=G(U,NEB(N),TAU(N),I,KN)
      DELU=0.05
      DO 80 I1=1,50
         DGDU=(G(U+DELU,NEB(N),TAU(N),I,KN)-GU)/DELU
         DELTAU=-GU/DGDU
         U=U+DELTAU
         GU=G(U,NEB(N),TAU(N),I,KN)
         IF (ABS(GU).LE.0.001) THEN
            CCHI=U*TAU(N)
            GOTO 85
         ENDIF
 80   CONTINUE
         CCHI = 0.0
         WRITE(*,205)
         IF (CHKDOT .GT. 1) WRITE(11,205)
C****DETERMINE DERIVATIVES AT COLLECTOR (1-) FROM B.C.
 85    IF (CHKDOT .GT. 1)
     &WRITE(11,206) EGRADA,ALPHA2,TAU(1),ENR/NEB(1),
     &JNET,ECHI,PHIB,ENE,EALPHA,CCHI,CALPHA,IFLAG,RCODE
      DPH = -CCHI/TAU(N)
      IF(DPH.LT.0.0000001) DPH = 0.0000001
      CALPHA=(1.0/TAU(N))*(3.14159265/2)*( (1.0 + ERF(SQRT(DPH)))
     + - (1./2.)*(1.0 + ERF(SQRT(4.0*DPH))) )**2 / ( EXP(-DPH)
     + - (1./4.)*EXP(-4.0*DPH) )**2
      LCCHI = 0.0
      IF(CCHI.LT.0.0) THEN
         LCCHI = CCHI
         CCHI = 0.0
      ENDIF
      CTETA=-I*(CCHI-TAU(N)/2.0)
      CTZ=CTETA/K(N)
      CDETA=ALOG(K(N)/K(N-1))*DZ/(K(N)-K(N-1))
      NBC0A=TAU(1)+TAUN(1)
      NBC0B=SQRT(PI/EALPHA/8.0)/LAMDAR/KN/MUI(1)-ENE*NEB(1)/K(1)*
     +       (TAU(1)-1.0)-DTAUNDZ
```

```
      NBC0C=I*NEB(1)/K(1)*(ECHI-TAU(1)/2.0)-I/MUEA(1)
      NBC1A=TAU(N)+TAUN(N)
      NBC1B=-SQRT(PI/CALPHA/8.0)/LAMDAR/KN/MUI(N)-CNE*NEB(N)/K(N)*
     +        (TAU(N)-1.0)+DTAUNDZ
      NBC1C=-I*NEB(N)/K(N)*(CCHI-TAU(N)/2.0)-I/MUEA(N)
      TBC0A=1.0
      TBC0B=ENE*NEB(1)/KN+I/2.0
      TBC0C=-ENE*NEB(1)/KN-I*ECHI
      TBC1A=-1.0
      TBC1B=CNE*NEB(N)/KN-I/2.0
      TBC1C=-CNE*NEB(N)/KN+I*CCHI
      NEBA(0)=(NBC0A*LAMNEB)/(2.0*DZ)
      NEBB(0)=-LAMNEB*NBC0B
      NEBC(0)=-NBC0A*LAMNEB/(2.0*DZ)
      NEBV(0)=NBC0B*(1.0-LAMNEB)*NEB(1)+NBC0C-(1.0-LAMNEB)*
     +         NBC0A*(NEB(2)-NEB(0))/(2.0*DZ)
      TAUA(0)=TBC0A*LAMTAU/(2.0*DETAP)
      TAUB(0)=-LAMTAU*TBC0B
      TAUC(0)=-TBC0A*LAMTAU/(2.0*DETAP)
      TAUV(0)=TBC0B*(1.0-LAMTAU)*TAU(1)+TBC0C-(1.0-LAMTAU)*
     +         TBC0A*(TAU(2)-TAU(0))/(2.0*DETAP)
      NEBA(N+1)=(NBC1A*LAMNEB)/(2.0*DZ)
      NEBB(N+1)=-LAMNEB*NBC1B
      NEBC(N+1)=-NBC1A*LAMNEB/(2.0*DZ)
      NEBV(N+1)=NBC1B*(1.0-LAMNEB)*NEB(N)+NBC1C-(1.0-LAMNEB)*
     +           NBC1A*(NEB(N+1)-NEB(N-1))/(2.0*DZ)
      TAUA(N+1)=TBC1A*LAMTAU/(2.0*CDETA)
      TAUB(N+1)=-LAMTAU*TBC1B
      TAUC(N+1)=-TBC1A*LAMTAU/(2.0*CDETA)
      TAUV(N+1)=TBC1B*(1.0-LAMTAU)*TAU(N)+TBC1C-(1.0-LAMTAU)*
     +           TBC1A*(TAU(N+1)-TAU(N-1))/(2.0*CDETA)
C*****INITIALIZE GAMMAP & QKP FOR LOOP
      MURS=MUI(2)/MUEA(2)+MUI(1)/MUEA(1)*(1-2*DZ*(
     +     (0.5-RE)*ETZ/TAU(1)-0.5*DTAUNDZ/TAUN(1)))
      GAMMAP=0.5*(((MUI(1)+MUI(2))*(PC(1)-PC(0))
     +       )/DZ+I*MURS)
      QKP=(TAU(1)-TAU(0))/DETA
      MUIS=MUI(1)+MUI(2)
C-----------------------------------------------------------------
      DO 100 J=1,N
C-----UPDATE FOR NEW J
         GAMMAM=GAMMAP
         QKM=QKP
         DETA=DETAP
         MUISOLD=MUIS
         MURSOLD=MURS
         IF (J.NE.N) THEN
            DETAP=ALOG(K(J+1)/K(J))*DZ/(K(J+1)-K(J))
            MUIS=MUI(J)+MUI(J+1)
            MURS=MUI(J)/MUEA(J)+MUI(J+1)/MUEA(J+1)
         ELSE
            MURS=MURS+2*DZ*(MUI(N)/MUEA(N))*((0.5-RE)*CTZ/TAU(N)
     +           -0.5*DTAUNDZ/TAUN(N))
         ENDIF
C-----FIND AMBIPOLAR FLUX AT J+1/2
         GAMMAP=0.5*((MUIS*(PC(J+1)-PC(J)))/DZ+I*MURS)
C-----FIND MASS SOURCE AT J
         A=CA/TAU(J)**4.5
         NES2=NNB(J)*TAU(J)**1.5*EXP(CSAHA-EGNDB/TAU(J))
         D21B=F(7)*(1+F(8)/TAU(J))
```

```
      D32B=F(2)*EXP(F(3)/TAU(J))
      IB=A*NES2*(1+F(1)/NEB(J))/(1+D21B*(1+D32B/NEB(J))/NEB(J))
      P0=1+(F(4)/NEB(J))*(1+F(5)/NEB(J))/(1+F(6)/NEB(J))
      NUE=NEB(J)*NEB(J)/NES2
      MSOURCE(J)=NEB(J)*IB*(1-P0*NUE)
       IF (IDEN.EQ.1) MSOURCE(J)=NEB(J)*A*NES2
      NEBDOT(J)=RMUR*(GAMMAP-GAMMAM)/DZ+MSOURCE(J)
      NA(J)=RMUR*MUIS*(TAU(J+1)+TAUN(J+1))/2.0/DZ**2
      NB(J)=RMUR*(MUIS+MUISOLD)*(TAU(J)+TAUN(J))/2.0/DZ**2
      NC(J)=RMUR*MUISOLD*(TAU(J-1)+TAUN(J-1))/2.0/DZ**2
      ND(J)=I*(MURS-MURSOLD)*RMUR/DZ/2.0
     +        +NEB(J)*IB*(1.0+SQRT(P0/NES2)*NEB(J))
C     NS(J)=IB*(1.0-P0*NUE)
      NS(J)=-NEB(J)*IB*(1.0+SQRT(P0/NES2)*NEB(J))*SQRT(P0/NES2)
       IF (IDEN.EQ.1) NS(J)=A*NES2
      NEBA(J)=-DT*NA(J)*LAMNEB
      NEBB(J)=1.0+DT*NB(J)*LAMNEB-DT*NS(J)*LAMNEB
      NEBC(J)=-DT*NC(J)*LAMNEB
      NEBV(J)=NEB(J)+DT*NA(J)*(1.0-LAMNEB)*NEB(J+1)-DT*NB(J)*
     +          (1.0-LAMNEB)*NEB(J)+DT*NC(J)*(1.0-LAMNEB)*NEB(J-1)+
     +           DT*ND(J)+DT*NS(J)*(1.0-LAMNEB)*NEB(J)
      KDE=K(J)*(DETA+DETAP)/2
      QKP=(TAU(J+1)-TAU(J))/DETAP
      CONVECT=-(1.5)*I*(DETA*QKP+DETAP*QKM)/(2*KDE)
      SIGMA=NEB(J)*MUEA(J)
      POHMIC=I*(I/SIGMA+TAU(J)*(NEB(J+1)-NEB(J-1))
     +        /(2*DZ*NEB(J)))
      PBP=(F(9)*NNR/NR)*EXP(-F(10)/TAU(J))
      PB=(F(11)*NNR/NR)*EXP(-F(12)/TAU(J))
      CV(J)=1.5*NEB(J)+NNB(J)*(F(10)*PBP+F(12)*PB*NUE)
     +       /(TAU(J)*TAU(J))
      ESOURCE(J)=-ELOSSB*MSOURCE(J)
     +            -NNB(J)*PB*(2*NUE*NEBDOT(J)/NEB(J))
      TAUDOT(J)=((QKP-QKM)/KDE+CONVECT+POHMIC+ESOURCE(J))
     +           /CV(J)
      TA(J)=1.0/(DETAP*KDE*CV(J))
      TB(J)=(1.0/DETAP+1.0/DETA)/KDE/CV(J)
      TC(J)=1.0/DETA/KDE/CV(J)
      TS(J)=(CONVECT+POHMIC+ESOURCE(J))/CV(J)
      TAUA(J)=-DT*LAMTAU*TA(J)
      TAUB(J)=1.0+DT*LAMTAU*TB(J)
      TAUC(J)=-DT*LAMTAU*TC(J)
      TAUV(J)=TAU(J)+DT*(1.0-LAMTAU)*TA(J)*TAU(J+1)
     +          -DT*(1.0-LAMTAU)*TB(J)*TAU(J)
     +          +DT*(1.0-LAMTAU)*TC(J)*TAU(J-1)
     +          +TS(J)*DT
      IF (CHKDOT.EQ.3) WRITE(9,201) J,NEB(J),J,TAU(J),
     +    J,MSOURCE(J),J,PB,PBP,A,D21B,D32B,P0,IB,
     +    NUE,NES2,QKP,GAMMAP,DETAP,MURS
  100 CONTINUE
C-----------------------------------------------------------------
      NEBC(0)=NEBC(0)-NEBC(1)*NEBA(0)/NEBA(1)
      NEBB(0)=NEBB(0)-NEBB(1)*NEBA(0)/NEBA(1)
      NEBV(0)=NEBV(0)-NEBV(1)*NEBA(0)/NEBA(1)
      NEBA(0)=NEBB(0)
      NEBB(0)=NEBC(0)
      NEBA(N+1)=NEBA(N+1)-NEBA(N)*NEBC(N+1)/NEBC(N)
      NEBB(N+1)=NEBB(N+1)-NEBB(N)*NEBC(N+1)/NEBC(N)
      NEBV(N+1)=NEBV(N+1)-NEBV(N)*NEBC(N+1)/NEBC(N)
      NEBC(N+1)=NEBB(N+1)
```

```
      NEBB(N+1)=NEBA(N+1)
      TAUC(0)=TAUC(0)-TAUC(1)*TAUA(0)/TAUA(1)
      TAUB(0)=TAUB(0)-TAUB(1)*TAUA(0)/TAUA(1)
      TAUV(0)=TAUV(0)-TAUV(1)*TAUA(0)/TAUA(1)
      TAUA(0)=TAUB(0)
      TAUB(0)=TAUC(0)
      TAUA(N+1)=TAUA(N+1)-TAUA(N)*TAUC(N+1)/TAUC(N)
      TAUB(N+1)=TAUB(N+1)-TAUB(N)*TAUC(N+1)/TAUC(N)
      TAUV(N+1)=TAUV(N+1)-TAUV(N)*TAUC(N+1)/TAUC(N)
      TAUC(N+1)=TAUB(N+1)
      TAUB(N+1)=TAUA(N+1)
      ALPHA(0)=-NEBA(0)/NEBB(0)
      DO 110 I1=1,N
         ALPHA(I1)=-NEBA(I1)/(NEBC(I1)*ALPHA(I1-1)+NEBB(I1))
110   CONTINUE
      ALPHA(N+1)=0.0
      BETA(0)=NEBV(0)/NEBB(0)
      DO 120 I1=1,N+1
         BETA(I1)=(NEBV(I1)-NEBC(I1)*BETA(I1-1))/(NEBC(I1)
     +              *ALPHA(I1-1)+NEBB(I1))
120   CONTINUE
      NEBU(N+1)=BETA(N+1)
      DO 130 I1=N,0,-1
         NEBU(I1)=ALPHA(I1)*NEBU(I1+1)+BETA(I1)
130   CONTINUE
      ALPHA(0)=-TAUA(0)/TAUB(0)
      DO 140 I1=1,N
         ALPHA(I1)=-TAUA(I1)/(TAUC(I1)*ALPHA(I1-1)+TAUB(I1))
140   CONTINUE
      ALPHA(N+1)=0.0
      BETA(0)=TAUV(0)/TAUB(0)
      DO 150 I1=1,(N+1)
         BETA(I1)=(TAUV(I1)-TAUC(I1)*BETA(I1-1))/(TAUC(I1)
     +              *ALPHA(I1-1)+TAUB(I1))
150   CONTINUE
      TAUU(N+1)=BETA(N+1)
      DO 160 I1=N,0,-1
         TAUU(I1)=ALPHA(I1)*TAUU(I1+1)+BETA(I1)
160   CONTINUE
      DO 170 I1=0,N+1
         TAUDOT(I1)=(TAUU(I1)-TAU(I1))/DT
         NEBDOT(I1)=(NEBU(I1)-NEB(I1))/DT
170   CONTINUE
      IF (CHKDOT.EQ.3) THEN
         WRITE(9,202) (I1,NEBDOT(I1),I1,TAUDOT(I1),I1=0,N+1)
         WRITE(9,203) (I1,ALPHA(I1),I1,BETA(I1),I1=0,N+1)
         WRITE(9,204) (I1,NEBU(I1),I1,TAUU(I1),I1=0,N+1)
      ENDIF
    RETURN
C
201  FORMAT('NEB(',I2,')=',F8.3,'  TAU(',I2,')=',F8.3,
    &'  MSOURCE(',I2,')=',F8.3/'J=',I2,'  PB=',F8.3,
    &'  PBP=',F8.3/'A=',F8.3,'  D21B=',F8.3,'  D32B=',F8.3/
    &'P0=',F8.3,'  IB=',F8.3/'NUE=',F8.3,'  NES2=',F8.3/
    &'QKP=',F8.3,'  GAMMAP=',F8.3/'DETAP=',F8.3,'  MURS=',F8.3)
202  FORMAT('NEBDOT(',I2,')=',F8.3,'  TAUDOT(',I2,')=',F8.3)
203  FORMAT('ALPHA(',I2,')=',F8.3,'  BETA(',I2,')=',F8.3)
204  FORMAT('NEBU(',I2,')=',F8.3,'  TAUU(',I2,')=',F8.3)
205  FORMAT(//2X,'COLLECTOR SHEATH FAILED TO CONVERGE',//)
206  FORMAT(/1X,'EGRADA=',F7.3,3X,'ALPHA2=',F7.3/
```

```
     &1X,'RLE=',F5.2,3X,'EMISS=',F9.1,3X,'JNET=',F7.4/
     &1X,'ECHI=',F7.3,3X,'PHIB=',F7.3,1X,'ENE=',F10.3,3X,
     &'EALPHA=',F7.4/1X,'CCHI=',F7.3,3X,'CALPHA=',F7.4/1X,
     &'IFLAG=',I1,3X,'RCODE=',A1)
      END
C*********************************************************************
      FUNCTION G(UX,NEB,TAU,I,KN)
C*********************************************************************
      REAL UX,NEB,TAU,I,KN,SQX,GX
      DOUBLE PRECISION ERF
      IF(UX.LE.0.0)THEN
         SQX=0.0
      ELSE
         SQX=SQRT(UX)
      ENDIF
C     G=UX*LOG(1.0+ERF(SQX)) - LOG(NEB*SQRT(TAU)/I/KN/2.0)
      G=UX - LOG(NEB*SQRT(TAU)/I/KN/2.0)
      RETURN
      END
C*********************************************************************
      FUNCTION ERF(X)
C*********************************************************************
      DOUBLE PRECISION X1,SUM,ERF,ERFX,P(3,6),Q(3,6),PI,TSUM1,TSUM2
      INTEGER IPOWER(3)
      DATA IPOWER/2,1,-2/
      PI=3.1415926535898
      TSUM1=0.0
      TSUM2=0.0
      X1=X
      IF (X1 .LT. 0.0) X1=-X1
      IF (X1 .GT. 5.93) THEN
         ERFX=1.0
         GOTO 1240
      END IF
      IF (X1 .EQ. 0.0) THEN
         ERF=0.0
         GOTO 1245
      ELSE
         IFLAG=1
      END IF
      IF (X1 .LE. 4.0 .AND. X1 .GE. 0.47) IFLAG=2
      IF (X1 .GT. 4.0) IFLAG=3
      DO 1205 J=1,6
         TSUM1=TSUM1 + P(IFLAG,J) * (X1**(IPOWER(IFLAG)*(J-1)))
         TSUM2=TSUM2 + Q(IFLAG,J) * (X1**(IPOWER(IFLAG)*(J-1)))
 1205 CONTINUE
      SUM=TSUM1/TSUM2
      GOTO (1210,1220,1230),IFLAG
 1210 ERFX=X1*SUM
      GOTO 1240
 1220 ERFX=1.0 - DEXP(-X1*X1)*SUM
       GOTO 1240
 1230 ERFX=1.0 - DEXP(-X1*X1)/X1*(1.0/DSQRT(PI)+(1.0/(X1*X1)*SUM))
 1240 ERF=ERFX
      IF (X .LT. 0.0) ERF=-ERFX
 1245 RETURN
C***************P(IFLAG,J)******Q(IFLAG,J)******
      DATA P(1,1)/3.20937758913847D+03/,P(1,2)/3.774852376853D+02/
      DATA P(1,3)/1.1386415415105D+02/,P(1,4)/3.16112374387057/
      DATA P(1,5)/1.85777706184603D-01/,P(1,6)/0.0/
```

```
DATA Q(1,1)/2.84423683343917D+03/,Q(1,2)/1.2826165077372D+03/
DATA Q(1,3)/2.44024637934444D+02/,Q(1,4)/2.36012909523441D+01/
DATA Q(1,5)/1.0/,Q(1,6)/0.0/,P(2,1)/2.2898992851659D+01/
DATA P(2,2)/2.6094746956075D+01/,P(2,3)/1.4571898596926D+01/
DATA P(2,4)/4.2677201070898/,P(2,5)/5.6437160686381D-01/
DATA P(2,6)/-6.0858151959688D-06/,Q(2,1)/2.2898985749891D+01/
DATA Q(2,2)/5.1933570687552D+01/,Q(2,3)/5.0273202863803D+01/
DATA Q(2,4)/2.6288795758761D+01/,Q(2,5)/7.5688482293618/
DATA Q(2,6)/1.0/,P(3,1)/-6.58749161529838D-04/
DATA P(3,2)/-1.60837851487423D-02/,P(3,3)/-1.2578172611123D-01/
DATA P(3,4)/-3.60344899949804D-01/,P(3,5)/-3.05326634961232D-01/
DATA P(3,6)/-1.63153871373021D-02/,Q(3,1)/2.3352049762687D-03/
DATA Q(3,2)/6.05183413124413D-02/,Q(3,3)/5.2790510295142 8D-01/
DATA Q(3,4)/1.87295284992346/,Q(3,5)/2.56852019228982/,Q(3,6)/1/
END
```

```
C                                                        DOS FILE PRED3.FOR
C*************************************************************************
      SUBROUTINE INITIAL(TE,TC,EWF,CWF,PN,NSTEPS,DTP,T2,AN,AT,
     &CN,CT,BN,BT,TCHAR,SMR,ARECN,DELTAT,SN,ST,TAU,NEB,LS,pc)
C*************************************************************************
      REAL CA,CSAHA,CNE,ENE,ECHI,CCHI,EALPHA,CALPHA,LAMNEB,LAMTAU
      REAL DT,DTAUNDZ,DTP,T2,AN,AT,CN,CT,BN,BT,RE,KN,TCHAR,PN
      REAL SMR,LAMDAR,NR,TE,TC,ENR,I,ARECN,EGNDB,ELOSSB,MUI(0:150)
      REAL TAU(0:150),NEB(0:150),DELTAT,SN,ST,PI,TAUN(0:150),NNB(0:150)
      REAL NEBCAL(0:150),FYEN,LAMDAE,LAMDAI,EWF,CWF,J,RMUR,LCCHI
      REAL ESOURCE(0:150),CV,JRIC,VALUE,PHISDAT(154,6),PHIBDAT(21,6)
      INTEGER N,IDEN,CHKDOT,OFILE,EFIX,CFIX,NSTEPS,LS,pc
C
      COMMON /PRED/ CA,CSAHA,DT,DTAUNDZ,DZ,EGNDB,ELOSSB,ENR,I,IDEN,KN
      COMMON /PRED/ LAMDAR,LAMNEB,LAMTAU,MUI,N,NNB,NNR,NR,PI,RE,RMUR
      COMMON /PRED/ TAUN,EFIX,CFIX,CHKDOT,FYEN,ENE,ECHI,CCHI,CNE
      COMMON /PRED/ EALPHA,CALPHA,CV,ESOURCE,LCCHI
      COMMON /XSHEATH/ PHISDAT,PHIBDAT
C
      WRITE(*,150)
C*****READ FILE INDATA.DAT
      READ(2,151) TE,TC,EWF,CWF,PN,D,J,DTP,T2,CHKDOT,OFILE,pc,N,LS
      REWIND(2)
      CLOSE(2)
C*****READ FILE PRECOR.DAT
C     CALL DATAINT
C*****SET NUMERICAL PARAMETERS, RECOMPILATION REQUIRED TO CHANGE
      AN=0.5
      AT=0.5
      CN=0.5
      CT=0.5
      BN=1.0-CN
      BT=1.0-CN
      PI=3.1415926
      IDEN=0
      RE=0.0
      FYEN=1.0
      NR=1.0E14
      DELTAT=DTP/NSTEPS
      LAMNEB=1.0
      LAMTAU=1.0
C*****SET TRANSPORT PROPERTIES
      LAMDAE=1.0/32.3/PN
      LAMDAI=1.0/96.6/PN
      LAMDAR=LAMDAI/LAMDAE
      KN=LAMDAE/D
      TCHAR=D/(KN*3.75*(TE**.5))
      SMR=1.0/492.2
C*****EXECUTE OFILE SELECTION SETTING
      IF (OFILE .EQ. 1) THEN
         READ(8,152) ENE,CNE,ECHI,CCHI,EALPHA,CALPHA,N
         READ(8,154) (NEB(I1),TAU(I1),I1=0,N+1)
         REWIND(8)
      ELSE
         ENE=0.8
         CNE=0.8
         ECHI=3.0
         CCHI=3.0
         EALPHA=0.5
```

```
         CALPHA=0.5
         DO 10 I1=0,N+1
            NEB(I1)=I1
            NEBCAL(I1)=(NEB(I1)-1)/(N-1)
            NEB(I1)=4.0*(KN+NEBCAL(I1)*(1-NEBCAL(I1)))
            TAU(I1)=2700/TE
   10    CONTINUE
      ENDIF
C*****MISCELANEOUS DEFAULTS
      ARECN=0.31
      EGNDB=3.896/8.609E-05/TE
      ELOSSB=EGNDB
      SN=DELTAT*(N-1)**2*3*LAMDAR*SMR*(BN+CN)
      ST=DELTAT*(N-1)**2*0.667*(RE+2)*2**(RE+0.5)*(BT+CT)/FYEN
C*****NONDIMENSIONALIZE CURRENT AND CALCULATE RICHARDSON EMISSION
      VALUE=EXP(-11600.0*EWF/TE)
      ENR=(7.676E+14*(TE)**1.5*VALUE)/NR
      I=J / (KN*NR*(3.1265322E-13)*SQRT(TE))
      JRIC=120.0*TE*TE*(EXP(-11600.0*EWF/TE))
C*****OUTPUT INITIALIZATION DATA TO PRNTOUT.DAT
      WRITE(9,155) TE,TC,EWF,CWF,PN,D,J,CHKDOT,OFILE,N,
     &             JRIC,NR,TCHAR,I,ENR,KN,SMR,LAMDAR,
     &             NSTEPS,T2,DELTAT,DTP,LS
      IF (CHKDOT.GT.1) THEN
          WRITE(9,160) ECHI,ENE,EALPHA,CCHI,CNE,CALPHA,AN,AT,
     &                 BN,BT,CN,CT,SN,ST,LAMNEB,LAMTAU,ELOSSB,
     &                 ARECN,EGNDB,IDEN,FYEN,RE
          WRITE(9,159) (I1,NEB(I1),I1,TAU(I1),I1=1,N)
      ENDIF
      WRITE(9,161)
C*****CHECK FOR UNREAL CURRENT CONDITION  J/JR > 1.0
      IF (2*KN*I/ENR .GE. 1.0) THEN
         WRITE(*,153)
         STOP
      ENDIF
      RETURN
C
C-----------------------------------------------------------------
  150 FORMAT(1X,'*****************************************'/
     &1X,'*****                                     *****'/
     &1X,'*****          TEC    START               *****'/
     &1X,'*****                                     *****'/
     &1X,'*****************************************'///)
  151 FORMAT(F8.1/F8.1/F6.3/F6.3/F6.3/F6.3/F7.2/F5.2/F6.1/
     &I1/I1/I3/I3/I3)
  152 FORMAT(F9.4/F9.4/F8.3/F8.3/F9.4/F9.4/I3)
  153 FORMAT(1X,'***SMALL J IS TOO LARGE...CASE TERMINATED***'//)
  154 FORMAT(2F8.3)
  155 FORMAT(12X,'    TEC INITIAL DATA SUMMARY'/
     &1X,'-------------------------------------------------'//
     &1X,'PHYSICAL OPERATING CONDITIONS-----'//
     &1X,'    EMITTER TEMPERATURE    (TE)=',F8.1,' KELVIN'/
     &1X,'  COLLECTOR TEMPERATURE    (TC)=',F8.1,' KELVIN'/
     &1X,'  EMITTER WORK FUNCTION   (EWF)=  ',F6.3,' EV'/
     &1X,'COLLECTOR WORK FUNCTION   (CWF)=  ',F6.3,' EV'/
     &1X,'     CONVERTOR PRESSURE    (PN)=  ',F6.3,' TORR'/
     &1X,'          GAP THICKNESS     (D)=  ',F6.3,' MM'/
     &1X,'      OPERATING CURRENT     (J)= ',F7.3,' AMPS/CM^2'//
     &1X,'    TEC FUNCTION SETTINGS-----'//
     &1X,'       DIAGNOSTIC LEVEL  (CHKDOT)=  ',I1/
```

```
     &1X,'       RESTART SEQUENCE    (OFILE)=  ',I1/
     &1X,'          POINT DENSITY        (N)=',I3//
     &1X,'PHYSICAL PARAMETERS EVALUATED-----'//
     &1X,' RICHARDSON CURRENT     (JRIC)=',E9.2,' AMPS/CM^2'/
     &1X,'   REFERENCE DENSITY      (NR)=',E9.2,' 1/CM^3'/
     &1X,' CHARACTERISTIC TIME   (TCHAR)=  ',F7.4,' SECS*E-06'/
     &1X,'       NONDIM CURRENT       (I)=  ',F7.4/
     &1X,'      NONDIM EMISSION     (ENR)=  ',F8.3,'(NRIC/NR)'/
     &1X,'       KNUDSEN NUMBER      (KN)=  ',F7.4/
     &1X,'     SQRT(MASS RATIO)     (SMR)=  ',F7.4/
     &1X,'MEAN FREE PATH RATIO (LAMDAR)=  ',F7.4//
     &1X,'TIME SETTINGS-----'/4X,'NSTEPS=',I3/
     &4X,'     T2=',F6.1/4X,'DELTAT=',F6.3/4X,'    DTP=',F6.3/
     &4X,'     LSF=',I3)
  159 FORMAT(4X,'NEB(',I2,')=',F8.3,'    TAU(',I2,')=',F8.3)
  160 FORMAT(//1X,'ADVANCED DIAGNOSTIC OUTPUT-----'//
     &4X,'ECHI=',F5.1,' ENE=',F7.4,' EALPHA=',F7.4/
     &4X,'CCHI=',F5.1,' CNE=',F7.4,' CALPHA=',F7.4/
     &4X,'AN=',F7.4,'  AT=',F7.4/4X,'BN=',F7.4,'  BT=',F7.4/
     &4X,'CN=',F7.4,'  CT=',F7.4/4X,'SN=',F7.4,'  ST=',F7.4/
     &4X,'LAMNEB= ',F5.2/4X,'LAMTAU=',F5.2/4X,'ELOSSB= ',F6.3/
     &4X,'ARECN= ',F6.3/4X,'EGNDB= ',F6.3,/4X,'IDEN=',I1/
     &4X,'FYEN=  ',F5.2/4X,'RE=  ',F5.2//
     &1X,'STARTUP DENSITY AND TEMPERATURE RATIOS-----')
  161 FORMAT(/1X,'------------------------------------',
     &'---------------')
      END
C
```